Fall 12-20-2017

Parameter Estimation Technique for Models in PSS/E using Real-Time Data and Automation

Malavika Vasudevan Menon
University of New Orleans, New Orleans, mvasudev@uno.edu

Fall 12-20-2017

Parameter Estimation Technique for Models in PSS/E using Real-Time Data and Automation

Malavika Vasudevan Menon

Parameter Estimation Technique for Models in PSS/E using Real-Time Data and Automation

A Thesis

Submitted to the Graduate Faculty of the
University of New Orleans
in partial fulfillment of the
requirements of the degree of

Master of Science
in
Engineering
Electrical Engineering

By

Malavika Vasudevan Menon

B-Tech. Mahatma Gandhi University, 2014

December, 2017

To my parents, and sister.

Acknowledgement

First and foremost, I offer my sincerest gratitude to my supervisor, Dr. Parviz Rastgoufard, who has supported me throughout my thesis with his patience and knowledge. His encouragement and support have been a major contribution to the completion of my thesis. I am grateful to the UNO - Power and energy Research Laboratory for all the opportunities and experiences.

I sincerely thank Rastin Rastgoufard for his constant motivation by assigning different Python projects and guiding me to learn everything I know about Python. His expertise and knowledge have been crucial throughout my thesis and research work.

I would like to express my sincere gratitude to Dr. Ittiphong Leevongwat for his technical support and valuable suggestions throughout my thesis and my time at school. His patience and way of teaching along with his cheerful attitude made research work and learning enjoyable.

I further heartfully thank Dr. Ebrahim Amiri for his constant motivation and moral support. I also thank all the faculty and staff of the University of New Orleans for their support and providing me with quality education.

Finally, I would like to thank my parents, Ajitha Menon and M.V. Menon, and sister, Mrinalini Menon for their constant support and unconditional love throughout my life. None of this would have been possible without them. I also would like to thank my friends for being there for me always and lifting my spirits when I needed it the most.

Contents

List of Figures

List of Tables

Abstract

The purpose of this thesis is to use automation to create appropriate models in PSS/E with the data from Hardware-in-Loop real-time simulations. With the increase in technology of power electronics, the use of High Voltage Direct Current Technology and Flexible Alternating Current Transmission System devices in the electrical power system have increased tremendously. Static Var Compensators are widely used and it is important to have accurate and reliable models for studies relating to power systems planning and interaction. An automation method is proposed to find the parameters of an SVC model in PSS/E with the data from the Hardware-in- loop real-time simulation of the SVC physical controller using Hypersim. The effect of the SVC on the system under steady state and fault conditions are analyzed with HIL simulation of an SVC physical controller in Hypersim and its corresponding model in PSS/E in the IEEE 14 bus system. The parameters of the SVC model in PSS/E can be effectively varied to bring its response closer to that of the response from HIL simulations in Hypersim. An error function is used as a measure to understand the extent of difference between the model and the physical controller.

Keywords: Electrical, Power and Energy

Chapter 1
Problem Statement and Historical Review

1.1 Introduction

Todays power systems network is an enormous and complex network of interconnections which includes buses, generators, transmission lines etc. This network is expanding and increasing with growing load demands and requires the installation of new generators or lines or extension of existing infrastructure. This increase in demand also leads to the unstable operation of the power system and causes the system to be less reliable. Electric utilities have the responsibility of maintaining the safety of their systems and planning for the future power needs of their customers [2].

Flexible AC Transmission Systems (FACTS) controllers enable the efficient utilization of the existing transmission and generator facilities instead of adding new facilities to the infrastructure [17]. It requires lower investment and does not lead to any environmental constraints. Devices such as Static VAR Compensators (SVC), Static Synchronous Compensator (STATCOM), Thyristor Controlled Series Compensator (TCSC), Static Synchronous Series Compensator (SSSC) and Unified Power Flow Controller (UPFC) are popular FACTS controllers. Other than improving the voltage profile and reactive power FACTS devices offer a wide range of benefits. FACTS technologies helps in the increase of power transfer capabilities by 20-30% by the increase of the system flexibility [17]. They also improve the

loading ability of the system. The increase in the inclusion of renewables in the system such as wind turbines leads to the absorption of large amounts of VARs (Volt-Amperes Reactive) due to it being induction generators. Facts devices offer faster and smooth switching capacitor operations along with voltage regulations and power factor corrections compared to the traditional switched capacitors which causes stress due to frequent switching that leads to transients to the grid and reduction of the life cycle of the capacitors [24].

SVC is one of the earliest and most commonly used FACTS devices due to its reasonable cost and numerous advantages. It is found to be one of the mostly widely used FACTS devices in China [3]. Analysis of the power system network is required to study and improve it during different network events and addition of different units to meet demands. This has been done by modeling the system and simulating the network events in power system software. Simulation based analysis of the planning and design of power systems have been done extensively for decades [3]. This type of analysis can be of many uses such as in the planning and design of power systems which helps to decide future system requirements and parameter selection for control systems, in the operation of the power system to determine limits for operation and requirement for specific protection schemes, and in the fault analysis to understand weak regions and analyze events that lead to major disturbances. Simulations can help analyze the network and device surrounding the area of the fault in the pre-fault, fault and post-fault durations.

Power system engineers use different software such as PSS/E, PSLF, EMTP, TSAT, Hypersim, and RTDS and so on. Each software is different and has its own advantages and limitations. PSS/E and PSLF have the capacity to model very large systems and are mainly used to run load flow analysis in different contingencies. EMTP and MATLAB have the

ability to simulate and study transients and involve in circuit element based modeling. The past few decades has the seen the evolution of simulation tools which were driven by the rapid evolution of computing technologies. The capacity of simulation based tools to solve complex problems in less time was enabled due the decrease in cost and the increase in performance of computer technologies [31]. This led to the origin of digital real time simulators which exploit advanced digital hardware and advanced computing methods to solve differential equations which represents the power system in the speed of real world time. Hypersim and RTDS are examples of real time simulators which can be used to study electromagnetic transients in micro seconds. They also enable the analysis of physical hardware devices with Hardware-in-loop (HIL) simulations which can connect the physical controller to the simulator through input/output (I/O) channels.

With the growth of computing technologies and increase in the simulation and problem solving capabilities, it is important to model devices and the system as accurate as possible for us to understand and analyze the effects of these devices on the system as well as other devices in the system and vice versa. At this time, it cannot be acceptable to question the accuracy of the model used for analysis. After the commissioning of HVDC and FACTS devices, the customers are usually provided with a black box model of their device. The maintenance of the model is hard during the lifetime of the equipment. This can be due to the fact that these models are based on a particular version of the simulation tool as the models require certain static libraries that might be linked to the version and thus disabling the model from following the actual control changes. Long term expertise is not necessarily provided by the manufactures for model maintenance [31]. The manufacturer also supplies physical replicas of the control system. The replica is a precise copy of the actual control

units installed on site.

This thesis aims in creating appropriate models in PSS/E for stability analysis studies with the data from the field. A method of automation is proposed to find the parameters of an SVC in PSS/E with the data from the Hardware-in-loop real-time simulation of the SVC physical controller using Hypersim. It analyzes the dynamic and transient response of the system with the SVC connected to it while subjecting it to different network events such as three phase bus faults. The system dynamics are kept to a minimum to reduce the difference between the software platforms and to focus on the dynamics of the SVC. The responses are compared and an error function is used to measure the amount of difference between the model and the replica. Selection of the parameters of the SVC model in PSS/E is based on how close the response of the SVC is in PSS/E to that of the response in Hypersim with the SVC physical controller. The comparison process is automated and the parameter set with the least error function value is chosen.

1.1.1 Challenges in Power System Planning

Power system planning is one of the most important parts of maintaining a reliable and secure power system network. Guidelines and standards are issues to enable a smooth process even with which it would face numerous challenges which can be seen below [4] :

- Collection of wide variety of data from multiple sources
- Cooperative approach to developing, validating, specifying and using new planning methods, tools and models
- Effective sharing and access to data

- Uncertainty in future demand including active and reactive power profiles under network events
- Need for an array of models, standards and processes to address distribution networks

1.1.2 Time Frames in Reactive Power Analysis

NERC has issued a time frame for the reactive power planning and voltage control to clearly understand the systems reactive capability requirements in [22] which can be seen below:

- Steady State / Pre-Contingency: Individual elements such as generators and dynamic reactive resources are maintained at a desired voltage set point value to ensure other voltages are maintained in the desired voltage range. Manual adjustments are required to maintain this schedule. In this state, the grid is said to be operating in a secure state which means no violations can be seen and thus no outage conditions are to happen.
- Transient: After a major network event or disturbance, the transient voltage stability is analyzed with different transient stability tools. There are two main transient voltage responses that can be seen in this period
  - Transient voltage dip: dips or sags which are caused by oscillations which change the active and reactive power flow and thus the voltage.
  - Delayed voltage recovery: Delayed recovery in voltage due to fault as well as stalling and restarting of induction motor which results in reactive power demand.
- Mid-term Dynamics : After the first swing during transients, if the system is stable, the oscillations begin to dampen and return to a new steady state condition this period

during transition is called mid-term dynamics. The analysis during this period includes the results of the automatic control devices and is within 3 minutes following an event

- Long term dynamics / Post-contingency: Once the system attains equilibrium, pose contingency analysis is performed to ensure the system is stable and secure. The system has to attain acceptable operating limits within 30 minutes following an event

This thesis deals with the accuracy of models and the selection of parameters for the simulation models which falls under the category of power system planning and design.

1.2 Historical Background

Power electronics controllers will have greater significance over the reliability of the grid and its performances over the next couple of years. The use of real time simulators and hardware in the loop analysis are growing as can be seen in [31] which involves performing simulations with different SVC replicas connected to the same simulator to study the levels of interaction between the replicas and to improve the model of SVC in off-line simulations. A Hardware-in the-loop test facility called SMARTE was set up which uses Hypersim simulator to verify various modeling techniques and to test interoperability with the absence of adverse interactions. This paper uses 3 study replicas of SVC controllers from 2 different manufacturers which are connected to the 225kV substations situated in the West of France, which is considered as the weak zone of the French grid. A large number of capacitors and 5 SVCs were installed in this zone to control voltage during events. The required part of the network involving substations, lines, autotransformers, generation units and the SVC were modeled in the Hypersim software. The replicas were connected to the simulator via input

and output signals (IO). Different types of network events such as transformer fault, line fault or bus faults were simulated to examine the SVCs reaction by observing the positive sequence voltage, reactive power and TCR firing angle.

The compatibility of generator models in different Power system simulation software such as PSS/E, EMTP and Hypersim is shown in [20]. PSS/E is used to study electro-mechanical dynamics whereas Hypersim and EMTP are used for electromagnetic dynamics and thus the dynamic results between PSS/E and Hypersim are different. This paper is required to achieve identical system results in order to compare the results of an SVC model in PSS/E to that of the HIL simulation with the SVC replica in Hypersim. The IEEE 14 bus system along with the models of the generator and excitation system were modeled in all three software. To study the transients, a same network event such as bus faults were applied in different location and the voltage profiles were plotted against each other. Sensitivity analysis of the excitation system is carried out and the parameters with the most sensitivity are varied within a specific range in one software to match the other software.

For over two decades, real-time simulators have been used by utilities, independent system operators (ISO), manufacturers, research institutes and universities to test a range of controls like HVDC, FACTS, generator controls, distributed generation, and smart grid [6]. The HIL test which is an advanced test method allows the prototype (replica) of a unique device to be analyzed under a range of realistic situations safely, frequently and efficiently. This paper deals with the testing of a digital controller for a DC-DC buck converter and DC-AC converter. These converters consist of basic elements such as switches, diodes and inverters that are used in other devices such as FACTS, HVDC which predominant in power systems network. It was found that HIL testing is useful to analyze the effectiveness of power electronic controllers by

being an intermediate step during the progress of an end product, reducing the development cost and risks that are encountered during testing.

The complexity and size of power system network has led to the extensive use of FACTS devices where they are not only able to improve the voltage and angle stability but also add flexible operation capabilities. FACTS devices such as SVC, STATCOM, TCSC and SSSC have their own characteristic and constraints and are represented by different models and mathematical equations which depend on time frame and issue under analysis. For RCP and HIL testing to be purposeful and relevant, it is important that the real-time simulations be accurate portrayal of the real-world response. The accuracy and credibility of HIL testing is shown in [25] by running a real-time simulation of an induction motor drive and comparing it against a physical implementation of the same. Modeling was done of both the motor and inverter in the Opal- RT platform to compare it to the actual motor drive. Motor control was enabled with the implementation of Field Oriented Control (FOC) and tests were run to examine both the steady state and dynamic response of the motor. While current outputs for different frequencies were used to compare results in the case of steady state, the motor start up stage was used to analyze the dynamic response. The results were highly close and the waveforms overlapped with disregard able errors which validated the credibility of the real-time HIL simulations.

The power system network of the present day is an intricate interconnected network which is increasing every day to meet the increase in demands. Addition of new lines and generators creates many environmental and economical restraints. Reactive power generation i.e., FACTS devices is the one way to counteract this problem. The applications of the four main FACTS devices which are STATCOM, SVC, TCSC and SSSC can be seen in [21]. Every

FACTS device has their own unique characteristics and limitations. The weakest bus is chosen from the standard IEEE 14 bus system with the use of continuation power flow (CPF) and then to determine the best location. The maximum loading factor (lambda) was taken as the metric to analyze the different devices. When placed on bus 14, lambda increased by 0.0808 for STATCOM, 0.0504 for SVC, 0.0348 for SSSC and 0.0332 for TCSC. When comparing average costs, STATCOM was found to be the most expensive followed by SVC and TCSC. It was found that advantages or savings by installing FACTS devices would outweigh the additional costs in acceptable time [21].

Functional applications of real-time simulations for power and energy systems include design and modeling, prototyping or rapid prototyping, testing, and teaching and training. Developing a new model and designing a new device can be easily done with real-time simulations as it produces results faster with higher accuracy [10]. It helps in creating prototypes which are approximates of the real system that can be used in testing and modification of the devices when and as required [3]. The most common application is testing as it allows the modeling of the surrounding area which represents real physical field environments [10]. It is a valuable tool in teaching and training as live feedback allows understanding the response of the systems when changes and disturbances are brought into the system [3]. The extensive and growing use of real-time simulations can be seen in [10] which mentions examples in super large EMT real-time simulation, protection, device interoperability, and PMU, Hybrid phasors/ EMT applications, HVDC testing, FACTS and D-FACTS testing, Smart grid/ Distribution system applications and Multi-physics applications. It is evident that real-time simulations in power systems valuable and predominant.

The steady state effect of an SVC on the IEEE 14 bus system can be seen in [23]. The

SVC was modeled as a fixed shunt capacitor in MATLAB/Simulink and connected to the weakest buses of the system. The load is then increased by 10% and 20%. The voltage profiles and reactive power profiles were analyzed of the base case against the profiles for when the SVC is connected to the system. It was clear from the profiles that the SVC plays a great importance in the voltage profile as well as the reactive power profile during load variations in the system.

A study on the transient stability improvement of a system with the use of FACTS devices is seen in [30]. MATLAB is used as the platform for modeling and analyzing the dynamic system. The sim Power block set enables the modeling of power system network and element. This paper analyzed the effect of FACTS controllers like SVC, STATCOM and SSSC on the IEEE 5 machine 14 bus system. A 3-phase fault was applied on different buses with the SVC connected to the system at different buses. The fault is applied at 0.5 secs and cleared after 0.1 secs. The results were analyzed and it was found that the time taken to attain system stability decreased with the use of FACTS devices and the best case was found when the SVC was connected at Bus 4. It was also found that the maximum overshoot values for relative rotor angle positions decreased with the use of the FACTS controller and the best case was found when the SVC was connected at Bus 3. This shows that transients are stabilized faster with the use of FACTS devices.

The comparison of transient stability analysis and real time digital simulation can be seen in [8]. Traditionally, real time simulators did not have the ability to simulate large-scale power systems. The KEPS real Time Digital Simulator is the largest RTDS produced with the ability to simulate large scale systems, the results of which are compared to that of transient stability analysis software, PSS/E. It was found that most of the results were very

similar but had cases which exhibited differences. The main differences were found to be the method in which the programs solved the differential equations which corresponds to the system. Three disturbances were applied to the systems and the differences were analyzed in detail.

According to the review of the above papers, it can be seen that creating accurate and precise models in transient stability analysis platform is necessary and important. Also, a methodical and efficient process of finding the parameters for the model has never been performed with python automation. The focus of this thesis is to increase the accuracy of the model of the SVC in PSS/E by finding the best set of parameters that would bring it closer to that of the SVC physical controller with the least error function.

1.3 Scope of Work

The aim of this thesis is to create appropriate models in PSS/E for stability analysis studies with the data from the field. An automation method is proposed to find the parameters of an SVC model in PSS/E with the results from the HIL simulation of the SVC physical controller. Different sets of parameters are assigned to the SVC model and the system voltages along with the MVAR output of the SVC are compared when a three phase bus fault is applied and cleared after a certain time along with the loss of a line. Chapter 2 describes the mathematical background of the components used in the test system. This chapter is important as it is necessary to know the underlying mathematics to understand and analyze the behavior of each component. Chapter 3 provides an insight on what the focus of this thesis is and an overall description of the methodology used in this research. Chapter 4 lists all the models

and components used in the test system. The process to find the best locations for the SVC is also elaborated in this chapter. It allows us to see and analyze the dynamic responses of the SVCs incorporating the differences in different platforms. Chapter 5 shows the results of the analysis with error function table along with the voltage responses of the parameters with the least error function. This is followed by the conclusion in Chapter 6 which analyzes the results along with the future work.

Chapter 2

Mathematical Background

2.1 Introduction

Representation of the power system components mathematically is the first and most important step in analyzing power systems and its stability. Power system planning and operations depend extensively on tools which use models to ensure reliable and efficient operation. There are different types of modeling depending on the type and requirement of the equipments.

The mathematical modeling of all the electrical components used in the test system for this thesis is dealt with in this chapter.

2.2 Static Var Compensator Modelling

Static Var Compensator is a type of FACTS device that is a shunt compensator which has been in use since the 1970s [11]. It is used to influence the natural electrical characteristics of the transmission line to increase the power for transmission and to control the voltage profile. It consists of a set of power electronic devices for providing fast-acting reactive power. The output of the SVC can be adjusted to produce either capacitive or inductive currents which

control the bus voltage of the electrical power system [1]. Thyristors play a significant part in control of the reactive power flow which is done by controlling the firing angle [18]. The one-line diagram of an SVC is shown in Figure 2.1.

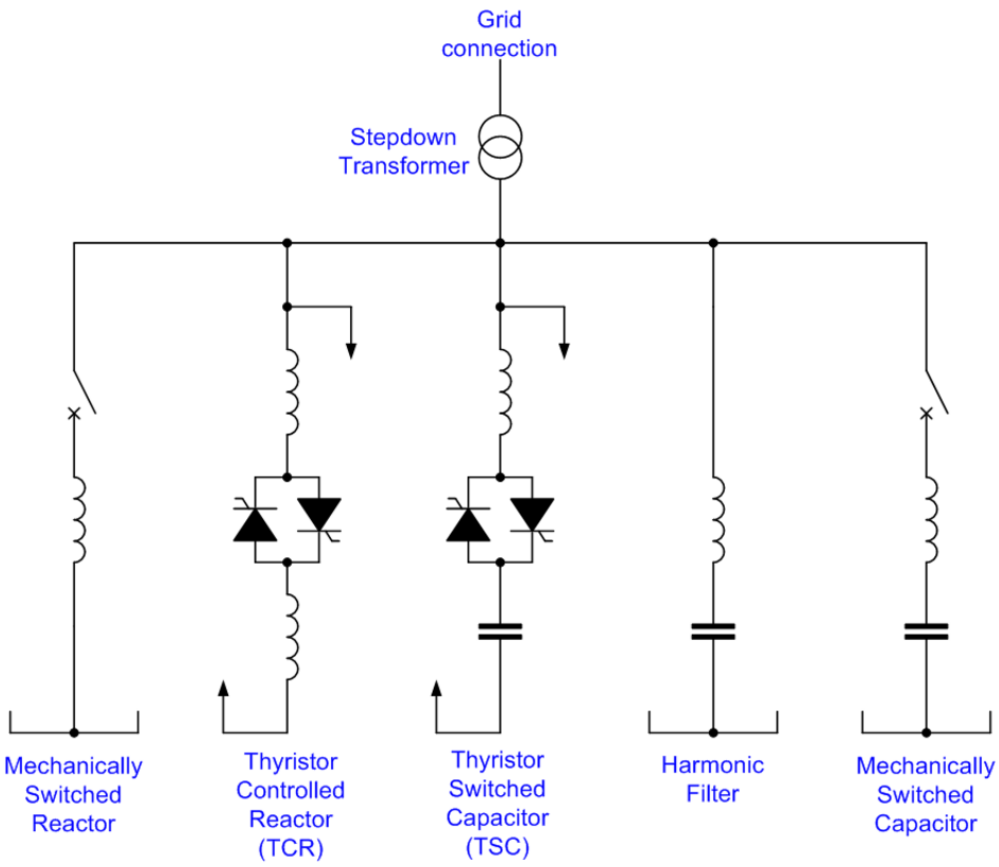

Figure 2.1: SVC one-line diagram

The SVC constitutes one or more banks of fixed or switched capacitors or reactors. Components which can be used to design an SVC are:

- Thyristor Switched Capacitor
- Thyristor Controlled/Switched Reactor
- Harmonic Filters
- Mechanically Switched Capacitor/ Mechanically Switched Reactor

2.2.1 Thyristor Switched Capacitor

The thyristor Switched Capacitor consists of a capacitor connected in series with a bidirectional valve and, mostly, a current limiting reactor. The current limiting reactor is used to limit the effects of the capacitor switching [12]. The SVC in the study involves 3 TSC units which results in a 0/+300 Mvar SVC.

The current through the TSC branch at any given time is given by [12, 18],

$$i(t) = \Big(I\cos(\omega_0 t + \alpha)\Big) - \Big(I\cos(\alpha)\cos(\omega_r t) + nB_c\Big(V_{Co} - \frac{n^2}{n^2-1}V\sin(\alpha)\Big)\sin(\omega_r t)\Big) \quad (2.1)$$

In the equation above, the first part represents the steady state equation and the second part represents the equation for the oscillatory transients. We assume that the TSC comprises of capacitance, C and inductance, L with a sinusoidal input voltage. ω_0 is the nominal angular frequency, α is the current firing angle , ω_r is the resonant frequency, n is the per unit natural frequency and V_{Co} is the voltage across the capacitor.

The current amplitude and n is given by,

$$I = V\frac{B_C B_L}{B_C + B_L} \quad (2.2)$$

$$n = \frac{1}{\sqrt{\omega_0{}^2 LC}} = \sqrt{\frac{X_C}{X_L}} \quad (2.3)$$

B_C and B_L is the capacitor and reactor susceptance and X_C and X_L are the capacitor and

reactor reactance respectively. The TSC resonant frequency ω_r is given by,

$$\omega_r = n\omega_0 = \frac{1}{\sqrt{LC}} \tag{2.4}$$

Thus, the magnitude of the TSC current can be given as,

$$I = V\frac{B_C B_L}{B_C + B_L} = VB_C\frac{n^2}{n^2 - 1} \tag{2.5}$$

The SVC is represented as a one line diagram with a simplified block diagram of the control units in Figure 2.2. It consists of a measuring system which measures the voltage to be controlled. The voltage regulator determines the SVC susceptance needed to keep the voltage at a desired value. This is done with the use of the voltage error which is the difference between the measured voltage V_m and the reference voltage V_{ref}. The distribution unit determines which TSCs and TSRs needs to be switched in and out and finds the firing angle of TCR. The synchronizing unit uses a Phase locked loop pulse generator to send the required

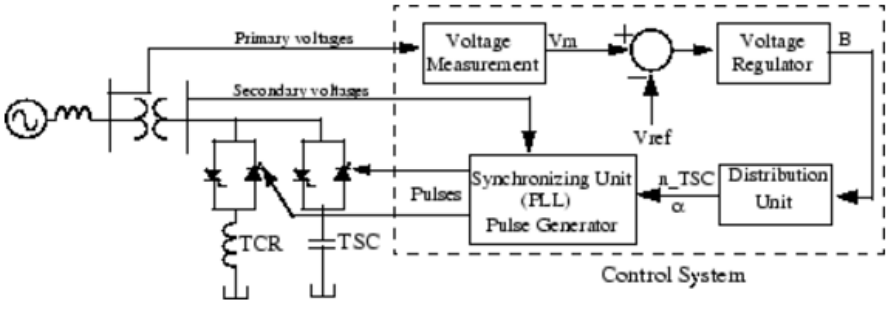

Figure 2.2: Simplified block diagram of SVC unit

2.3 Generator Modeling

There are different types of models for the synchronous generator depending on type of analysis and requirement. The classical generator model is used in this study. One of the simplest yet useful representation of the synchronous generator is the classical model [16]. There are a few assumptions taken into consideration while representing the synchronous generator by a classical model [16]. They are:

- The field current is assumed constant and exciter dynamics are not of concern
- The effect of damper windings is ignored
- The mechanical power input is assumed to be constant during the study period
- The saliency of the generator is neglected

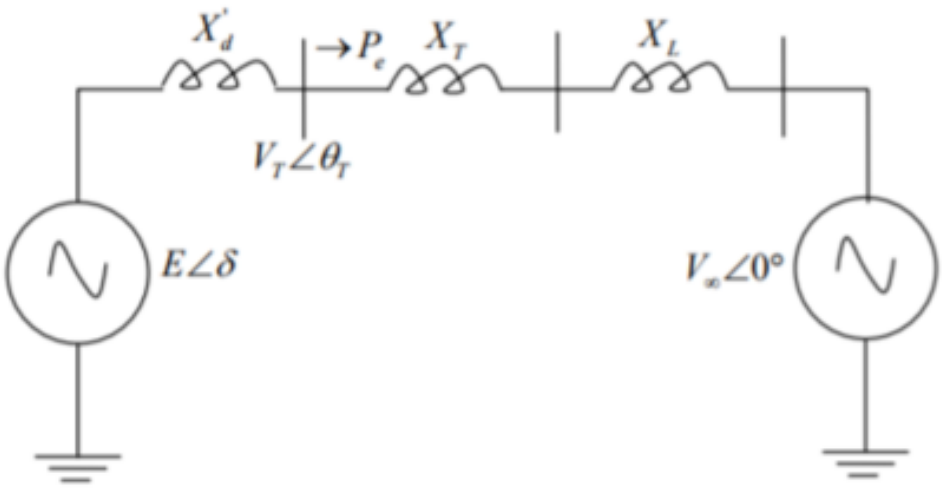

Figure 2.3: Simplified block diagram of SVC unit

The classical model representation can be seen in Figure 2.3. $E\angle\delta$ represents the complex internal voltage of the generator and X represents the reactance. The generator is assumed to be connected to an infinite bus is through a transformer and line and the bus voltage is represented as V. The generator internal voltage angle delta is defined with respect to bus voltage. The input mechanical power is P_i and output electrical power is P_o

The electrical power output can be found to be,

$$P_o = \frac{EV_\infty}{X} \sin\delta \tag{2.6}$$

The reactance, X is a combination of the transient reactance, $X_d{}'$, line reactance X_L and transformer reactance X_T.

Maximum power is transferred when $\delta = 0$ which is,

$$P_{max} = \frac{EV_\infty}{X_d{}' + X_T + X_L}, at\delta = 90\,\text{deg} \tag{2.7}$$

The synchronous machine also has a mechanical system model and the dynamics of the rotational mechanical system is represented as,

$$J\frac{d^2\theta_m}{dt^2} = T_m - T_e \tag{2.8}$$

Where J is the inertia constant of the rotating machine. The mechanical input torque due to the prime mover and the electrical torque is represented by T_m and T_e. The mechanical angle of the rotor field axis with respect to the stator reference is θ_m. θ_m is made a constant

in steady state by measuring it with respect to a synchronously rotating reference and hence,

$$\theta_m = \delta_m + \omega_{ms} t \tag{2.9}$$

The manipulation of the above equations leads to the equation given below,

$$\frac{d^2\delta}{dt^2} = \frac{\pi f_s}{H} \tag{2.10}$$

This is called the swing equation of the synchronous generator which helps to analyze the response of the generator. H is the machine inertia constant. If $P_m = P_{max} \sin\delta$, then there will be no speed change and no angle change. But if they are not equal due to some disturbance in the system, then either the speed will increase or decrease with respect to time.

In synchronous generators, the rotor has damper windings which causes it to act as an induction motor during transients. This effect needs to be considered which evaluating stability and leads to the equation,

$$\frac{H}{\pi f_s}\frac{d^2\Delta\delta}{dt} + D\frac{d\Delta\delta}{dt} + P_s\Delta\delta = 0 \tag{2.11}$$

Where D is the damping coefficient and Ps is the synchronizing torque or power. Similarly, the generator reactive power output is given by,

$$Q_o = \frac{V_\infty(E\cos(\delta) - V_\infty)}{X_d{}' + X_L + X_T} \tag{2.12}$$

Classic model has two main advantages beside its simplicity. First, all the voltages and currents are phasors in the network reference frame, whereas in higher order models d q representation is needed. The second important advantage is that the generator reactance can be treated in similar way as transmission line reactances and can be combined with network elements to form reduced admittance matrix.

2.4 Exciter Modeling

The basic function of an excitation system is to supply the required direct current to the field winding of the synchronous generator. It automatically adjusts the field current to retain the required terminal voltage.

R_e and L_e represent the resistance and inductance of the exciter field, then the voltage is given by,

$$V_R = R_e i_e + L_e \frac{d}{dt} i_e \tag{2.13}$$

and hence,

$$\Delta V_R = R_e \Delta i_e + L_e \frac{d}{dt} (\Delta i_e) \tag{2.14}$$

The exciter field i_e produces the rectified armature voltage V_f of the exciter which is given by,

$$\Delta V_f = K_1 \Delta i_e \tag{2.15}$$

Here, K_1 is the rectified armature volts per ampere of exciter field current. This yields,

$$\Delta V_f(s)\frac{K_e}{1+sT_e}\Delta V_R(s) \tag{2.16}$$

where,

$$K_e = \frac{K1}{R_e} \qquad\qquad T_e = \frac{L_e}{R_e} \tag{2.17}$$

The Figure 2.4 given shows the Simple Excitation System (SEXS) model provided by PSS/E. The SEXS model represents the general characteristics of a range of tuned excitation systems [28]. The first block with time constant T_a and T_b, represents the transient gain reduction needed to follow satisfactory dynamic behavior and the second block with the gain, K, time contant, T_e with the corresponding limits E_max and E_min portrays the basic excitation power source.

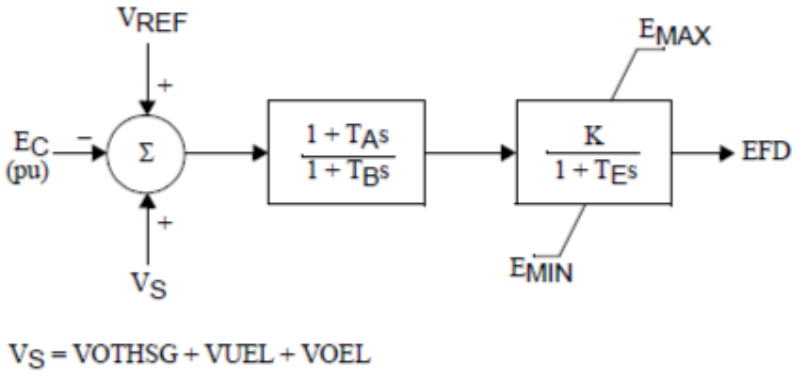

Figure 2.4: Simple Excitation System in PSS/E [27]

2.5 Transmission Line Modeling

Transmission lines are conductors that transfer electrical signals from one place to another. Transmission lines can be classified based on the transmission line length, amount of power transfer capability and the conductor used for the transmission line [5]. Modeling for transmission lines are characterized by 5 parameters : Resistance per unit length (R), Shunt conductance per unit length (G), Inductance per unit length (L) and Shunt capacitance per unit length (c) and increment of length as seen in Figure 2.5.

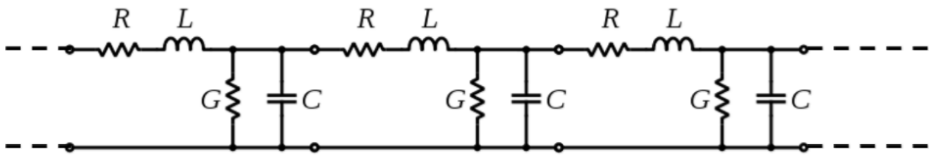

Figure 2.5: Transmission line circuit diagram

The voltage and current at a distance k from the receiving end of a distributed parameter line is given by,

$$\bar{V} = \frac{\bar{V}_R + Z_o \bar{I}_R}{2} e^{\gamma k} + \frac{\bar{V}_R - Z_o \bar{I}_R}{2} e^{-\gamma k} \tag{2.18}$$

$$\bar{I} = \frac{\bar{V}_R / Z_o + \bar{I}_R}{2} e^{\gamma k} - \frac{\bar{V}_R / Z_o - \bar{I}_R}{2} e^{-\gamma k} \tag{2.19}$$

The characteristic impedance is represented as Z_o, propagation constant is γ, attenuation constant is α and phase constant is β can be seen below,

$$Z_o = \sqrt{\frac{j\omega L + R}{j\omega C + G}},$$
$$\gamma = \sqrt{(j\omega L + R)(j\omega C + G)} = \alpha + j\beta$$

This study includes π lines in the test system and the voltage and current equations for π lines are represented as given below, where, S and R represent sending and receiving end of the transmission line.

$$\bar{V}_S = \bar{V}_R \cosh(\gamma l) + Z_c \bar{I}_R \sinh(\gamma l) \tag{2.20}$$

$$\bar{I}_S = \bar{I}_R \cosh(\gamma l) + \frac{\bar{V}_R}{Z_c} \sinh(\gamma l) \tag{2.21}$$

The characteristic impedance is given by,

$$Z_e = Z_o \sinh(\gamma l) \tag{2.22}$$

When $\gamma l \ll 1$, then, the transmission line is considered negligble, which gives,

$$Z_e = Z_c \sinh(\gamma l) \approx Z_c \gamma l \approx zl = Z \tag{2.23}$$

and,

$$\frac{Y_e}{2} = \frac{1}{Z_c} \tanh(\frac{\gamma l}{2}) \approx \frac{1}{Z_c} \frac{\gamma l}{2} \approx \frac{\gamma l}{2} = \frac{Y}{2} \tag{2.24}$$

2.6 Transformer Modeling

A transformer is an electrical device that takes electricity of one voltage and changes it into another voltage [14]. They are used to change voltage levels as well as to control to the voltage and reactive power flow. It works on the principle of electromagnetic induction typically where, the primary is connected to a voltage supply and converts it into a magnetic field and the secondary then converts the alternating magnetic field into electric power with

the required voltage level based on the number of windings in the coils. The equivalent circuit diagram of a two-winding transformer is shown below in Figure 2.6

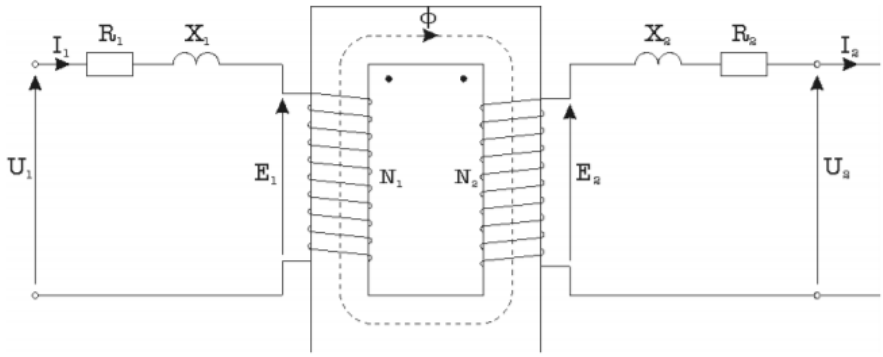

Figure 2.6: Diagram of 2-winding transformer

R_1 and R_2 represent the primary and secondary winding resistance and X_1 and X_2 represent the primary and secondary winding leakage reactance respectively. Number of turns in the primary and secondary are n_1 and n_2.

The voltage at the primary and secondary side is represented as given below,

$$\bar{v}_1 = Z_1\bar{i}_1 + \frac{n_1}{n_2}\bar{v}_2 - \frac{n_1}{n_2}Z_2\bar{i}_2 \tag{2.25}$$

$$\bar{v}_2 = \frac{n_2}{n_1}\bar{v}_1 - \frac{n_2}{n_1}Z_1\bar{i}_1 + Z_2\bar{i}_2 \tag{2.26}$$

If we consider the nominal values, the above equation is represented as given below,

$$\bar{v}_1 = (\frac{n_1}{n_{1o}})^2 Z_{1o}\bar{i}_1 + \frac{n_1}{n_2}\bar{v}_2 - \frac{n_1}{n_2}(\frac{n_2}{n_{2o}})^2 Z_{2o}\bar{i}_2 \tag{2.27}$$

$$\bar{v}_2 = \frac{n_2}{n_1}\bar{v}_1 - \frac{n_2}{n_1}(\frac{n_1}{n_{1o}})^2 Z_{1o}\bar{i}_1 + (\frac{n_2}{n_{2o}})^2 Z_{2o}\bar{i}_2 \tag{2.28}$$

Z_{1o} and Z_{2o} represent the primary and secondary tap position whereas n_{1o} and n_{2o} represent the primary and secondary number of turns.

The per unit representation of the voltage equations are as seen below,

$$\bar{v}_1 = \bar{n}_1^2 \bar{Z}_{1o}\bar{i}_1 + \frac{\bar{n}_1}{\bar{n}_2}\bar{v}_2 - \bar{n}_2^2\frac{\bar{n}_1}{\bar{n}_2}\bar{Z}_{2o}\bar{i}_2 \tag{2.29}$$

$$\bar{v}_2 = \frac{\bar{n}_2}{\bar{n}_1}\bar{v}_1 - \bar{n}_1^2\frac{\bar{n}_2}{\bar{n}_1}\bar{Z}_{1o}\bar{i}_1 + \bar{n}_2^2\bar{Z}_{2o}\bar{i}_2 \tag{2.30}$$

where,

$$\bar{n}_1 = \frac{n_1}{n_{1o}} \tag{2.31}$$

$$\bar{n}_2 = \frac{n_2}{n_{2o}} \tag{2.32}$$

Transformer Losses:

The transformer losses mainly comprise of winding and core losses. As the transformer capacity increases, the transformer efficiency tend to increase. Transformers consists of only electrical losses.

Core Losses : Core losses or iron losses depend on the magnetic properties of the material used for the core. Core loss comprises of Hysteresis loss and Eddy current loss. Hysteresis loss is due to the reversal of magnetization in the core and is given by,

$$W_h = \eta {B_{max}}^{1.6} f V \tag{2.33}$$

It can be seen the loss depends on the flux density, B_{max}, Volume, V, frequency of magnetic reversals, f. η is Steinmetz hysteresis constant.

The eddy currents formed due to the induced emf in the core or iron body of the transformer causes the eddy current loss. The eddy currents dissipate energy in the form of heat.

Copper Loss : Copper loss is caused because of the resistance of the transformer windings. Copper loss in transformer varies with the load. Copper loss due to the primary is ${I_1}^2 R_1$ and secondary winding is ${I_2}^2 R_2$. Where, I is the current and R is the resistance and 1 and 2 represent the primary and secondary respectively.

2.7 Load Modeling

A load is a device that is connected to a power system network that consumes power. Load models represents the mathematical relationship between voltage and power. The voltage is the input and the power, which can be either active or reactive is the output of the model. Load models are used to analyze the stability of power systems such as steady state stability, transient stability, long-term and voltage control. There are different types of load models that depend on usage such Residential, commercial and industrial. Loads are very difficult to model as there will be a variation in the load depending on time and practically, there is no constant load. Loads can be motors, furnaces, appliances, lamps etc. There are different types of load modeling - static, dynamic or a combination of both [15].

Static Load Models :

Static load models are models that represent the active and reactive powers as a function of the magnitude and/or frequency of voltage. There are different types of static load models. The

most common types are constant power, constant current, constant impedance, polynomial, exponential, slope values, frequency dependent.

Traditionally, the type of static load model used in the exponential load model which is shown in Equation 2.34. It is a non-linear model in which the active and reactive power are related to voltage as an exponential equation. Here, np and nq are parameters of the load model.

$$P = P_O\left(\frac{V}{V_O}\right)^{n_p} \tag{2.34}$$

$$Q = Q_O\left(\frac{V}{V_O}\right)^{n_q} \tag{2.35}$$

Constant power, constant current and constant impendance models are special cases of the exponential model.

Constant power load models are models in which the active and reactive powers are a constant and are independent of the change in voltage. The models can be represented as given below,

$$P = P_O\left(\frac{V}{V_O}\right)^{0} = P_O \tag{2.36}$$

$$Q = Q_O\left(\frac{V}{V_O}\right)^{0} = Q_O \tag{2.37}$$

Here, $n_p = n_q = 0$. Similarly, $n_p = n_q = 1$ for constant current models and $n_p = n_q$ =2 for constant impedance models.

Dynamic Load Models :

The importance of load models has increased during the last decade. It represents the time

and voltage dependence of load. The modeling of dynamic load models is required to study internal oscillations, stability of voltage and long-term stability analysis. The most commonly used load models are Induction motor model, state space model and the transfer function model.

An equivalent circuit diagram of the induction motor load model is shown in Figure 2.7. A considerable part of loads consists of induction motors.

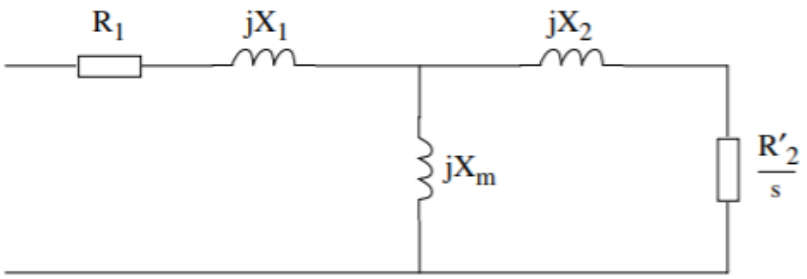

Figure 2.7: Circuit Diagram of Induction motor load model

The per unit change in speed that represents the induction motor load model is given by,

$$\Delta\omega = \frac{1}{2Hs}(\Delta T_a - D\Delta\omega) \tag{2.38}$$

ΔT_a represents the accelerating torque, T_e and T_m are the electrical and mechanical torques, D is the mechanical damping and H is the motor and drive inertia.

Chapter 3

Main Focus and Contribution

3.1 Introduction

The focus of this thesis is to use automation to create appropriate models in PSS/E with the data from the field. This technique is used to find the parameters of an SVC in PSS/E with the data from the Hardware-in-loop real-time simulation of the SVC physical controller using Hypersim.

Power system planning is an important aspect in transmission for every utility and transient stability analysis tools such as PSS/E are most commonly used. It is necessary to make the models in use as accurate as possible and update them regularly. Python programming language is used to find the parameters of the SVC model in PSS/E in a fast and efficient manner. This process ensures that the SVC model in PSS/E behaves similar to the actual SVC which is represented by the SVC physical controller.

3.1.1 Hypersim

Hypersim is the most advanced system which can simulate over 1000 3-phase buses in real-time with high precision to study 3-phase electro-magnetic and electro-mechanical transients and complex events which involves interaction between several controls, protection, HVDC and

FACTS System. It is known as the power system simulator of tomorrow with a proven track record and constant updating to increase its performance, reliability and ease of use. Real-time simulation enables execution at the same pace as real-world clock. This property allows the availability of Rapid Control Prototyping (RCP) and Hardware-in-the-loop simulation [31].

3.1.2 SVC Physical Controller

The SVC physical controller or replica is an exact copy of the actual control cubicles installed on the site. The SVC physical controller in the study is a 0/+300 Mvar SVC with 3 TSC units. 2 TSCs are three-phase Y configuration and provides 75 Mvar whereas the third TSC is delta configuration and provides 150 Mvar.

3.1.3 PSS/E

Power System Simulation for Engineering (PSS/E) is a transient stability analysis tool which is widely used for planning of and analysis of power system networks. PSS/E is composed of a comprehensive set of programs for studies of power system transmission network and generation performance in both steady-state and dynamic conditions. PSS/E offers the ability to drive itself from batch scripts using IPLAN, IDEV, and Python where IPLAN and IDEV are PSS/E specific batch scripts. From its introduction in 1976, PSS/E has offered comprehensive modeling capabilities.

3.2 Methodology

The methodology of this thesis is to find the parameters of the SVC model in PSS/E to achieve results similar to that of the results with the SVC physical controller HIL simulation in Hypersim. There are parameters that are unique to the SVC such as active range of voltage control loop, size of reactor etc and depends on the design of the SVC needed to be modeled. The methodology followed in this thesis can be divided into two parts analysis before the addition of the SVC and analysis after the addition of the SVC model and parameter manipulation. Analysis of the system before the addition of the SVC is important as this step is required to reduce the difference between the two software platforms in-order to clearly analyze the response of the SVC. It includes the steady state analysis and the dynamics analysis. This forms the base for the rest of the analysis conducted in the thesis. The generation of the test matrix can be seen in the test system chapter and explains the selection of test cases. The system is subject to different network disturbances with the addition of different network elements. This helps us select locations for the SVC that show the least difference between the two software platforms. Analysis after the addition of SVC involves applying different three phase bus faults and analyzing the dynamic response of the SVC model in PSS/E against the SVC physical controller. The parameter manipulation automation technique is then used to find the right set of parameters for the SVC model in PSS/E and make its response similar to that of the SVC physical controller. The methodology followed can be seen in the following sections with their flow charts.

3.2.1 Before addition of SVC

3.2.1.1 Steady State Analysis

Steady state studies are restrained to small and gradual changes in the system operating conditions. It concentrates on restricting the bus voltages to their nominal values and to make sure that the difference between the bus phase angles between are not too large and analyzes the overloading power of equipment and transmission lines. This analysis is done with the use of power flow calculations. The power flow analysis applies to the balanced, steady-state operation of the power system and deals with positive-sequence models of all system components.

The basic data required for power flow calculations such as line impedances and charging admittances, transformer impedances and tap ratios, admittances of shunt connected devices such as capacitors and reactors, load consumption at each bus, power output and voltage magnitude of each generator along with its maximum and minimum reactive power outputs are entered into the system models in Hypersim with modeling of single line diagram of the test system and/or as raw data in the case of PSS/E. The load flow is calculated and the results are analyzed. If the results match, we move on to the next phase or we are required to make changes to the parameters of the network elements such that the power flow results are similar. This forms the basis of our study as the dynamic analysis is dependent on this.

The IEEE 14 bus system is considered as the test system with the test data shown in Chapter 4. The data is assigned to the models in PSS/E and Hypersim and the Newton Raphson load flow analysis is performed. The results such as voltages, line and transformer

currents are compared. In our study, the comparison yielded matching results and did not need any modifications to the parameters - they are shown in chapter 5.

3.2.1.2 Dynamic Analysis

The power flow model is taken as the base case for the dynamic analysis studies. Hypersim has the ability to run dynamics and generate results with static voltage sources whereas PSS/E cannot do so without a dynamic element. Therefore, a dynamic element needs to be added in PSS/E with its appropriate parameters. The dynamic model of a generator is considered here in this thesis.

The generator dynamic model includes the rotor model, excitation system model, governor model and stabilizer model. The response of the governor and stabilizer models to electromagnetic transients are slow and hence only the rotor model and exciter models are included. For this study, it is necessary to reduce the system dynamics to reduce the differences between the two software packages.

A near-ideal voltage source is modeled in PSS/E using GENCLS generator and SEXS exciter models whereas an ideal voltage source is used in Hypersim. The GENCLS generator model is a constant internal voltage and the SEXS excitation system model is a simplified excitation systems offered by PSS/E. Parameters are assigned to the models and dynamic analysis is performed on both the elements.

The generator and exciter models are first tried and analyzed on a three-bus system by assigning parameters to the models. A three-phase bus fault is applied at Bus-2 and the results are analyzed. The windowed rms values of the bus voltages are plotted for the analysis. The 3-bus system modeled is shown in Figure 3.1 and the results can be seen in Figure 3.2.

Once a near-ideal source was modeled in the 3 bus system, the model was used in the 14 bus system of our concern. The near ideal voltage source was fine-tuned with the help of the parameter manipulation script which is explained in the following sections and parameters were chosen based on the least error function value to reduce differences between the test systems.

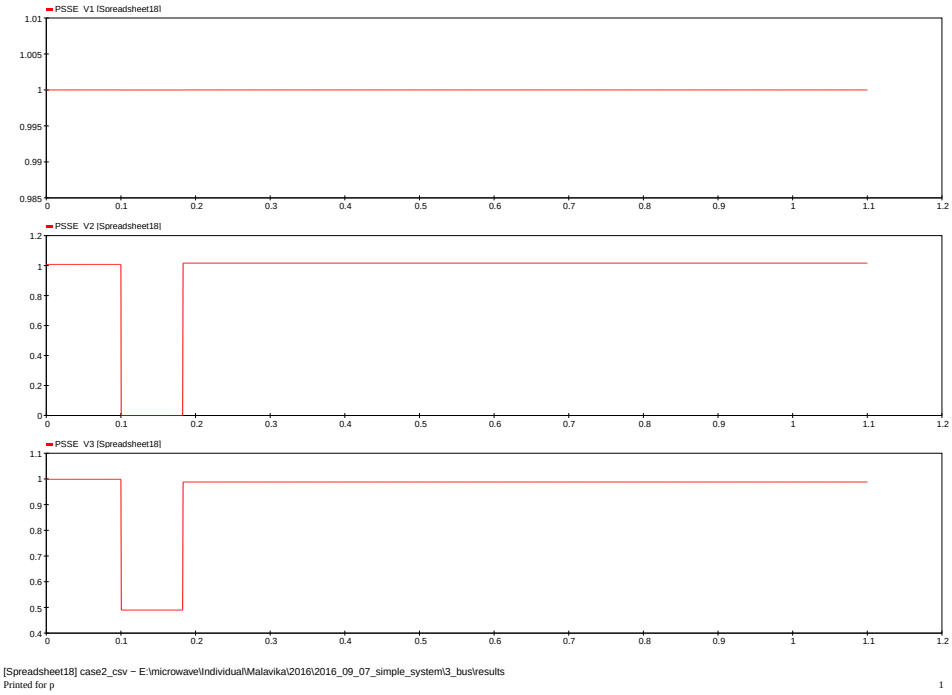

Figure 3.1: 3-Bus Test System

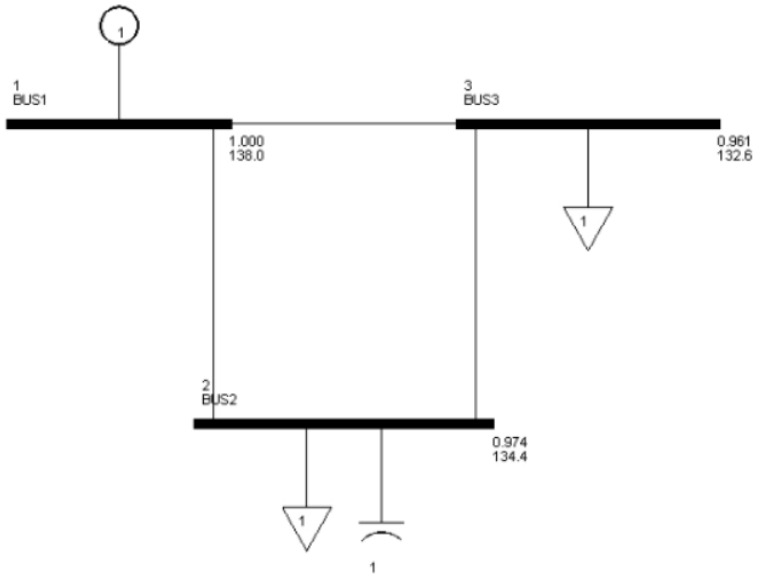

Figure 3.2: 3-Bus Test System Voltages with Fault at Bus-2

A three-phase bus fault is applied on different buses of the test system. Faults are not applied on buses 1 and 2 since they are generator buses as well as bus 8 as it results in the isolation of the bus from the system and does not produce a desirable response. This consideration is taken throughout this thesis. The three phase fault is applied on buses 3,4,5,6,7,9,10,11,12,13 and 14 , after a certain period of time the faults are cleared along with the removal of a transmission line connected to the particular bus. The bus voltages of the 14 buses from PSS/E and Hypersim are compared and plotted against each other.

To clearly understand the extent of similarity between the two software packages, an error function is used. The method to find the error function and the corresponding equations used are seen in the section 3.3. The application of the three-phase bus fault is taken as base case. The test system is then subject to the addition of a shunt capacitor of capacitance 18 MVar

and 45MVar along with the application of bus fault in both software platforms. The addition of a circuit element forms case 1 and case 2 respectively. Capacitors were chosen as the extra circuit element as it injects MVar similar to TSC units in the SVC. All the 14 bus voltages in all three cases were compared against each other. The capacitors are placed on all buses except the generator buses. This led to 132 cases with 14 bus voltages for each case. The error function was used to calculate the extent of difference between the 3 cases in PSS/E and Hypersim. For a bus voltage for a particular fault scenario, if the error of bus voltage was found to be less than 0.05 pu% in all three cases, then the bus was a viable location for the SVC. This process was followed in all 132 cases and a test matrix was created with the optimal location for SVC with the appropriate fault scenario. This method allows us to find locations which show least variation in both software platforms when the test system is subject to different network disturbances and changes. When the SVC model or Physical controller are placed in these locations, their responses can be analyzed easily.

3.2.2 After addition of SVC

Once the optimal placement of the SVC is determined and a test matrix is created, the simulations are run to find the right parameters and analyze the response of the SVC model in PSS/E against the HIL simulation of the SVC physical controller in Hypersim. A range of values are assigned to each parameter from which a parameter set is created for each iteration and assigned to the SVC.The SVC is then placed at different locations and three phase bus faults are applied to analyze the dynamic response in both software packages. The 14 bus voltages were compared against each-other by plotting their responses for a visual analysis as

well as the use of the error function for a measurable analysis. The parameters which result in least error is chosen as the desired set.

The result of the real-time Hypersim HIL simulation with the SVC physical controller is considered accurate and taken as the reference. The PSS/E offers a couple of models to represent Static Var Devices. Figure 3.3 shows a general block diagram of the controlled reactor model in PSS/E which characterizes a controlled reactor approximated by a single time constant and limits which relates the fundamental frequency admittance to the output signal of the control unit [28].

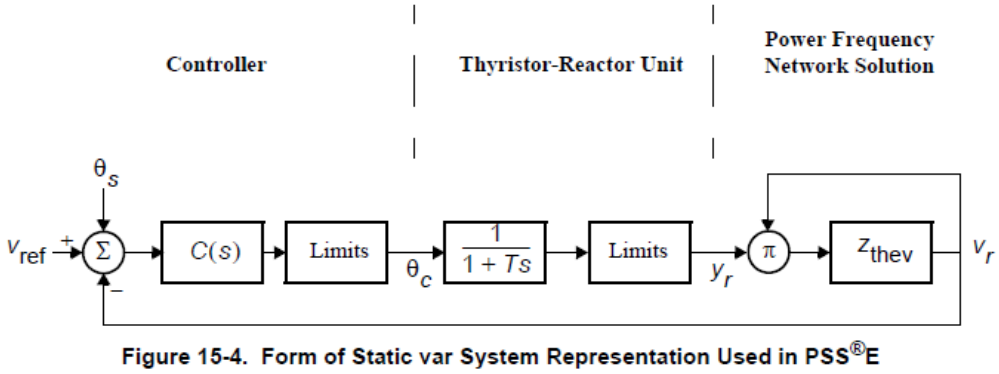

Figure 15-4. Form of Static var System Representation Used in PSS®E

Figure 3.3: General form of reactor models [28]

The model used in this thesis to represent the SVC physical controller in use is the CSVGN3 which can be seen IN Figure 3.4. It represents a Silicon-Controlled Rectifier (SCR) controlled shunt reactor along with a parallel capacitor. The voltage error which is the difference between the input voltage and the reference voltage (V_{REF}) and/or the auxiliary voltage (VOTHSG) controls the SCR gate. C_{BASE} specifies the size of the capacitor, V_{MAX} and V_{MIN} specify the active range of the voltage control loop, R_{MIN} is the effective reactive

admittance of the reactor. T_5 is the time constant that allows an approximation of delays in the reactors response to control signals, transient gain reduction is represented by T_1 through T_4 and K is the steady state voltage control gain. Parameters such as Vref, Rmin, Cbase are specific to a particular SVC and cannot be varied. The fine-tuning of this SVC model is done by the varying the parameters K and T1 through T5.

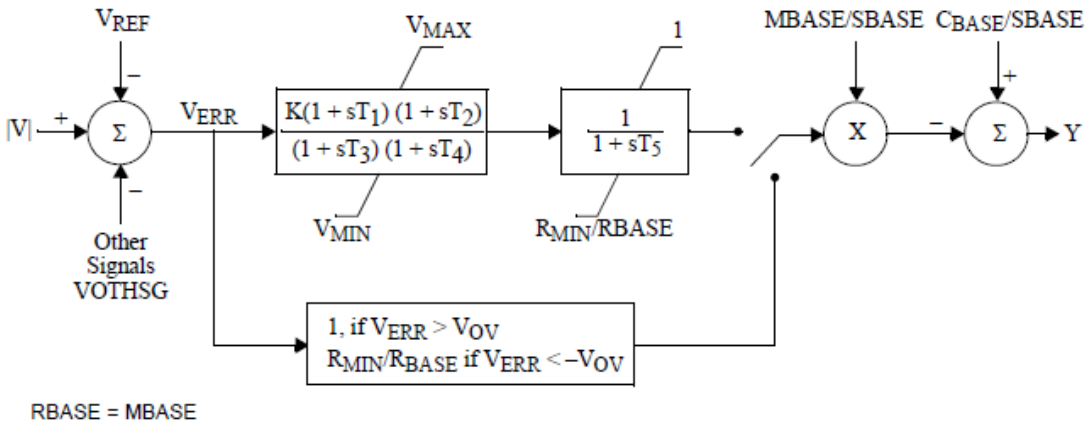

Figure 3.4: CSVGN3 model [27]

3.3 Automation Process

PSS/E offers the ability to drive itself from batch scripts using IPLAN, IDEV, and Python. IPLAN and IDEV are PSS/E specific batch scripts. The PSS/E Application Program Interface (API) document defines the application interface to various engineering functions in PSS/E. It consists of the function explanation of the API routine, along with the syntax for calling the routine in different languages and a detailed explanation of the arguments used in the functions. This document was used to understand automation of PSS/E with python. In

this thesis, Python is used to automate the dynamics process in PSS/E and then take the data and results to find the error and plot the voltage waveforms. Python has the ability to run hundreds of different PSS/E simulations for a given network which is much faster than executing PSS/E itself [29]. Figure 3.5 shows the flow chart for the automation process of running dynamics in PSS/E.

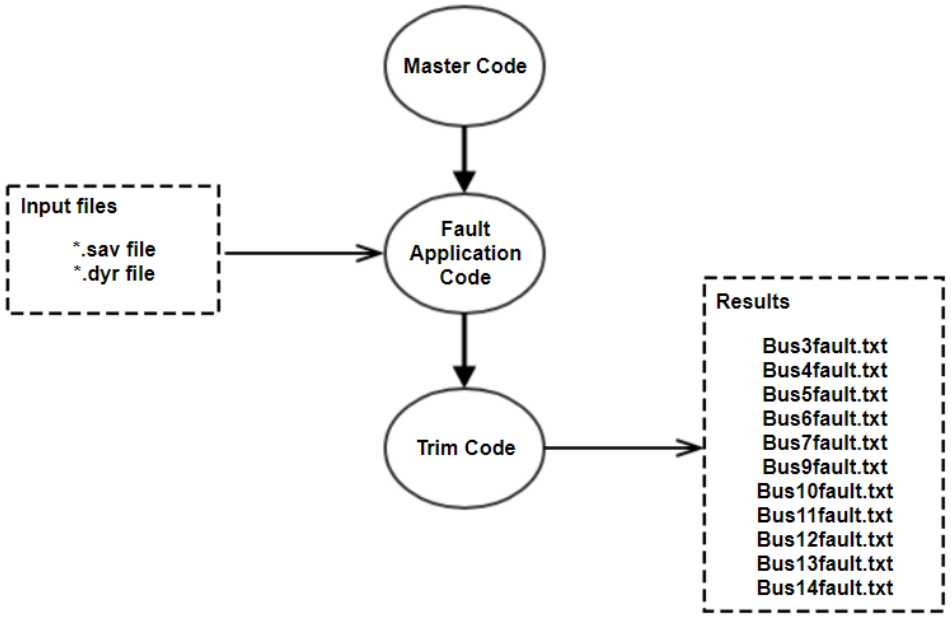

Figure 3.5: Flow chart of PSS/E automation

The master code specifies all the buses at which faults need to be applied and the corresponding lines that need to be disconnected after the removal of the fault. This enables us to run all the necessary bus faults for a particular scenario or choose the faults that the study requires. The master code is also used to call the rest of the python files needed to perform the operations for the three phase faults as well as extract and use the results for the error function.

Once the master code chooses the first fault scenario, the fault application code is called which takes the *.sav file (saved case file) and the *.dyr file (dynamics data file) along with the bus fault location and line to be removed. The loadflow function performs the Full Newton-Raphson method (FNSL) to solve the load flow of the case. The convertlf function performs the fixed slope decoupled Newton-Raphson power flow calculation (FDNS), converts generators from power flow representation to prepare for dynamic studies (CONG), calculates sparsity preserving ordering of buses for processing of network matrices (ORDR),factorizes the network admittance matrix (FACT), and runs the switching study network solutions (TYSL).The crtsnap function performs the operations which modifies the network solution parameters, performs CONG, ORDR, FACT, TYSL and generates the conec, conet and compile file. The tstep function performs the operations which again performs the CONG, ORDR, FACT & TYSL and starts the process for fault application with a specified time step. It specifies the time at which the bus fault is applied and its duration. It runs the case (steady-state) for a specified amount of time (psspy.run()) and then applies a very large negative shunt impedance on a given bus (psspy.shunt data) for another specified duration. A transmission line is then disconnected (psspy.branch data()) and the bus fault is removed. The shunt impedance (if present in the bus) is re-attached to the bus (psspy.shunt data()). The duration of the entire simulation is also specified. A case.out file is generated at the end of the simulation.The assign_channels function assigns all the channels that is included in the case.out file. It includes the Mvar output of the SVC (psspy.machine array channel) and all the voltages of the 14 buses (psspy.voltage channel). Save_txt function then converts the case.out file into a text file. All the functions are called in the order of the function explanations.

The trim code helps modify the data in to a usable format for plotting and data manipulation. The data contains the voltage and Mvar values and the corresponding time throughout simulation run. This is the process used to run the dynamic simulation in PSS/E with Python.

The results obtained from PSS/E then need to be compared against the already available Hypersim results. Since there are no changes made to the parameters in Hypersim, the results always remain the same and are accessed when needed. The comparison process starts with finding the error function value. The Mvar and voltage data from both software platforms are linearly interpolated into a common time frame. For each bus fault, the absolute values of the difference between the interpolated values of Hypersim and PSS/E are added together and averaged by the total number of values taken during the difference calculation. The error function which is the error in terms of parameters, the total error by bus faults are taken and averaged by the number of bus faults. These errors have a unit of per unit percent. Equation 3.1 represents the error difference for each bus fault and Equation 3.2 represents the error difference for a set of parameters.

$$(Error\_by\_bus\_fault)_B = \frac{\sum_1^N |V_{PSS/E}(t) - V_{Hypersim}(t)|}{N} \times 100 \tag{3.1}$$

$$(Error\_by\_parameters) = \frac{\sum_1^B (Error\_by\_bus\_fault)}{B} \tag{3.2}$$

In Equation 3.1 and Equation 3.2 B represents the number of bus faults and N represents the number of voltage points taken for the difference calculation. These errors are then tabulated in ascending order along with the corresponding parameters for easy analysis of the results. The error function is expressed in percent per unit or pcu.

Once the basic process of running dynamics was automated, the parameter manipulation process is then inserted in the initial stages before running the dynamics. The dynamic data is imported via the dynamic data file (*.dyr) into PSS/E. In this study, it includes the generator dynamic parameters and the SVC dynamic parameters. The template code enables us to enter a set of values for each parameter as an array. The code would take values one by one and create a dynamics data file each time which will be given as an input while running the dynamics. Each time the dynamics is run with a new dynamics data file in PSS/E, the results are then taken and the comparison is made with the results from Hypersim to generate the error table as well as plots for visual analysis.The flow chart that corresponds to the automation process followed in this study can be seen in Figure 3.6

The responses of the SVC model in PSS/E is analyzed for different values of a parameter. Parameters K, T_1, T_2, T_3, T_4 and T_5 are studied to see its effect on this SVC model. Three different values are taken for each parameter and the Mvar output of the SVC model is analyzed.

Figure 3.7 - Figure 3.12 show that all the parameters have an effect on the transients in the pre-fault and post-fault cases when varied individually.

In-order to find the parameters of the SVC, the first step involves varying the parameters individually and then move on to varying the parameters simultaneously.

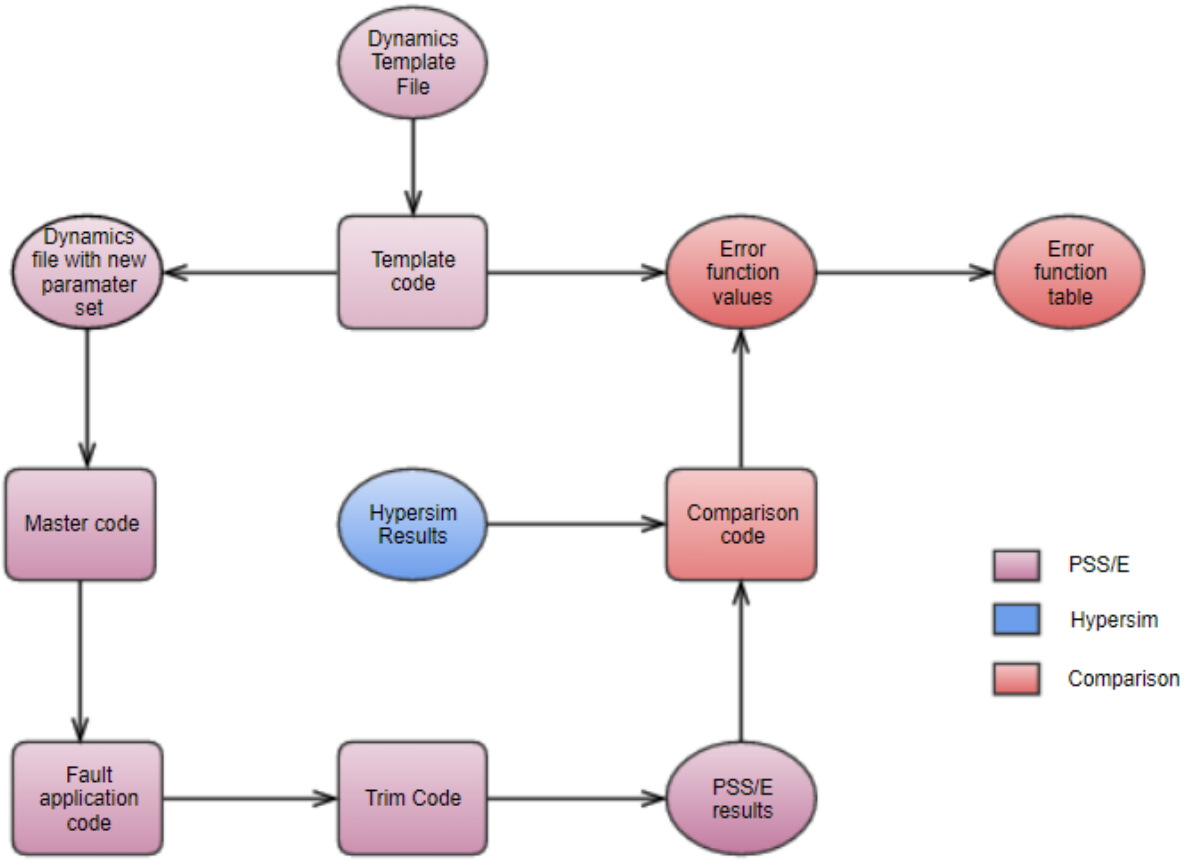

Figure 3.6: Flow chart of complete automation process

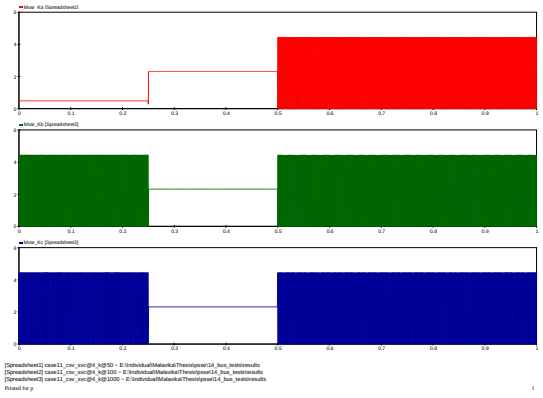

Figure 3.7: Variation of K ; Mvar output of SVC Model with respect to time

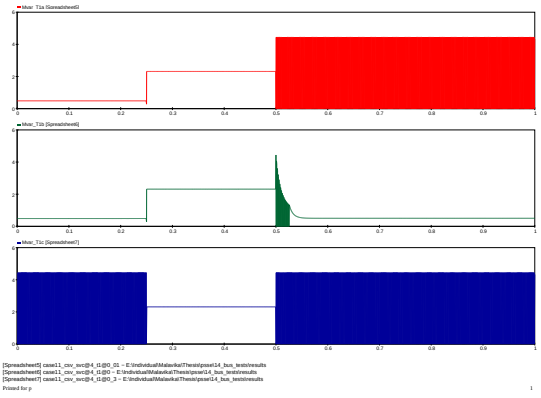

Figure 3.8: Variation of T_1 ; Mvar output of SVC Model

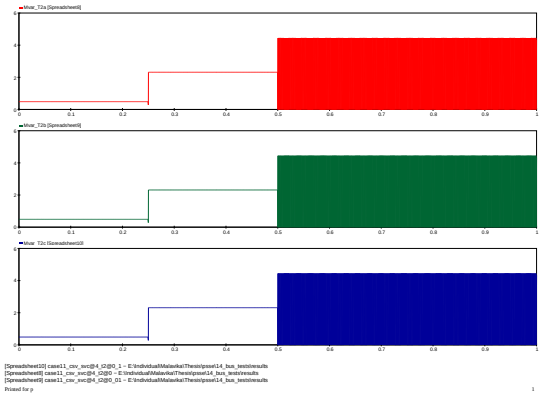

Figure 3.9: Variation of T_2 ; Mvar output of SVC Model with respect to time

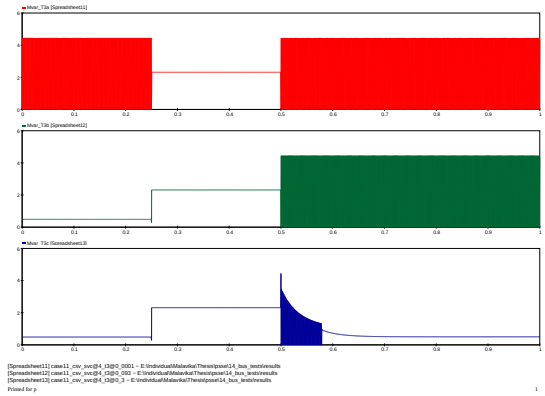

Figure 3.10: Variation of T_3 ; Mvar output of SVC Model

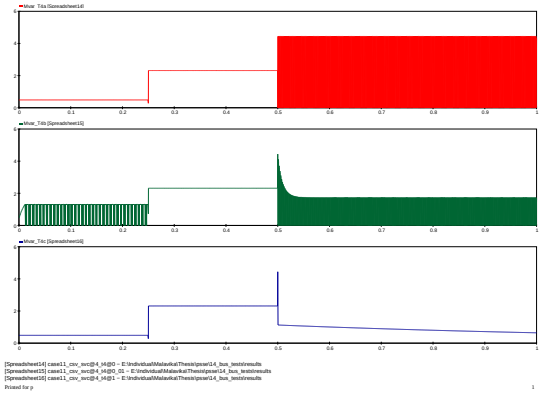

Figure 3.11: Variation of T_4 ; Mvar output of SVC Model with respect to time

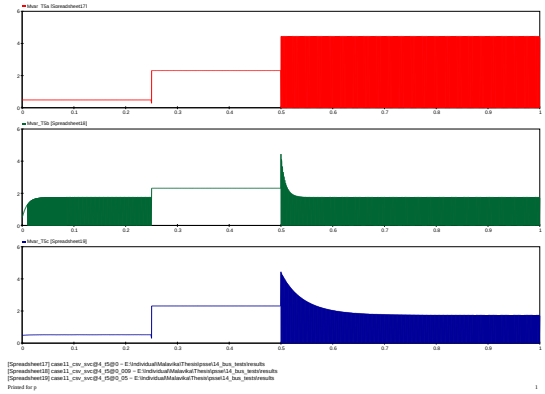

Figure 3.12: Variation of T_5 ; Mvar output of SVC Model

Chapter 4

Test System

4.1 Introduction

This thesis uses the IEEE 14 bus system as the test system. The standard IEEE 14 bus test case represents a portion of the American Electric Power System (in the Midwestern US) as of February, 1962. The system consists of 14 buses, 5 synchronous machines, 3 of which are synchronous compensators and 11 loads. It has a shunt capacitor and a total of 3 transformers of which, 2 are two-winding transformers and 1 is a three-winding transformer. For simplicity, we consider a two-winding equivalent of the three-winding transformer which leads to a total of 18 transmission lines. The total load of the system is 254 MW and 73.5 Mvar and has a base voltage of 138 kV with a 100 MVA base power. The basis of this thesis involves the comparison of the transient stability software, PSS/E against the real-time software, Hypersim. Th difference are reduced by reducing the system dynamics and hence the synchronous generators are replaced by near-ideal generators or ideal voltage sources. The voltage sources are placed on Bus 1 and Bus 2 with Bus 1 considered as the slack bus. The test system can be seen in Figure 4.1.

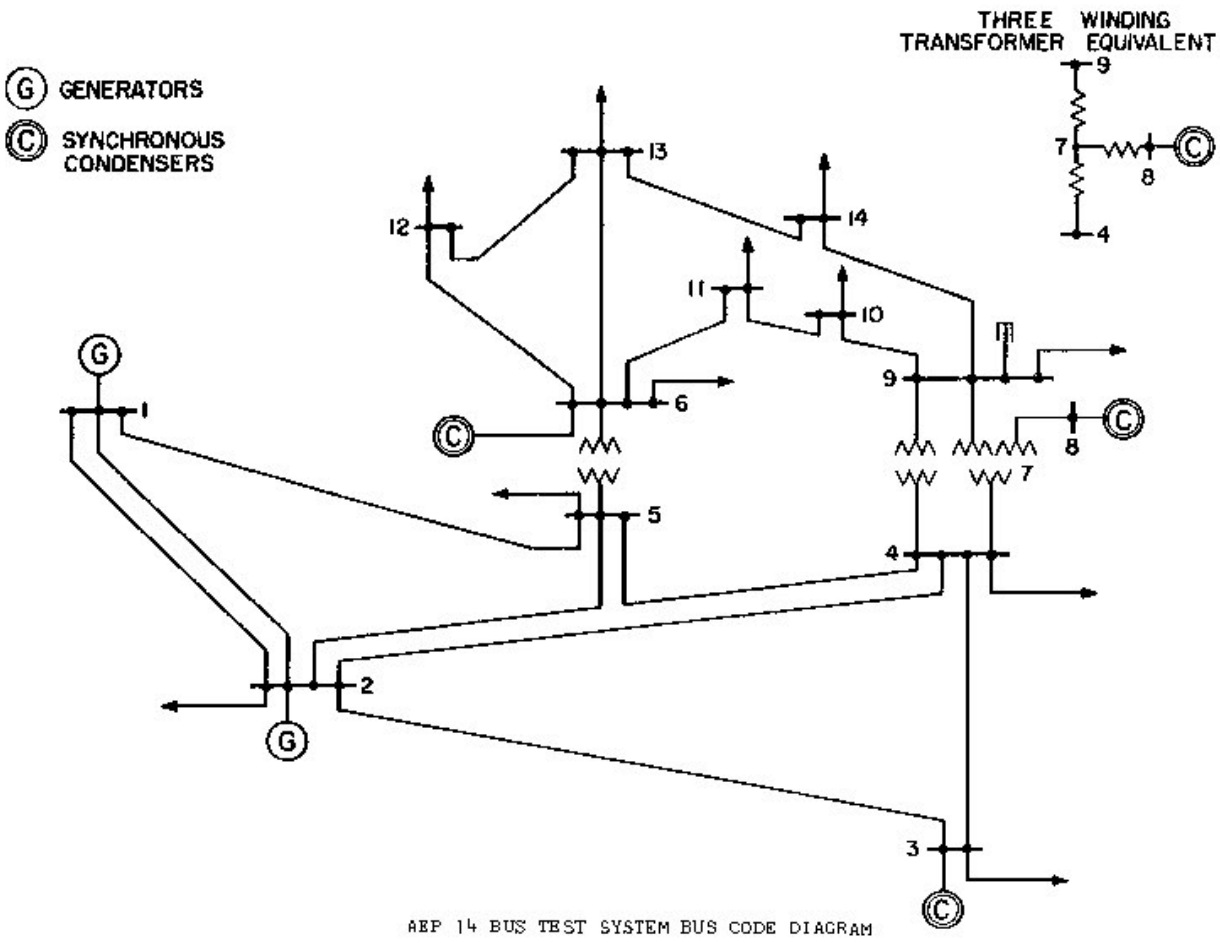

Figure 4.1: IEEE 14 Bus Test System [2]

4.2 Bus Data

The bus data consists of the bus voltage and the bus angles. The initial values of the voltage in pu and the angle in pu can be seen in Table 4.1. The pu representation of the bus voltages use a 100 MVA base value along with the voltage base of 138kV. The voltage sources are placed on Bus 1 and Bus 2. Bus 1 is considered as the slack bus which makes Bus 2 the PV bus. All other buses 3-14 are PQ buses.

Table 4.1: Bus Data

Bus	Base Voltage (kV)	Voltage (pu)	Angle (Deg)
1	138	1.06000	0.0000
2	138	1.04500	-4.9826
3	138	1.01000	-12.7250
4	138	1.01767	-10.3128
5	138	1.01951	-8.7738
6	138	1.07000	-14.2209
7	138	1.06152	-13.3596
8	138	1.09000	-13.3596
9	138	1.05593	-14.9385
10	138	1.05099	-15.0972
11	138	1.05691	-14.7906
12	138	1.05591	-15.0755
13	138	1.05038	-15.1562
14	138	1.03553	-16.0336

4.3 Transmission lines

Parameters such as resistance, inductance, capacitance and conductance helps in the modelling of transmission lines. These parameters form the line impedance and the line admittance (susceptance) and are dependent on the type of conductor used and the length of the transmission line. Table 4.2 shows the transmission line parameters for the 17 lines in the 14-bus system. In this study, all transmission lines are considered as π lines and the double line between Bus 1 and Bus 2 is replaced by a single transmission line.

Table 4.2: Transmission Line Parameters

Bus	Resistance (pu)	Reactance (pu)	Suceptance (pu)
1 to 2	0.01938	0.05917	0.05280
1 to 5	0.05403	0.22304	0.04920
2 to 3	0.04699	0.19797	0.04380
2 to 4	0.05811	0.17632	0.03400
2 to 5	0.05695	0.17388	0.03460
3 to 4	0.06701	0.17103	0.01280
4 to 5	0.01335	0.04211	0.00000
6 to 11	0.09498	0.19890	0.00000
6 to 12	0.12291	0.25581	0.00000
6 to 13	0.06615	0.13027	0.00000
7 to 8	0.00000	0.17615	0.00000
7 to 9	0.00000	0.11001	0.00000
9 to 10	0.03181	0.08450	0.00000
9 to 14	0.12711	0.27038	0.00000
10 to 11	0.08205	0.19207	0.00000
12 to 13	0.22092	0.19988	0.00000
13 to 14	0.17093	0.34802	0.00000

4.4 Transformer data

The system has 3 two-winding transformers with the modification of the three-winding transformer to a two-winding one. The parameters such as reactance and ratio used for the transformers are shown in Table 4.3.

Table 4.3: Transformer Parameters

Bus	Reactance (pu)	Ratio (pu)
4 to 7	0.20912	0.978
4 to 9	0.55618	0.969
5 to 6	0.25202	0.932

4.5 Load data

There are 11 loads in the 14-bus system and have been modelled as PQ loads in this study. The load parameters are the active power in MW and reactive power in MVar drawn by the loads. The parameters taken for the study can be seen in Table 4.4.

Table 4.4: Load Parameters

Bus	Pload (MW)	Qload (MVar)
2	21.700	12.700
3	94.200	19.000
4	47.800	-3.900
5	7.600	1.600
6	11.200	7.500
9	29.500	16.600
10	9.000	5.800
11	3.500	1.800
12	6.100	1.600
13	13.500	5.800
14	14.900	5.000

4.6 Generator / Voltage Source

There are two synchronous generators in the standard IEEE 14 bus system. The generator connected to Bus 1 is the slack bus and makes up for the difference between the demand and the generated power caused by the system losses. The initial load flow parameters of the two generators are seen in Table 4.5. These parameters are only sufficient to run load flow and perform steady state analysis. For dynamic analysis, to study transient and sub-transient response, a more detailed set of parameters need to be included to the model.

Table 4.5: Generator Parameters

Bus	Base (MVA)	PGen (MW)	QGen (MVar)	QMax (MVar)	QMin (MVar)	VSch (pu)
1	615	232.392	-16.549	0.000	0.000	1.060
2	60	40.000	43.556	50.000	-40.000	1.045

These parameters are included in the dynamics data file (*.dyr) and can be seen below in Table 4.6 and Table 4.7.

Table 4.6: Generator (GENCLS) Dynamic Parameters

Parameter	Value (pu)
H	0.05
D	0.005

Table 4.7: Exciter (SEXS) Parameters

Parameter	Value
T_A/T_B	0.001
T_B	0.10
K	0.50
T_E	0.01
E_{MIN}	0
E_{MAX}	1

4.7 Synchronous Condensers and Shunt Elements

The IEEE 14 bus system has three synchronous condensers. Synchronous condensers are generators with no active power generation, i.e, Pgen = 0 MW which can be seen in Table 4.8. The synchronous condensers are converted to shunt capacitors for easy analysis and to reduce

the system dynamics. The system contains only one shunt element. This shunt capacitor is a

Table 4.8: Synchronous Condensers

Bus	Base (MVA)	PGen (MW)	QGen (MVar)	QMax (MVar)	QMin (MVar)	VSch (pu)
3	60	0.000	25.075	40.000	0.000	1.010
6	25	0.000	12.730	24.000	-6.000	1.070
8	25	0.000	17.623	24.000	-6.000	1.090

fixed capacitor placed at Bus 9 with a fixed reactive power generation of 19 MVar.

4.8 Static Var Compensators

The static Var Compensator can be represented either as a switched shunt or a generator to run power flow and dynamics in PSS/E. The SVC physical controller taken into consideration is a 0/+300 MVar SVC with Thyrsitor Switched Capacitors (TSC). In this study, we represent the model as a generator. The initial load flow parameters that are used for the SVC is seen in *******.

Table 4.9: SVC Parameters

Base (MVA)	PGen (MW)	QGen (MVar)	QMax (MVar)	QMin (MVar)	VSch (pu)
300	0.000	25.075	300.000	0.5	1.00

Similar to the generator modeling, the SVC required a detailed set of parameter to run dynamics which can be seen in Table 4.10. T_1 - T_5 depends on the time step of the simulation. An intial range of parameters are chosen based on the specifications given by PSS/E [28]. For simplicity, parameters such as R_{MIN}, V_{MAX}, V_{MIN}, C_{BASE}, V_{OV} are given constant values based on the design of the SVC

Table 4.10: SVC (CSVGN3) dynamic Parameters

Parameter	Value Range
K	> 50 and < 1000
T_1	<0.5
T_2	<0.5
T_3	<1=0.5
T_4	<0.5
T_5	< 0.05
R_{MIN}	Admittance of reactor
V_{MAX}	Maximum value of Voltage control loop
V_{MIN}	Minimum value of Voltage control loop
C_{BASE}	Size of capacitor < 500
V_{OV}	Over ride Voltage ≤ 0.5

Chapter 5

Analysis of Results

5.1 Introduction

For the analyzing the system in PSS/E against the HIL simulation of the system in Hypersim, the 14 bus voltages, Mvar output of the SVC and the transmission line currents were taken as the data for comparison. The fault is applied at 0.25 secs and cleared at 0.5 secs with a total run time of 1 sec.

5.2 Test Case Model

The modified IEEE 14 bus system modeled in PSS/E and Hypersim can be seen in Figure 5.1 and Figure 5.2. The test system in Hypersim displays the fault breakers for all scenarios of bus faults analyzed in this study. with the near-ideal voltage source and ideal voltage source. The test case was modeled with the control blocks present in the software with Graphical User Interface to enter the parameters in the case of Hypersim and as raw data in PSS/E which can later be used to generate the one-line diagram in PSS/E. For the dynamic analysis, built-in block for GENCLS and SEXS were present in PSS/E.

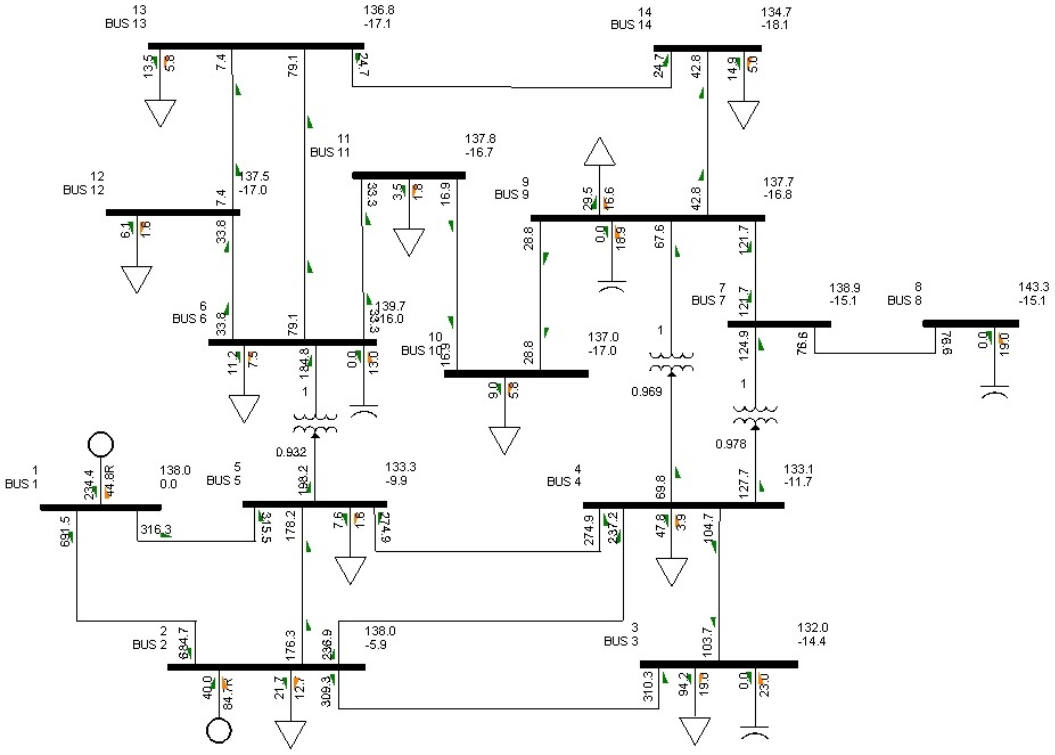

Figure 5.1: 14-bus Test System in PSS/E

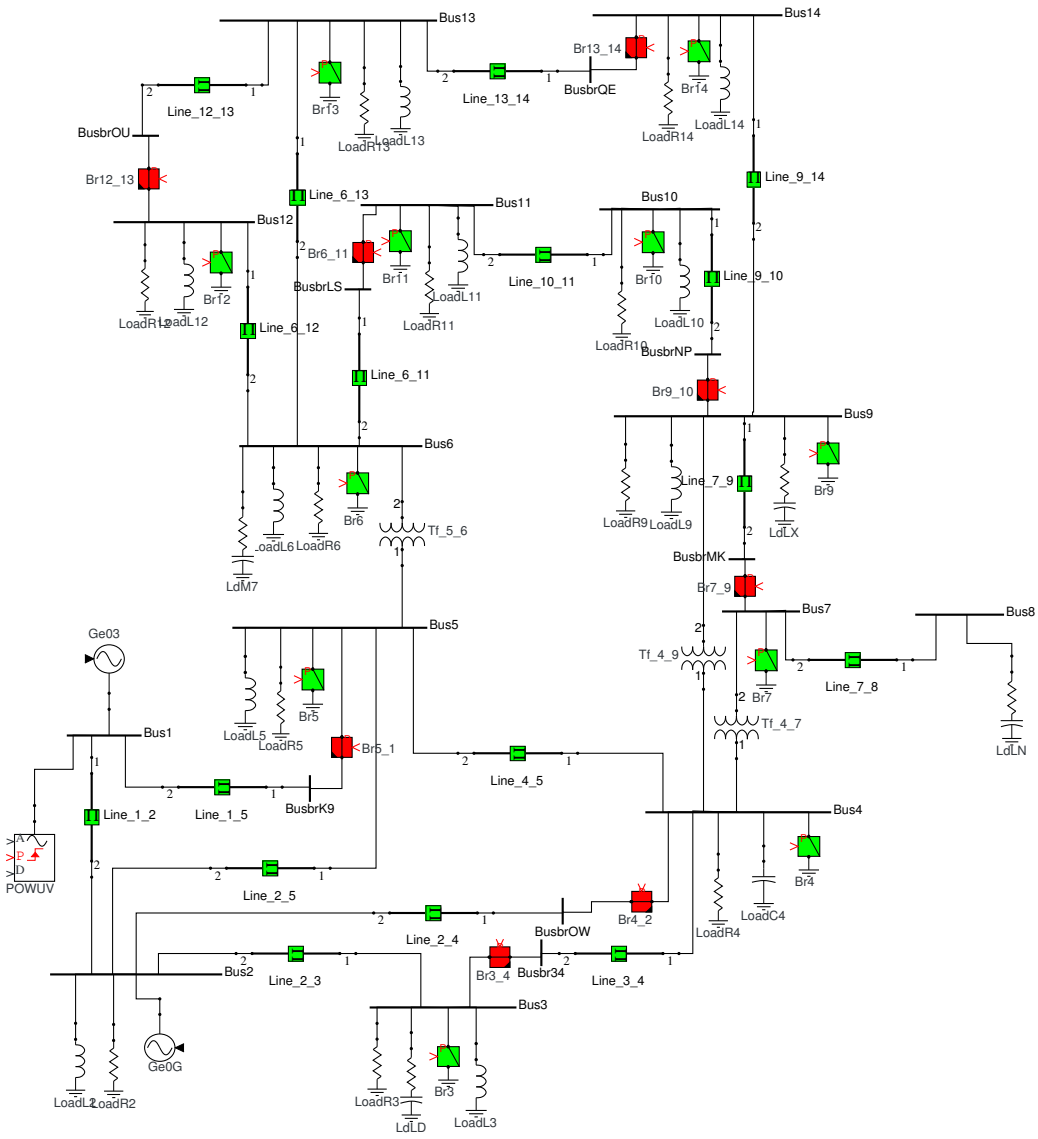

Figure 5.2: 14-bus Test System in Hypersim

5.3 Before addition of SVC

5.3.1 Steady State Analysis

The bus voltages and transmission line currents from PSS/E and Hypersim are taken into consideration for the comparison of steady state analysis. The power flow analysis is performed

	PSS/E		Hypersim	
Bus	$\|V\|$	$\angle\theta$	$\|V\|$	$\angle\theta$
1	138.00	0.00	138.00	0.00
2	138.00	−5.87	138.00	−6.08
3	132.04	−14.30	132.04	−14.73
4	133.18	−11.60	133.12	−12.21
5	133.31	−9.70	133.32	−10.23
6	139.65	−16.00	139.65	−16.23
7	138.87	−15.10	138.86	−15.61
8	143.32	−15.05	143.32	−15.49
9	137.53	−16.61	137.62	−17.30
10	137.00	−17.02	136.98	−17.54
11	137.77	−16.73	137.80	−16.88
12	137.45	−16.98	137.48	−17.35
13	136.80	−17.12	136.78	−17.43
14	134.66	−17.89	134.69	−18.98

Table 5.1: Voltages (kV RMS) compared between PSSE and Hypersim

using the Full Newton-Raphson method and the data is compared.

The differences between the two software platforms are analyzed and were found to be negligible to be considered. A similar study was done in [20] were the transformer currents were taken into account. Th results from our analysis were close to that if [20] The steady state data comparison led us to see that the two models responded similarly with negligible differences in steady state.

5.3.2 Dynamic Analysis

The test system in both software platforms are subject to three-phase bus faults along with the removal of a transmission line after the fault is cleared. The voltage waveform at all 14 buses are taken into consideration for the analysis. Figure 5.3 shows the voltage waveforms at all buses when a fault is applied at Bus-5 at 0.15 secs and cleared at 0.2 secs. The

Line	PSS/E	Hypersim
1 to 2	691.2	691.99
1 to 5	316.1	315.49
2 to 3	308.3	309.58
2 to 4	236.7	236.99
2 to 5	176.3	177.60
3 to 4	102.2	104.76
4 to 5	273.8	274.33
6 to 11	33.3	33.27
6 to 12	33.6	33.80
6 to 13	78.9	79.13
7 to 8	76.6	76.68
7 to 9	121.2	121.99
9 to 10	28.7	28.91
9 to 14	42.6	42.83
10 to 11	16.9	16.61
12 to 13	7.4	7.43
13 to 14	24.7	24.66

Table 5.2: Currents (A RMS) compared between PSSE and Hypersim

voltage waveforms from PSS/E and Hypersim are overlapped against eachother for a clear understanding.

The bus fault scenario can be split into three cases : Pre-fault, fault and Post-fault. The source voltage used in both the software are ideal or near-ideal source and hence there are no transients in either of the response during the pre-fault case. PSS/E always starts from steady state conditions irrespective of the source modeled. During fault, the response in both platforms are almost the same. The voltage dip has some differences in certain bus voltages and can be neglected. The voltage drop in the case of Hypersim in ramped due to the resistance in the breaker in the Hypersim software. Once the fault is cleared, both the softwares retain the same steady state condition. The ramped increase again can be seen in Hypersim during fault clearing.

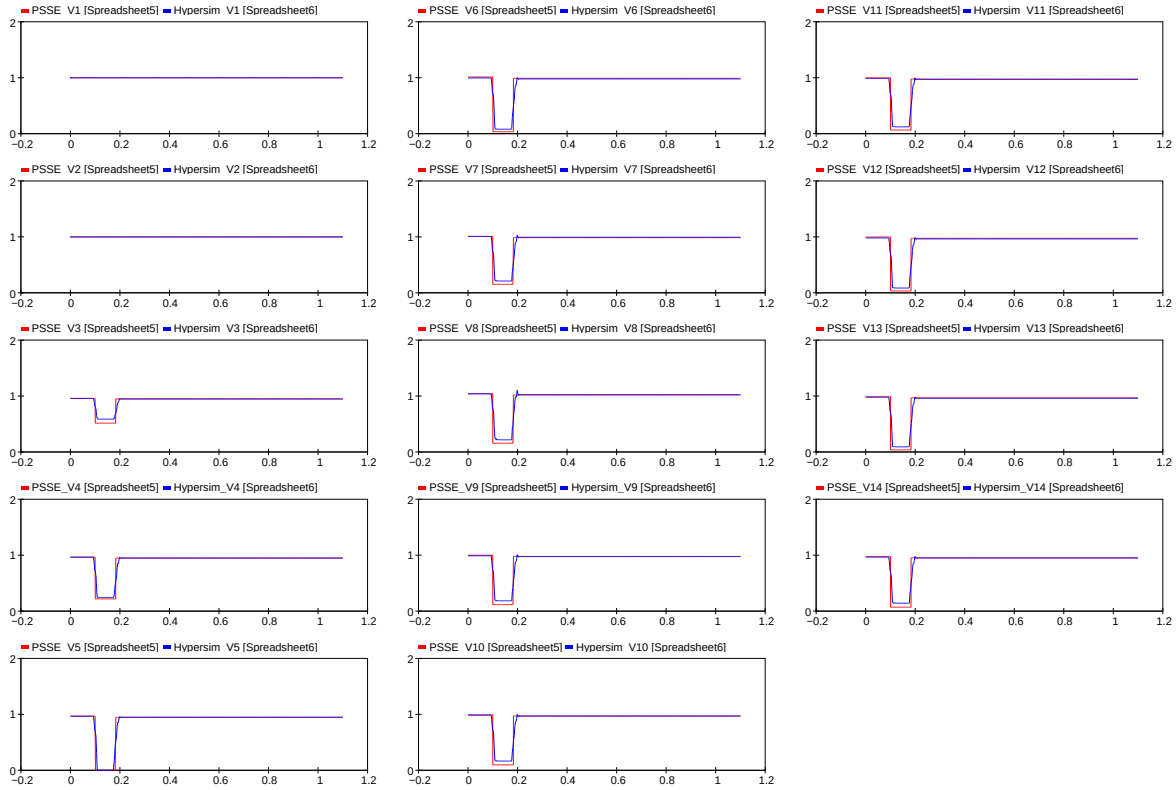

Figure 5.3: Comparison between PSS/E and Hypersim test case with Bus-5 fault

The parameters of the near-ideal source was chosen with the parameter manipulation script which would bring the least difference between the two software platforms and the desired results can be seen in the output voltage waveforms.

Text Matrix Generation:

To clearly analyze the response of the SVC it was necessary to place the SVC model and/or connect the SVC physical controller at bus locations that showed least variations to system disturbances. Capacitor elements of different capacitances were placed at different buses

along with the fault scenarios. The voltage waveform of the base case along with the 2 other cases with the addition of capacitor elements can be seen in Figure 5.4. In Figure 5.4 three cases have been overlapped against each other - The first one is the base case i.e., the test system, the second one is the test system along with a 18Mvar capacitor at Bus-4 and the third with a 45 Mvar capacitor at Bus-4. A fault is applied on Bus-5 on the test cases in PSS/E and Hypersim.

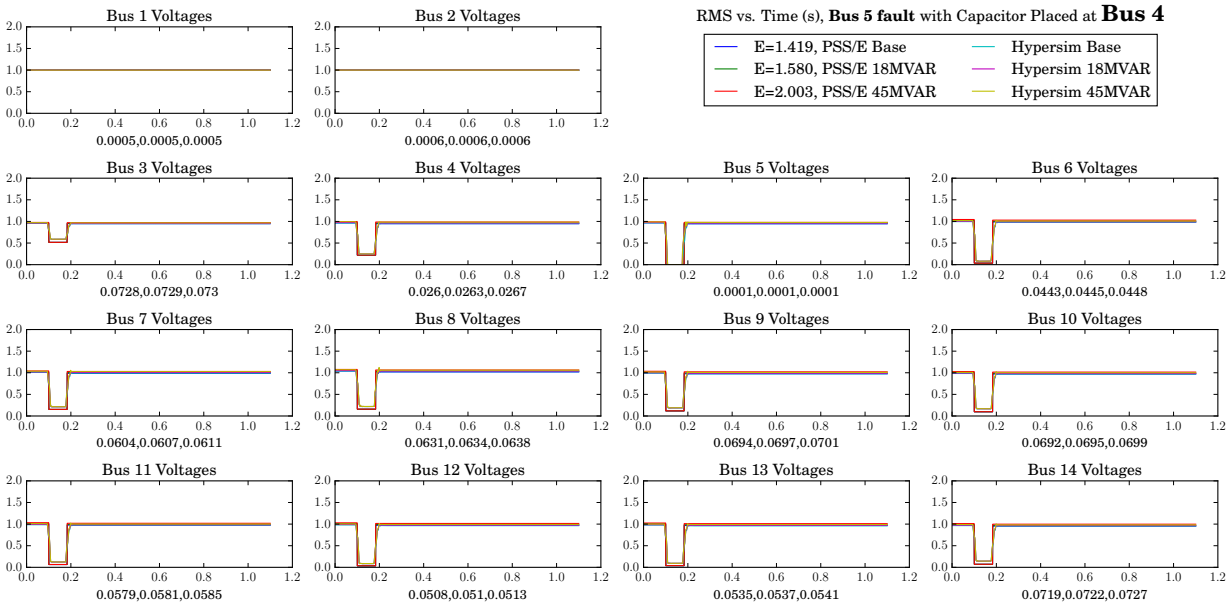

Figure 5.4: Voltage waveforms of the base case and capacitor added at Bus-4

This process is done such that capacitors are placed on all buses from 3-14 and bus faults are applied on all buses from 3-7 and 9-14. This leads to 132 scenarios. The waveforms like Figure 5.4 are studied ad their differences are analyzed. If the steady state waveforms match, then the difference in the two platforms are biggest at the dip (during the fault). The difference between the voltages (in pu) are calculated for each waveform at the dip and those values with <0.03 pu. The error values shown in the legend is the total error between

Hypersim and PSS/E for the three scenarios whereas the values shown under each plot is the error difference at the dip for each scenario. A table is also created which shows the error differences at a time during the fault. The Figure 5.5 - Figure 5.15 show the error values when a Bus-4 fault is applied with capacitors placed from Bus-3 to Bus-14.

Location	Diff Base Case	Diff 18Mvar Case	Diff 45Mvar Case
Bus4_voltage1:	0.0006	0.0006	0.0006
Bus4_voltage2:	0.0006	0.0006	0.0005
Bus4_voltage3:	0.0661	0.0683	0.0717
Bus4_voltage4:	0.0001	0.0001	0.0001
Bus4_voltage5:	0.0095	0.0095	0.0095
Bus4_voltage6:	0.0523	0.0523	0.0523
Bus4_voltage7:	0.0291	0.0291	0.0291
Bus4_voltage8:	0.0304	0.0304	0.0305
Bus4_voltage9:	0.0425	0.0425	0.0425
Bus4_voltage10:	0.0476	0.0476	0.0476
Bus4_voltage11:	0.0522	0.0522	0.0522
Bus4_voltage12:	0.0619	0.0619	0.0619
Bus4_voltage13:	0.0632	0.0632	0.0632
Bus4_voltage14:	0.0597	0.0597	0.0597

Figure 5.5: Bus 4 fault with capacitor at Bus 3

Location	Diff Base Case	Diff 18Mvar Case	Diff 45Mvar Case
Bus4_voltage1:	0.0006	0.0006	0.0006
Bus4_voltage2:	0.0006	0.0005	0.0005
Bus4_voltage3:	0.0661	0.0661	0.0661
Bus4_voltage4:	0.0001	0.0001	0.0001
Bus4_voltage5:	0.0095	0.0097	0.01
Bus4_voltage6:	0.0523	0.0526	0.053
Bus4_voltage7:	0.0291	0.0292	0.0294
Bus4_voltage8:	0.0304	0.0306	0.0308
Bus4_voltage9:	0.0425	0.0427	0.043
Bus4_voltage10:	0.0476	0.0479	0.0482
Bus4_voltage11:	0.0522	0.0524	0.0528
Bus4_voltage12:	0.0619	0.0622	0.0627
Bus4_voltage13:	0.0632	0.0635	0.064
Bus4_voltage14:	0.0597	0.06	0.0604

Figure 5.6: Bus 4 fault with capacitor at Bus 5

Location	Diff Base Case	Diff 18Mvar Case	Diff 45Mvar Case
Bus4_voltage1:	0.0006	0.0006	0.0006
Bus4_voltage2:	0.0006	0.0006	0.0006
Bus4_voltage3:	0.0661	0.0661	0.0661
Bus4_voltage4:	0.0001	0.0001	0.0001
Bus4_voltage5:	0.0095	0.0099	0.0106
Bus4_voltage6:	0.0523	0.0549	0.0596
Bus4_voltage7:	0.0291	0.0298	0.0322
Bus4_voltage8:	0.0304	0.0307	0.0364
Bus4_voltage9:	0.0425	0.0439	0.0466
Bus4_voltage10:	0.0476	0.0493	0.0523
Bus4_voltage11:	0.0522	0.0543	0.0581
Bus4_voltage12:	0.0619	0.0646	0.0692
Bus4_voltage13:	0.0632	0.0658	0.0704
Bus4_voltage14:	0.0597	0.0618	0.0653

Figure 5.7: Bus 4 fault with capacitor at Bus 6

Location	Diff Base Case	Diff 18Mvar Case	Diff 45Mvar Case
Bus4_voltage1:	0.0006	0.0006	0.0006
Bus4_voltage2:	0.0006	0.0005	0.0005
Bus4_voltage3:	0.0661	0.0661	0.0661
Bus4_voltage4:	0.0001	0.0001	0.0001
Bus4_voltage5:	0.0095	0.0096	0.0097
Bus4_voltage6:	0.0523	0.053	0.0535
Bus4_voltage7:	0.0291	0.031	0.0354
Bus4_voltage8:	0.0304	0.0331	0.0398
Bus4_voltage9:	0.0425	0.0441	0.0466
Bus4_voltage10:	0.0476	0.049	0.0508
Bus4_voltage11:	0.0522	0.0532	0.0542
Bus4_voltage12:	0.0619	0.0627	0.0632
Bus4_voltage13:	0.0632	0.064	0.0647
Bus4_voltage14:	0.0597	0.0609	0.0622

Figure 5.8: Bus 4 fault with capacitor at Bus 7

Location	Diff Base Case	Diff 18Mvar Case	Diff 45Mvar Case
Bus4_voltage1:	0.0006	0.0006	0.0006
Bus4_voltage2:	0.0006	0.0005	0.0005
Bus4_voltage3:	0.0661	0.0661	0.0661
Bus4_voltage4:	0.0001	0.0001	0.0001
Bus4_voltage5:	0.0095	0.0096	0.0106
Bus4_voltage6:	0.0523	0.0539	0.0644
Bus4_voltage7:	0.0291	0.0464	0.1161
Bus4_voltage8:	0.0304	0.0865	0.2563
Bus4_voltage9:	0.0425	0.0518	0.0949
Bus4_voltage10:	0.0476	0.0542	0.0882
Bus4_voltage11:	0.0522	0.0554	0.0749
Bus4_voltage12:	0.0619	0.0637	0.0751
Bus4_voltage13:	0.0632	0.0652	0.0779

Figure 5.9: Bus 4 fault with capacitor at Bus 8

Location	Diff Base Case	Diff 18Mvar Case	Diff 45Mvar Case
Bus4_voltage1:	0.0006	0.0006	0.0006
Bus4_voltage2:	0.0006	0.0005	0.0005
Bus4_voltage3:	0.0661	0.0661	0.0661
Bus4_voltage4:	0.0001	0.0001	0.0001
Bus4_voltage5:	0.0095	0.0097	0.0098
Bus4_voltage6:	0.0523	0.0533	0.0545
Bus4_voltage7:	0.0291	0.0302	0.0321
Bus4_voltage8:	0.0304	0.0313	0.0334
Bus4_voltage9:	0.0425	0.0443	0.047
Bus4_voltage10:	0.0476	0.0493	0.0518
Bus4_voltage11:	0.0522	0.0535	0.0555
Bus4_voltage12:	0.0619	0.0629	0.0643
Bus4_voltage13:	0.0632	0.0643	0.0658
Bus4_voltage14:	0.0597	0.0612	0.0634

Figure 5.10: Bus 4 fault with capacitor at Bus 9

Location	Diff Base Case	Diff 18Mvar Case	Diff 45Mvar Case
Bus4_voltage1:	0.0006	0.0006	0.0006
Bus4_voltage2:	0.0006	0.0006	0.0005
Bus4_voltage3:	0.0661	0.0661	0.0661
Bus4_voltage4:	0.0001	0.0001	0.0001
Bus4_voltage5:	0.0095	0.0097	0.01
Bus4_voltage6:	0.0523	0.0537	0.056
Bus4_voltage7:	0.0291	0.0303	0.0329
Bus4_voltage8:	0.0304	0.0313	0.037
Bus4_voltage9:	0.0425	0.0444	0.0479
Bus4_voltage10:	0.0476	0.0502	0.055
Bus4_voltage11:	0.0522	0.0542	0.0579
Bus4_voltage12:	0.0619	0.0633	0.0657
Bus4_voltage13:	0.0632	0.0647	0.0672
Bus4_voltage14:	0.0597	0.0615	0.0645

Figure 5.11: Bus 4 fault with capacitor at Bus 10

Location	Diff Base Case	Diff 18Mvar Case	Diff 45Mvar Case
Bus4_voltage1:	0.0006	0.0006	0.0006
Bus4_voltage2:	0.0006	0.0006	0.0006
Bus4_voltage3:	0.0661	0.0661	0.0661
Bus4_voltage4:	0.0001	0.0001	0.0001
Bus4_voltage5:	0.0095	0.0098	0.0104
Bus4_voltage6:	0.0523	0.0545	0.0588
Bus4_voltage7:	0.0291	0.0302	0.0334
Bus4_voltage8:	0.0304	0.0313	0.0441
Bus4_voltage9:	0.0425	0.0443	0.0473
Bus4_voltage10:	0.0476	0.0499	0.054
Bus4_voltage11:	0.0522	0.0555	0.0626
Bus4_voltage12:	0.0619	0.0641	0.0684
Bus4_voltage13:	0.0632	0.0654	0.0696
Bus4_voltage14:	0.0597	0.0618	0.0654

Figure 5.12: Bus 4 fault with capacitor at Bus 11

Location	Diff Base Case	Diff 18Mvar Case	Diff 45Mvar Case
Bus4_voltage1:	0.0006	0.0006	0.0006
Bus4_voltage2:	0.0006	0.0006	0.0005
Bus4_voltage3:	0.0661	0.0661	0.0661
Bus4_voltage4:	0.0001	0.0001	0.0001
Bus4_voltage5:	0.0095	0.01	0.0107
Bus4_voltage6:	0.0523	0.0559	0.0613
Bus4_voltage7:	0.0291	0.0301	0.0342
Bus4_voltage8:	0.0304	0.031	0.0409
Bus4_voltage9:	0.0425	0.0443	0.0483
Bus4_voltage10:	0.0476	0.0498	0.0538
Bus4_voltage11:	0.0522	0.0551	0.0596
Bus4_voltage12:	0.0619	0.0675	0.0758
Bus4_voltage13:	0.0632	0.0674	0.0736
Bus4_voltage14:	0.0597	0.0626	0.0674

Figure 5.13: Bus 4 fault with capacitor at Bus 12

Location	Diff Base Case	Diff 18Mvar Case	Diff 45Mvar Case
Bus4_voltage1:	0.0006	0.0006	0.0006
Bus4_voltage2:	0.0006	0.0006	0.0005
Bus4_voltage3:	0.0661	0.0661	0.0661
Bus4_voltage4:	0.0001	0.0001	0.0001
Bus4_voltage5:	0.0095	0.01	0.0107
Bus4_voltage6:	0.0523	0.0556	0.0614
Bus4_voltage7:	0.0291	0.0301	0.0341
Bus4_voltage8:	0.0304	0.031	0.0412
Bus4_voltage9:	0.0425	0.0443	0.0483
Bus4_voltage10:	0.0476	0.0498	0.0539
Bus4_voltage11:	0.0522	0.0549	0.0597
Bus4_voltage12:	0.0619	0.0659	0.0728
Bus4_voltage13:	0.0632	0.0677	0.0755
Bus4_voltage14:	0.0597	0.0628	0.0681

Figure 5.14: Bus 4 fault with capacitor at Bus 13

Location	Diff Base Case	Diff 18Mvar Case	Diff 45Mvar Case
Bus4_voltage1:	0.0006	0.0006	0.0006
Bus4_voltage2:	0.0006	0.0005	0.0005
Bus4_voltage3:	0.0661	0.0661	0.0661
Bus4_voltage4:	0.0001	0.0001	0.0001
Bus4_voltage5:	0.0095	0.0098	0.0102
Bus4_voltage6:	0.0523	0.0544	0.0577
Bus4_voltage7:	0.0291	0.0304	0.0335
Bus4_voltage8:	0.0304	0.0315	0.0444
Bus4_voltage9:	0.0425	0.0446	0.0475
Bus4_voltage10:	0.0476	0.0498	0.0528
Bus4_voltage11:	0.0522	0.0543	0.0575
Bus4_voltage12:	0.0619	0.0643	0.0683
Bus4_voltage13:	0.0632	0.066	0.0704
Bus4_voltage14:	0.0597	0.0642	0.0723

Figure 5.15: Bus 4 fault with capacitor at Bus 14

As we can see the bus voltage difference which are <0.3 pcu are bus 5,7,8,9 and 10 when capacitors are placed at bus 3 and 4 and bus 5,7,8 and 9 when capacitors are placed at bus

5,6,7,8,9,10,11,12,13 and 14 and bus 5 when capacitor is placed at bus 8. Since the voltage at bus 5 does not vary for bus 4 fault with various location of capacitor, this position is chosen as one of the test cases.

Similar tables which show the error function value for all bus fault scenarios are created and the cases with the least error (0.03 pu%) is marked. These cases form the test matrix which includes the bus fault location as well as the location for the placement of the SVC. In Figure 5.16 below, the locations and fault scenarios for testing the SVC model.

Test #	Test Description	
	Bus Fault Location	SVC Location
1	Bus 3	Bus 5
2	Bus 4	Bus 5
3	Bus 5	Bus 4
4	Bus 6	Bus 3
5		Bus 4
6		Bus 5
7	Bus 7	Bus 3
8		Bus 4
9		Bus 5
10	Bus 9	Bus 3
11		Bus 4
12	Bus 10	Bus 3
13		Bus 4
14		Bus 5
15	Bus 11	Bus 3
16		Bus 4
17		Bus 5
18	Bus 12	Bus 3
19		Bus 4
20		Bus 5
21	Bus 13	Bus 3
22		Bus 4
23		Bus 5
24	Bus 14	Bus 3
25		Bus 4
26		Bus 5

Figure 5.16: Test Matrix

5.4 Finding the parameters of SVC model

A range of values were given to each parameter - K, T_1, T_2, T_3, T_4 and T_5. K ranged from various values from 50-1000 initially. After every iteration, the range was reduced according to the error function and to get more accurate results. The ranges for T_1 - T_4 always remained < 0.5 and $T_5 < 0.05$. The parameters were varied based on the error function.

The comparison of the plots of the voltage waveforms with SVC placed at different locations with bus faults can been seen below. The MVar output of the SVC model in PSS/E and the Mvar output of the SVC physical controller along with the 14 bus voltages are overlapped against each other.

The first step involves varying the parameters individually. Error function tables are created in-order to analyze which parameter has least difference. A range of values are given to each parameter of the SVC model in PSS/E one at a time and the error function values are tabulated in ascending order of error between the response of PSS/E and Hypersim. This table helps us in creating a range for the variation of parameters are done simultaneously.

Figure 5.17 shows the error function table with varying values for parameter K when the SVC is placed at Bus-5 and a fault is applied on Bus-3.

Error(%)	K	$T1$	$T2$	$T3$	$T4$	$T5$	R_{min}	V_{max}	V_{min}	C_{base}	VOV
5.8494367998	50.0	0.01	0.0	0.093	0.0	0.0	0.0	1.0	0.0	300.0	0.07
5.85461228185	54	0.01	0.0	0.093	0.0	0.0	0.0	1.0	0.0	300.0	0.07
5.85894481648	52	0.01	0.0	0.093	0.0	0.0	0.0	1.0	0.0	300.0	0.07
7.45734610901	56	0.01	0.0	0.093	0.0	0.0	0.0	1.0	0.0	300.0	0.07
7.4936849499	58	0.01	0.0	0.093	0.0	0.0	0.0	1.0	0.0	300.0	0.07
7.50617502427	60	0.01	0.0	0.093	0.0	0.0	0.0	1.0	0.0	300.0	0.07
7.51450462637	70	0.01	0.0	0.093	0.0	0.0	0.0	1.0	0.0	300.0	0.07
7.53913738279	80	0.01	0.0	0.093	0.0	0.0	0.0	1.0	0.0	300.0	0.07
7.53917668161	100	0.01	0.0	0.093	0.0	0.0	0.0	1.0	0.0	300.0	0.07
7.54041581766	200	0.01	0.0	0.093	0.0	0.0	0.0	1.0	0.0	300.0	0.07
7.54689404594	300	0.01	0.0	0.093	0.0	0.0	0.0	1.0	0.0	300.0	0.07
7.54725700877	800	0.01	0.0	0.093	0.0	0.0	0.0	1.0	0.0	300.0	0.07
7.55124641725	500	0.01	0.0	0.093	0.0	0.0	0.0	1.0	0.0	300.0	0.07
7.55203306179	1000	0.01	0.0	0.093	0.0	0.0	0.0	1.0	0.0	300.0	0.07

Figure 5.17: Error function table for variation of K

The parameter K has been given values from 50-1000 and the corresponding error function is tabulated for each case. As seen in Figure 5.17 K= 50 has the least error.

The same scenario is used to create error function tables shown in Figure 5.18 - Figure 5.22 for variation of T_1 to T_5

Error(%)	K	$T1$	$T2$	$T3$	$T4$	$T5$	R_{min}	V_{max}	V_{min}	C_{base}	VOV
2.23780218082	50.0	0.005	0.0	0.093	0.0	0.0	0.0	1.0	0.0	300.0	0.07
2.24179192419	50.0	0.002	0.0	0.093	0.0	0.0	0.0	1.0	0.0	300.0	0.07
2.24320981885	50.0	0	0.0	0.093	0.0	0.0	0.0	1.0	0.0	300.0	0.07
5.8494367998	50.0	0.01	0.0	0.093	0.0	0.0	0.0	1.0	0.0	300.0	0.07
5.85535998938	50.0	0.009	0.0	0.093	0.0	0.0	0.0	1.0	0.0	300.0	0.07
7.53801875822	50.0	0.02	0.0	0.093	0.0	0.0	0.0	1.0	0.0	300.0	0.07
7.54005621537	50.0	0.03	0.0	0.093	0.0	0.0	0.0	1.0	0.0	300.0	0.07
7.54281419092	50.0	0.04	0.0	0.093	0.0	0.0	0.0	1.0	0.0	300.0	0.07

Figure 5.18: Case 1:Error function table for variation of T_1

Error(%)	K	$T1$	$T2$	$T3$	$T4$	$T5$	R_{min}	V_{max}	V_{min}	C_{base}	VOV
5.8494367998	50.0	0.01	0.002	0.093	0.0	0.0	0.0	1.0	0.0	300.0	0.07
5.8494367998	50.0	0.01	0.005	0.093	0.0	0.0	0.0	1.0	0.0	300.0	0.07
5.8494367998	50.0	0.01	0.009	0.093	0.0	0.0	0.0	1.0	0.0	300.0	0.07
5.8494367998	50.0	0.01	0.015	0.093	0.0	0.0	0.0	1.0	0.0	300.0	0.07
5.8494367998	50.0	0.01	0.01	0.093	0.0	0.0	0.0	1.0	0.0	300.0	0.07
5.8494367998	50.0	0.01	0.02	0.093	0.0	0.0	0.0	1.0	0.0	300.0	0.07
5.8494367998	50.0	0.01	0.03	0.093	0.0	0.0	0.0	1.0	0.0	300.0	0.07
5.8494367998	50.0	0.01	0.04	0.093	0.0	0.0	0.0	1.0	0.0	300.0	0.07
5.8494367998	50.0	0.01	0.05	0.093	0.0	0.0	0.0	1.0	0.0	300.0	0.07
5.8494367998	50.0	0.01	0.0	0.093	0.0	0.0	0.0	1.0	0.0	300.0	0.07
5.8494367998	50.0	0.01	0.1	0.093	0.0	0.0	0.0	1.0	0.0	300.0	0.07
5.8494367998	50.0	0.01	1e-06	0.093	0.0	0.0	0.0	1.0	0.0	300.0	0.07

Figure 5.19: Case 1:Error function table for variation of T_2

Error(%)	K	$T1$	$T2$	$T3$	$T4$	$T5$	R_{min}	V_{max}	V_{min}	C_{base}	VOV
2.2739100207	50.0	0.01	0.0	0.15	0.0	0.0	0.0	1.0	0.0	300.0	0.07
5.8494367998	50.0	0.01	0.0	0.093	0.0	0.0	0.0	1.0	0.0	300.0	0.07
5.85796312141	50.0	0.01	0.0	0.1	0.0	0.0	0.0	1.0	0.0	300.0	0.07
7.49194690893	50.0	0.01	0.0	0.08	0.0	0.0	0.0	1.0	0.0	300.0	0.07
7.53875984736	50.0	0.01	0.0	0.05	0.0	0.0	0.0	1.0	0.0	300.0	0.07
7.54424483396	50.0	0.01	0.0	0.02	0.0	0.0	0.0	1.0	0.0	300.0	0.07
7.54974123648	50.0	0.01	0.0	0.009	0.0	0.0	0.0	1.0	0.0	300.0	0.07
7.55178616896	50.0	0.01	0.0	0.005	0.0	0.0	0.0	1.0	0.0	300.0	0.07
7.5520476785	50.0	0.01	0.0	0.002	0.0	0.0	0.0	1.0	0.0	300.0	0.07

Figure 5.20: Case 1:Error function table for variation of T_3

Error(%)	K	$T1$	$T2$	$T3$	$T4$	$T5$	R_{min}	V_{max}	V_{min}	C_{base}	VOV
2.23686030583	50.0	0.01	0.0	0.093	0.002	0.0	0.0	1.0	0.0	300.0	0.07
2.25047663203	50.0	0.01	0.0	0.093	0.005	0.0	0.0	1.0	0.0	300.0	0.07
2.26193809201	50.0	0.01	0.0	0.093	0.01	0.0	0.0	1.0	0.0	300.0	0.07
2.2968058875	50.0	0.01	0.0	0.093	0.015	0.0	0.0	1.0	0.0	300.0	0.07
2.31917595488	50.0	0.01	0.0	0.093	0.02	0.0	0.0	1.0	0.0	300.0	0.07
2.49290820899	50.0	0.01	0.0	0.093	0.04	0.0	0.0	1.0	0.0	300.0	0.07
2.86273365609	50.0	0.01	0.0	0.093	0.08	0.0	0.0	1.0	0.0	300.0	0.07
2.99185964664	50.0	0.01	0.0	0.093	0.5	0.0	0.0	1.0	0.0	300.0	0.07
3.00554237311	50.0	0.01	0.0	0.093	0.1	0.0	0.0	1.0	0.0	300.0	0.07
3.32847795073	50.0	0.01	0.0	0.093	0.2	0.0	0.0	1.0	0.0	300.0	0.07
5.8494367998	50.0	0.01	0.0	0.093	0.0	0.0	0.0	1.0	0.0	300.0	0.07
5.8494367998	50.0	0.01	0.0	0.093	1e-06	0.0	0.0	1.0	0.0	300.0	0.07

Figure 5.21: Case 1: Error function table for variation of T_4

Error(%)	K	$T1$	$T2$	$T3$	$T4$	$T5$	R_{min}	V_{max}	V_{min}	C_{base}	VOV
2.2380086369	50.0	0.01	0.0	0.093	0.0	0.001	0.0	1.0	0.0	300.0	0.07
2.24046318811	50.0	0.01	0.0	0.093	0.0	0.002	0.0	1.0	0.0	300.0	0.07
2.24915673648	50.0	0.01	0.0	0.093	0.0	0.005	0.0	1.0	0.0	300.0	0.07
2.25947286155	50.0	0.01	0.0	0.093	0.0	0.009	0.0	1.0	0.0	300.0	0.07
2.26150843922	50.0	0.01	0.0	0.093	0.0	0.01	0.0	1.0	0.0	300.0	0.07
2.3204002133	50.0	0.01	0.0	0.093	0.0	0.02	0.0	1.0	0.0	300.0	0.07
2.49418020535	50.0	0.01	0.0	0.093	0.0	0.04	0.0	1.0	0.0	300.0	0.07
2.59456608434	50.0	0.01	0.0	0.093	0.0	0.05	0.0	1.0	0.0	300.0	0.07
5.8494367998	50.0	0.01	0.0	0.093	0.0	0.0	0.0	1.0	0.0	300.0	0.07

Figure 5.22: Case 1:Error function table for variation of T_5

Similarly, the error function tables for SVC at Bus-5 with a fault at Bus-11 for the parameters varied individually can be seen in Figure 5.23 - Figure 5.28

Error(%)	K	$T1$	$T2$	$T3$	$T4$	$T5$	R_{min}	V_{max}	V_{min}	C_{base}	VOV
6.95883556314	50.0	0.01	0.0	0.093	0.0	0.0	0.0	1.0	0.0	300.0	0.07
6.95939313706	54	0.01	0.0	0.093	0.0	0.0	0.0	1.0	0.0	300.0	0.07
6.95949787839	52	0.01	0.0	0.093	0.0	0.0	0.0	1.0	0.0	300.0	0.07
8.5617592908	56	0.01	0.0	0.093	0.0	0.0	0.0	1.0	0.0	300.0	0.07
8.59625625423	58	0.01	0.0	0.093	0.0	0.0	0.0	1.0	0.0	300.0	0.07
8.60969772822	60	0.01	0.0	0.093	0.0	0.0	0.0	1.0	0.0	300.0	0.07
8.62732837472	70	0.01	0.0	0.093	0.0	0.0	0.0	1.0	0.0	300.0	0.07
8.64116901221	80	0.01	0.0	0.093	0.0	0.0	0.0	1.0	0.0	300.0	0.07
8.64138872314	100	0.01	0.0	0.093	0.0	0.0	0.0	1.0	0.0	300.0	0.07
8.6416341707	200	0.01	0.0	0.093	0.0	0.0	0.0	1.0	0.0	300.0	0.07
8.64737525203	300	0.01	0.0	0.093	0.0	0.0	0.0	1.0	0.0	300.0	0.07
8.65112830232	500	0.01	0.0	0.093	0.0	0.0	0.0	1.0	0.0	300.0	0.07
8.65179022807	1000	0.01	0.0	0.093	0.0	0.0	0.0	1.0	0.0	300.0	0.07
8.65248648594	800	0.01	0.0	0.093	0.0	0.0	0.0	1.0	0.0	300.0	0.07

Figure 5.23: Case 2: Error function table for variation of K

Error(%)	K	$T1$	$T2$	$T3$	$T4$	$T5$	R_{min}	V_{max}	V_{min}	C_{base}	VOV
6.95883556314	50.0	0.01	0.002	0.093	0.0	0.0	0.0	1.0	0.0	300.0	0.07
6.95883556314	50.0	0.01	0.005	0.093	0.0	0.0	0.0	1.0	0.0	300.0	0.07
6.95883556314	50.0	0.01	0.009	0.093	0.0	0.0	0.0	1.0	0.0	300.0	0.07
6.95883556314	50.0	0.01	0.015	0.093	0.0	0.0	0.0	1.0	0.0	300.0	0.07
6.95883556314	50.0	0.01	0.01	0.093	0.0	0.0	0.0	1.0	0.0	300.0	0.07
6.95883556314	50.0	0.01	0.02	0.093	0.0	0.0	0.0	1.0	0.0	300.0	0.07
6.95883556314	50.0	0.01	0.03	0.093	0.0	0.0	0.0	1.0	0.0	300.0	0.07
6.95883556314	50.0	0.01	0.04	0.093	0.0	0.0	0.0	1.0	0.0	300.0	0.07
6.95883556314	50.0	0.01	0.05	0.093	0.0	0.0	0.0	1.0	0.0	300.0	0.07
6.95883556314	50.0	0.01	0.0	0.093	0.0	0.0	0.0	1.0	0.0	300.0	0.07
6.95883556314	50.0	0.01	0.1	0.093	0.0	0.0	0.0	1.0	0.0	300.0	0.07
6.95883556314	50.0	0.01	1e-06	0.093	0.0	0.0	0.0	1.0	0.0	300.0	0.07

Figure 5.24: Case 2: Error function table for variation of T_2

Error(%)	K	$T1$	$T2$	$T3$	$T4$	$T5$	R_{min}	V_{max}	V_{min}	C_{base}	VOV
3.82666007519	50.0	0.005	0.0	0.093	0.0	0.0	0.0	1.0	0.0	300.0	0.07
3.82776272297	50.0	0.002	0.0	0.093	0.0	0.0	0.0	1.0	0.0	300.0	0.07
3.82902865336	50.0	0	0.0	0.093	0.0	0.0	0.0	1.0	0.0	300.0	0.07
6.95883556314	50.0	0.01	0.0	0.093	0.0	0.0	0.0	1.0	0.0	300.0	0.07
6.95955850053	50.0	0.009	0.0	0.093	0.0	0.0	0.0	1.0	0.0	300.0	0.07
8.64165543044	50.0	0.02	0.0	0.093	0.0	0.0	0.0	1.0	0.0	300.0	0.07
8.64341974721	50.0	0.03	0.0	0.093	0.0	0.0	0.0	1.0	0.0	300.0	0.07
8.64719450436	50.0	0.04	0.0	0.093	0.0	0.0	0.0	1.0	0.0	300.0	0.07

Figure 5.25: Case 2: Error function table for variation of T_1

Error(%)	K	$T1$	$T2$	$T3$	$T4$	$T5$	R_{min}	V_{max}	V_{min}	C_{base}	VOV
3.84826064497	50.0	0.01	0.0	0.15	0.0	0.0	0.0	1.0	0.0	300.0	0.07
6.95811738033	50.0	0.01	0.0	0.1	0.0	0.0	0.0	1.0	0.0	300.0	0.07
6.95883556314	50.0	0.01	0.0	0.093	0.0	0.0	0.0	1.0	0.0	300.0	0.07
8.59402707228	50.0	0.01	0.0	0.08	0.0	0.0	0.0	1.0	0.0	300.0	0.07
8.6411808284	50.0	0.01	0.0	0.05	0.0	0.0	0.0	1.0	0.0	300.0	0.07
8.64756274328	50.0	0.01	0.0	0.02	0.0	0.0	0.0	1.0	0.0	300.0	0.07
8.64787275254	50.0	0.01	0.0	0.009	0.0	0.0	0.0	1.0	0.0	300.0	0.07
8.65049069967	50.0	0.01	0.0	0.005	0.0	0.0	0.0	1.0	0.0	300.0	0.07
8.65431340235	50.0	0.01	0.0	0.002	0.0	0.0	0.0	1.0	0.0	300.0	0.07

Figure 5.26: Case 2: Error function table for variation of T_3

Error(%)	K	$T1$	$T2$	$T3$	$T4$	$T5$	R_{min}	V_{max}	V_{min}	C_{base}	VOV
3.8198874682	50.0	0.01	0.0	0.093	0.002	0.0	0.0	1.0	0.0	300.0	0.07
3.82634269386	50.0	0.01	0.0	0.093	0.005	0.0	0.0	1.0	0.0	300.0	0.07
3.83211486222	50.0	0.01	0.0	0.093	0.01	0.0	0.0	1.0	0.0	300.0	0.07
3.83821755756	50.0	0.01	0.0	0.093	0.015	0.0	0.0	1.0	0.0	300.0	0.07
3.87485405104	50.0	0.01	0.0	0.093	0.02	0.0	0.0	1.0	0.0	300.0	0.07
3.96588604032	50.0	0.01	0.0	0.093	0.04	0.0	0.0	1.0	0.0	300.0	0.07
4.23730637501	50.0	0.01	0.0	0.093	0.08	0.0	0.0	1.0	0.0	300.0	0.07
4.34981851959	50.0	0.01	0.0	0.093	0.1	0.0	0.0	1.0	0.0	300.0	0.07
4.65175522101	50.0	0.01	0.0	0.093	0.2	0.0	0.0	1.0	0.0	300.0	0.07
4.7484369406	50.0	0.01	0.0	0.093	0.5	0.0	0.0	1.0	0.0	300.0	0.07
6.95883556314	50.0	0.01	0.0	0.093	0.0	0.0	0.0	1.0	0.0	300.0	0.07
6.95883556314	50.0	0.01	0.0	0.093	1e-06	0.0	0.0	1.0	0.0	300.0	0.07

Figure 5.27: Case 2: Error function table for variation of T_4

Error(%)	K	$T1$	$T2$	$T3$	$T4$	$T5$	R_{min}	V_{max}	V_{min}	C_{base}	VOV
3.82094597278	50.0	0.01	0.0	0.093	0.0	0.001	0.0	1.0	0.0	300.0	0.07
3.82226142447	50.0	0.01	0.0	0.093	0.0	0.002	0.0	1.0	0.0	300.0	0.07
3.82778672839	50.0	0.01	0.0	0.093	0.0	0.005	0.0	1.0	0.0	300.0	0.07
3.83242925892	50.0	0.01	0.0	0.093	0.0	0.009	0.0	1.0	0.0	300.0	0.07
3.83404902141	50.0	0.01	0.0	0.093	0.0	0.01	0.0	1.0	0.0	300.0	0.07
3.87509222906	50.0	0.01	0.0	0.093	0.0	0.02	0.0	1.0	0.0	300.0	0.07
3.96880945317	50.0	0.01	0.0	0.093	0.0	0.04	0.0	1.0	0.0	300.0	0.07
4.03636239738	50.0	0.01	0.0	0.093	0.0	0.05	0.0	1.0	0.0	300.0	0.07
6.95883556314	50.0	0.01	0.0	0.093	0.0	0.0	0.0	1.0	0.0	300.0	0.07

Figure 5.28: Case 2: Error function table for variation of T_5

The error tables tell us the value for each parameter which gives least error. Error tables were also created with SVC placed at Bus-3 and Bus-4 with faults applied on different locations. These tables can be seen in 6.2.

These best value of each parameter from the error function tables where taken and the response of the SVC model against the SVC physical controller is analyzed individually. The SVC is placed at Bus-4 and the fault is applied on Bus-5.

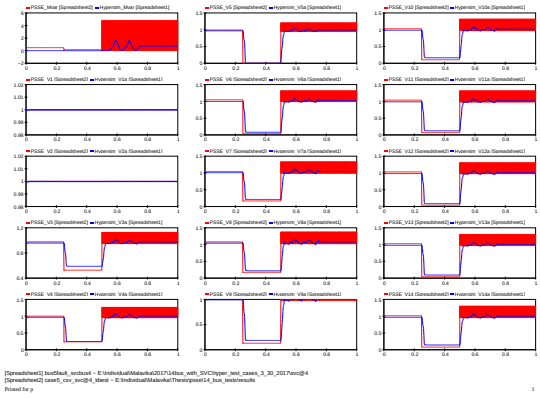

Figure 5.29: Comparison of response with best value of K

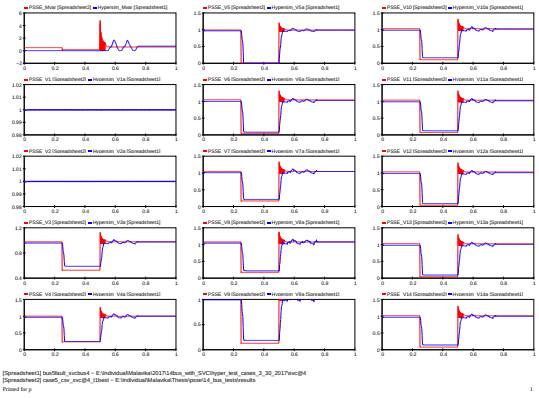

Figure 5.30: Comparison of response with best value of T_1

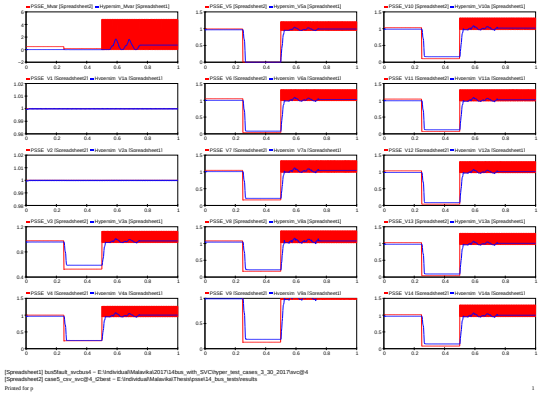

Figure 5.31: Comparison of response with best value of T_2

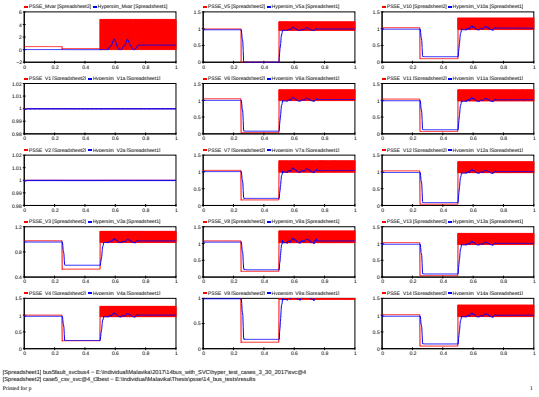

Figure 5.32: Comparison of response with best value of T_3

From the above graphs, it is seen that parameters T_1, T_4 and T_5 reduces the transients

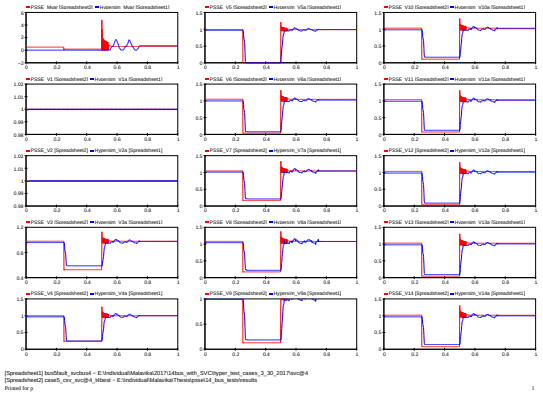

Figure 5.33: Comparison of response with best value of T_4

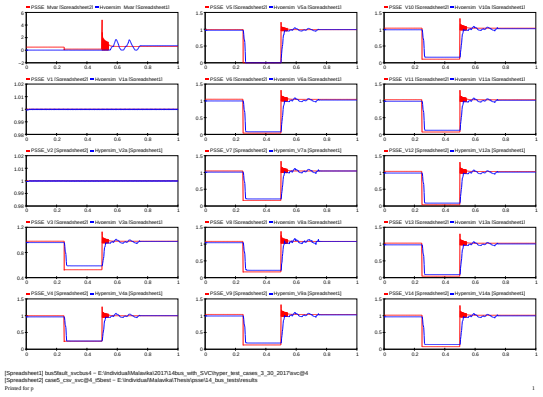

Figure 5.34: Comparison of response with best value of T_5

and shows a big effect on the response.

The parameters which had the least error was taken as the basis for selecting the range for variation simultaneously. This reduced the simulation time and also restricted the parameter range for an accurate results. Figure 5.35 shows the error function table when the SVC is placed at Bus-5 and a fault is applied on Bus-5 when all parameters are varied.

Error(%)	K	$T1$	$T2$	$T3$	$T4$	$T5$	R_{min}	V_{max}	V_{min}	C_{base}	VOV
2.20276153327	40	0	0.02	0.01	0.002	0.0001	0.0	1.0	0.0	300.0	0.07
2.20898699699	50.0	0	0.02	0.01	0.002	0.0001	0.0	1.0	0.0	300.0	0.07
2.21032665028	40	0	0.02	0.01	0.01	0.0001	0.0	1.0	0.0	300.0	0.07
2.21398712814	50.0	0	0.02	0.01	0.01	0.0001	0.0	1.0	0.0	300.0	0.07
2.21449890412	70	0	0.02	0.01	0.01	0.0001	0.0	1.0	0.0	300.0	0.07
2.21624904406	40	0	0.005	0.01	0.002	0.0001	0.0	1.0	0.0	300.0	0.07
2.21627851483	40	0	0.02	0.01	0.02	0.0001	0.0	1.0	0.0	300.0	0.07
2.21627851483	40	0	0.02	0.01	0.0001	0.0001	0.0	1.0	0.0	300.0	0.07
2.21627851483	40	0	0.002	0.01	0.0001	0.0001	0.0	1.0	0.0	300.0	0.07
2.21627851483	40	0	0.002	0.01	0.002	0.0001	0.0	1.0	0.0	300.0	0.07
2.21627851483	40	0	0.0	0.01	0.0001	0.0001	0.0	1.0	0.0	300.0	0.07
2.21627851483	40	0	0.005	0.01	0.0001	0.0001	0.0	1.0	0.0	300.0	0.07
2.21775776441	40	0	0.02	0.01	0.002	0.002	0.0	1.0	0.0	300.0	0.07
2.21812723435	50.0	0	0.005	0.01	0.002	0.0001	0.0	1.0	0.0	300.0	0.07
2.21936963201	40	0	0.02	0.01	0.01	0.002	0.0	1.0	0.0	300.0	0.07
2.21993603099	100	0	0.02	0.01	0.01	0.0001	0.0	1.0	0.0	300.0	0.07
2.2201002657	70	0	0.005	0.01	0.002	0.0001	0.0	1.0	0.0	300.0	0.07
2.22030157949	40	0	0.005	0.01	0.002	0.002	0.0	1.0	0.0	300.0	0.07
2.22136392834	50.0	0	0.0	0.01	0.0001	0.0001	0.0	1.0	0.0	300.0	0.07
2.22136392834	50.0	0	0.002	0.01	0.0001	0.0001	0.0	1.0	0.0	300.0	0.07

Figure 5.35: Error function table for variation of all parameters simultaneously

Similar simulations have been run for SVC at Bus-5 with fault at Bus-11, SVC at Bus-3

and SVC at Bus-4 with different faults and can be seen in appendix. The best parameters are analyzed from all cases and a parameter set was chosen based on what values were most common and had least error.

From the error function tables, for both variation of parameters individually and simultaneously, the best parameters from both cases are similar. This shows that these parameters chosen are independent of each other. The variation of parameters simultaneously is helpful to understand the parameter dependency and to find the best parameter when used as a set.

Figure 5.37 shows the response of the SVC in both software platforms. The SVC is placed on Bus-4 and a fault is applied on Bus-5. We can see that the voltage waveforms follow each other mostly. During the fault, there is a difference in the dip which was already present before the placement of the SVC. The difference is taken as the difference the two software platforms have amongst each other. It can also be seen that the when the model in PSS/E responds with many high-speed transients when the SVC physical controller has sudden variations.

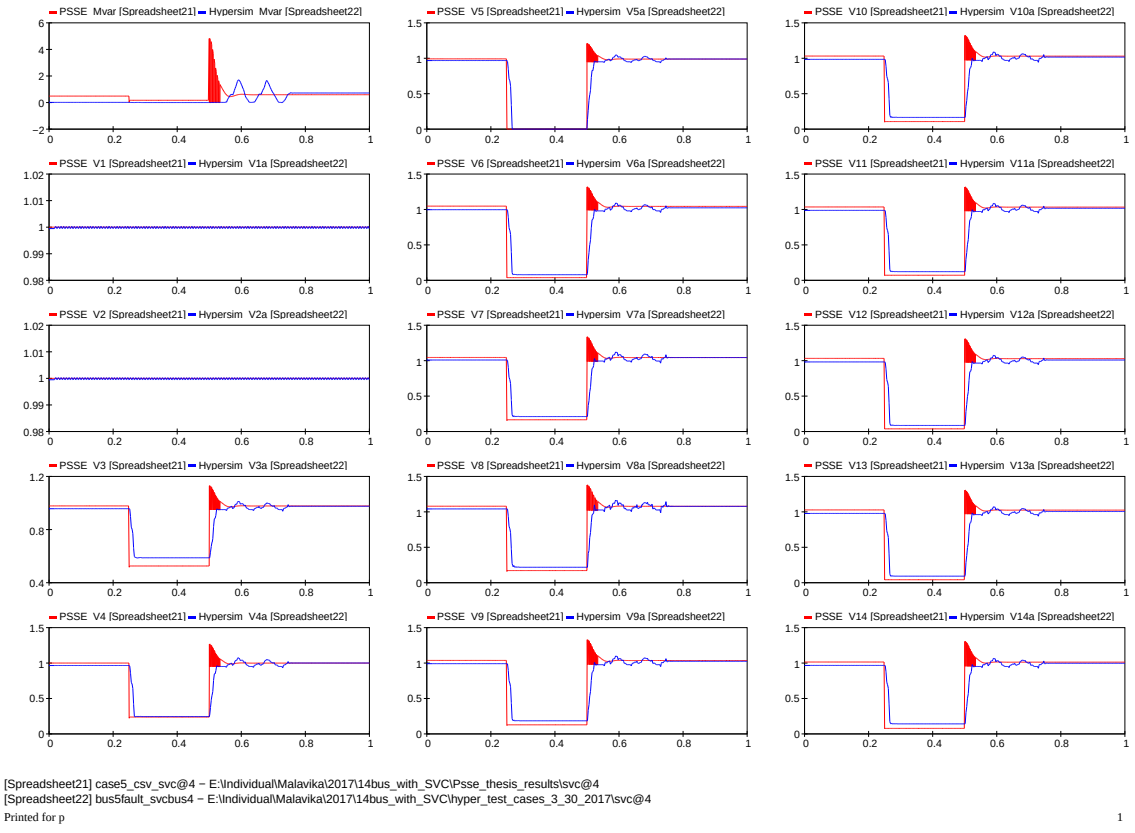

Figure 5.36: Response of the test system in PSS/E with new parameters for SVC and Hypersim HIL SVC at Bus-4 and a fault applied on Bus-5

With Figure 5.37, it is clear that the parameter finding methodology used has found the parameters for the SVC model that responds similar to the response of the SVC physical controller

For the purpose of validation and verification, the SVC model that was chosen to find the parameters for was already modeled when the physical controller / actual SVC installed. The response of the SVC model with the original parameters against the response of the SVC physical controller can be seen in Figure 5.37

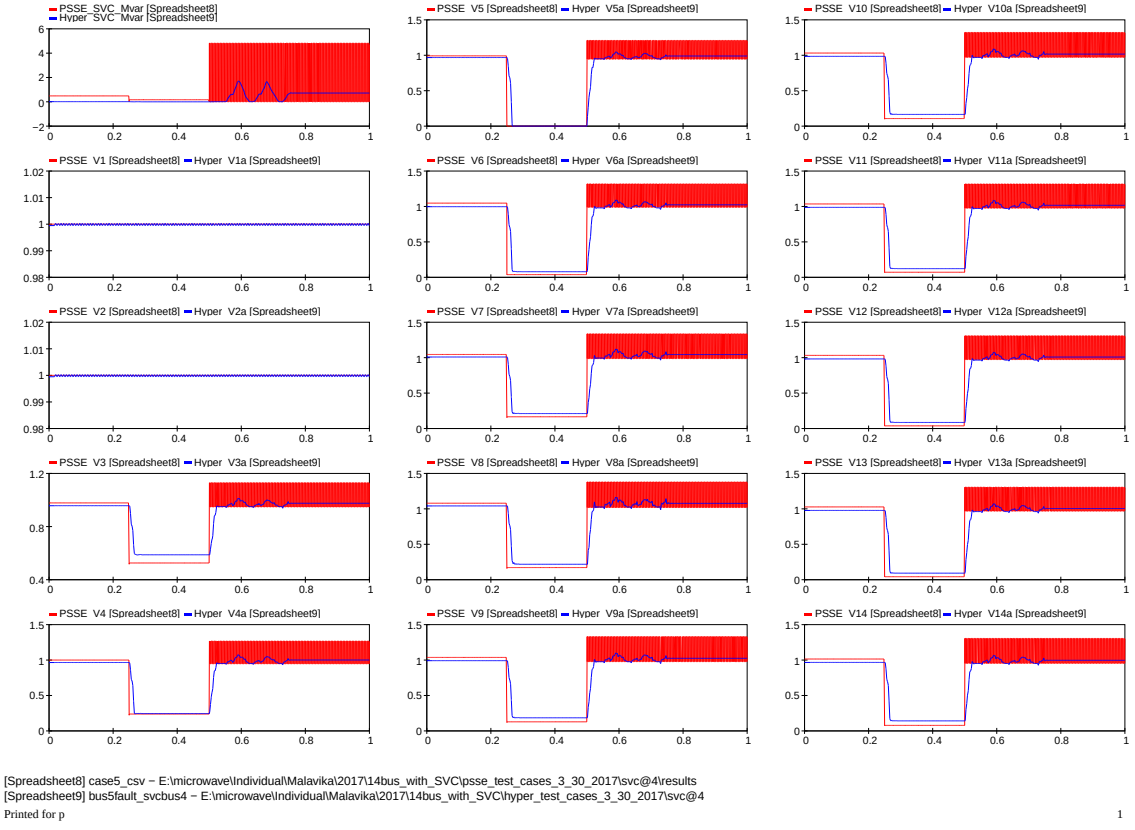

Figure 5.37: Response of the test system in PSS/E with original SVC and Hypersim HIL SVC at Bus-4 and a fault applied on Bus-5

From the above response, it can be seen that the response of the SVC with parameters found with this study is much more accurate than the response of the SVC with the original parameters. The new parameters chosen by the automation method proposed are seen in Table 5.3

The response of the SVC model in PSS/E with against the SVC physical controller for all cases of the test matrix can be seen in Figure 6.2.

Table 5.3: New SVC (CSVGN3) Parameters

Parameter	Value Range
K	50
T_1	0.0
T_2	0.002
T_3	0.15
T_4	0.002
T_5	0.001
R_{MIN}	0.0
V_{MAX}	1.0
V_{MIN}	0.0
C_{BASE}	300.0
V_{OV}	0.07

Chapter 6

Concluding Remarks and Future Work

6.1 Conclusion

This thesis focuses on the method of automation to create appropriate models in PSS/E with the data from the field.In this study, this methodology is used to find the appropriate model of an SVC in PSS/E with the data from the HIL real-time simulation of an SVC physical controller. Power system planning is an important aspect for the maintenance and reliability of the power system network. As the network increases in size and complexity the requirement of having more accurate and up-to-date models are necessary. The stability of the modified IEEE 14-Bus system is analyzed when subject to severe network disturbances in both PSS/E and Hypersim. Appropriate parameters were chosen for the SVC model in PSS/E with the SVC physical controller HIL simulation as reference. Automation played a key role in the process and highlighted its importance in terms of time and efficiency. The dynamic behavior of the SVC model was analyzed in PSS/E as well as the SVC physical control with HIL simulation in Hypersim. The main achievements of this research is summarized as given below,

- The modified IEEE 14-Bus test system is modeled successfully in PSS/E and Hypersim
- The steady state analysis is performed and the results were similar in both software platforms
- Near-ideal voltage source is modeled successfully. Dynamic analysis of the test system is performed in both the platforms.
- The process of running dynamics in PSS/E is successfully automated along with the automation of comparing the two platforms and finding the appropriate parameters based on the error function stated in chapter 3.
- The automation method is implemented successfully to modify parameters in PSS/E for the near-ideal voltage source based on the error function to reduce the difference between the two platforms
- The optimal location for the SVC is found to clearly analyze the response of the SVC when subject to network disturbances by reducing the difference of the two software.
- The parameters of the SVC is found with the methodology in chapter 3 to bring its response closer to the response of the SVC physical controller. Dynamic response of the SVCs are analyzed in PSS/E and Hypersim

6.2 Future Work

This study enables the use of automation techniques for modeling power system devices. The methodology proposed can be used in the modeling other components such as generators,

loads etc.

When the simulation software being used is updated, this methodology can also be used to update models of different components that are already in use with previous response of the model or response from the field. This helps in retaining the accuracy of the models and making the power system studies more reliable and effective.

This methodology can be used in any simulation software that enables its usage through scripting methods.

The models that are previously in use can be verified against the physical controller or the response of the devices from the field to ensure that the models in use are correct and reliable. This methodology can also be used to bring the responses of the models already in use closer to the required response and modify the models accordingly.

This study can also help in realizing that automation of various processes in power system studies are fast-approaching and inevitable. It enables reliable operation of analysis methodologies by reducing human error. It is also much faster and efficient when compared to manual testing and analysis. The data results can be modified and portrayed in various formats according to what is necessary and needed.

Bibliography

[1] IEEE Guide for the Functional Specification of Transmission Static Var Compensators. Technical report, IEEE Std. 1031, 2011.

[2] U.S. Energy Information Administration. How Electricity is Delivered to Consumers. https://www.eia.gov/Energyexplained/index.cfm?page=electricity_delivery, 2016.

[3] J Bélanger, P Venne, and JN Paquin. The What, Where and Why of Real-Time Simulation. *Planet RT*, 1(0):1, 2010.

[4] Keith Bell. Methods and Tools for Planning the Future Power System: Issues and Priorities. 2015.

[5] Arthur R. Bergen and Vijay Vittal. *Power Systems Analysis*. 2000.

[6] Seung Tae Cha, Qiuwei Wu, Arne Hejde Nielsen, Jacob Østergaard, and In Kwon Park. Real-Time Hardware-in-the-Loop (HIL) Testing for Power Electronics Controllers. In *Power and Energy Engineering Conference (APPEEC), 2012 Asia-Pacific*, pages 1–6. IEEE, 2012.

[7] Illinois Center for a Smarter Electric Grid (ICSEG). IEEE 14-Bus System. http://publish.illinois.edu/smartergrid/case-2-ieee-14-bus-systems, 2014.

[8] Paul Forsyth, Rick Kuffel, Rudi Wierckx, Jin-Boo Choo, Yong-Beum Yoon, and Tae-Kyun Kim. Comparison of Transient Stability Analysis and Large-Scale Real Time

Digital Simulation. In *Power Tech Proceedings, 2001 IEEE Porto*, volume 4, pages 7–pp. IEEE, 2001.

[9] Charles A. Gross. *Power System Analysis*. 1979.

[10] Xavier Guillaud, M Omar Faruque, Alexandre Teninge, Ali Hasan Hariri, Luigi Vanfretti, Mario Paolone, Venkata Dinavahi, Pinaki Mitra, Georg Lauss, Christian Dufour, et al. Applications of Real-Time Simulation Technologies in Power and Energy Systems. *IEEE Power and Energy Technology Systems Journal*, 2(3):103–115, 2015.

[11] Laszlo Gyugyi. Reactive Power Generation and Control by Thyristor Circuits. *IEEE Transactions on Industry applications*, (5):521–532, 1979.

[12] Narain G Hingorani, Laszlo Gyugyi, and Mohamed El-Hawary. *Understanding FACTS: Concepts and Technology of Flexible AC Transmission Systems*, volume 2. Wiley Online Library, 2000.

[13] P. K. Iyambo and R. Tzoneva. Transient Stability Analysis of the IEEE 14-Bus Electric Power System. In *AFRICON 2007*, pages 1–9, Sept 2007.

[14] Prabha Kundur, Neal J Balu, and Mark G Lauby. *Power System Stability and Control*, volume 7. McGraw-hill New York, 1994.

[15] Kerstin Lindén and Inger Segerqvist. Modelling of Load Devices and Studying Load or System Characteristics. Master's thesis, Chalmers University of Technology, August 1992.

[16] Jan Machowski, Janusz Bialek, and James Richard Bumby. *Power System Dynamics and Stability*. John Wiley & Sons, 1997.

[17] Surekha Manoj and PS Puttaswamy. Importance of FACTS Controllers in Power Systems. *International Journal of Advanced Engineering Technology*, 2(3):207–212, 2011.

[18] R Mohan Mathur and Rajiv K Varma. *Thyristor-based FACTS Controllers for Electrical Transmission Systems*. John Wiley & Sons, 2002.

[19] PM Menghal and A Jaya Laxmi. Real Time Simulation: Recent Progress & Challenges. In *Power, Signals, Controls and Computation (EPSCICON), 2012 International Conference on*, pages 1–6. IEEE, 2012.

[20] Sowmya Munukuntla, Rastin Rastgoufard, and Parviz Rastgoufard. Sensitivity Analysis of Synchronous Generators for Real-Time Simulations. In *Green Energy and Systems Conference (IGSEC), 2016 IEEE*, pages 1–6. IEEE, 2016.

[21] Shravana Musunuri and Gholamreza Dehnavi. Comparison of STATCOM, SVC, TCSC, and SSSC Performance in Steady State Voltage Stability Improvement. In *North American Power Symposium (NAPS), 2010*, pages 1–7. IEEE, 2010.

[22] North American Electric Reliability Council (NERC). Reliability Guideline - Reactive Power Planning. Technical report, 2016.

[23] Arun Pachori, Hemant Amhia, and Vikendra Moranya. Static VAR Compensation Technique for IEEE 14-Bus System. *International Journal of Emerging Technology and Advanced Engineering*, 3, 2013.

[24] Sidhartha Panda and NP Padhy. Power Electronics Based FACTS Controller for Stability Improvement of a Wind Energy Embedded Distribution System. *International Journal of Electronics, Circuits and Systems*, 1(1):30–37, 2007.

[25] Donghan Shi, Kun Han, Qi Chen, Peng Wang, Michael A Zagrodnik, and Gupta Amit. Credibility Analysis for Real-Time Hardware-in-the-Loop Simulation Compared Against Actual Plant. In *Power Electronics and Motion Control Conference (IPEMC-ECCE Asia), 2016 IEEE 8th International*, pages 2775–2778. IEEE, 2016.

[26] PTI Siemens. Application Program Interface PSS/E-32. Technical report, Schenectady, NY, USA, 2009.

[27] PTI Siemens. Model Library PSS/E-32. Technical report, Schenectady, NY, USA, 2009.

[28] PTI Siemens. Volume 2: Program Application Guide of PSS/E-32. Technical report, Schenectady, NY, USA, 2009.

[29] Don Somatilake. Execution of Python Program Scripts to Automate PSS/E Simulations. 2016.

[30] Rajeev Kumar Verma and Sangeeta Mishra. A Study on Transient Stability Improvement of 5-Machine 14-Bus System Using SVC. *International Journal on Recent and Innovation Trends in Computing and Communication*, 2, 2014.

[31] D. Petesch S. Dennetiér Y. Vernay, C. Martin. Hardware in the Loop Simulations to Test SVC Performances on the French Grid. *International Conference on Power Systems Transients*, 1, 2015.

Appendix

Appendix A

SVC placed at Bus-3 with Bus fault at Bus-6

Error(%)	K	$T1$	$T2$	$T3$	$T4$	$T5$	R_{min}	V_{max}	V_{min}	C_{base}	VOV
7.80770284558	50.0	0.01	0.0	0.093	0.0	0.0	0.0	1.0	0.0	300.0	0.07
7.80772808999	54	0.01	0.0	0.093	0.0	0.0	0.0	1.0	0.0	300.0	0.07
7.8077334789	52	0.01	0.0	0.093	0.0	0.0	0.0	1.0	0.0	300.0	0.07
7.80784707466	58	0.01	0.0	0.093	0.0	0.0	0.0	1.0	0.0	300.0	0.07
7.80789198314	56	0.01	0.0	0.093	0.0	0.0	0.0	1.0	0.0	300.0	0.07
7.80860901435	60	0.01	0.0	0.093	0.0	0.0	0.0	1.0	0.0	300.0	0.07
7.81104057629	100	0.01	0.0	0.093	0.0	0.0	0.0	1.0	0.0	300.0	0.07
7.81130319611	80	0.01	0.0	0.093	0.0	0.0	0.0	1.0	0.0	300.0	0.07
7.81145844473	70	0.01	0.0	0.093	0.0	0.0	0.0	1.0	0.0	300.0	0.07
7.81812369511	500	0.01	0.0	0.093	0.0	0.0	0.0	1.0	0.0	300.0	0.07
7.81818121246	800	0.01	0.0	0.093	0.0	0.0	0.0	1.0	0.0	300.0	0.07
7.81825959541	1000	0.01	0.0	0.093	0.0	0.0	0.0	1.0	0.0	300.0	0.07
7.81831846455	300	0.01	0.0	0.093	0.0	0.0	0.0	1.0	0.0	300.0	0.07
7.81854730006	200	0.01	0.0	0.093	0.0	0.0	0.0	1.0	0.0	300.0	0.07

Figure 1: Case A:Error Function Table of K varied

Error(%)	K	$T1$	$T2$	$T3$	$T4$	$T5$	R_{min}	V_{max}	V_{min}	C_{base}	VOV
3.04505653263	50.0	0	0.0	0.093	0.0	0.0	0.0	1.0	0.0	300.0	0.07
3.05206773975	50.0	0.002	0.0	0.093	0.0	0.0	0.0	1.0	0.0	300.0	0.07
7.70716211234	50.0	0.005	0.0	0.093	0.0	0.0	0.0	1.0	0.0	300.0	0.07
11.5687852508	50.0	0.015	0.0	0.093	0.0	0.0	0.0	1.0	0.0	300.0	0.07
12.5704102493	50.0	0.03	0.0	0.093	0.0	0.0	0.0	1.0	0.0	300.0	0.07
12.7691429707	50.0	0.009	0.0	0.093	0.0	0.0	0.0	1.0	0.0	300.0	0.07
12.8912659867	50.0	0.05	0.0	0.093	0.0	0.0	0.0	1.0	0.0	300.0	0.07
12.9641494233	50.0	0.02	0.0	0.093	0.0	0.0	0.0	1.0	0.0	300.0	0.07
13.1664175115	50.0	0.0095	0.0	0.093	0.0	0.0	0.0	1.0	0.0	300.0	0.07
13.1902581668	50.0	0.01	0.0	0.093	0.0	0.0	0.0	1.0	0.0	300.0	0.07
13.6235368464	50.0	0.04	0.0	0.093	0.0	0.0	0.0	1.0	0.0	300.0	0.07

Figure 2: Case A:Error Function Table of T_1 varied

Error(%)	K	$T1$	$T2$	$T3$	$T4$	$T5$	R_{min}	V_{max}	V_{min}	C_{base}	VOV
13.1902581668	50.0	0.01	0.002	0.093	0.0	0.0	0.0	1.0	0.0	300.0	0.07
13.1902581668	50.0	0.01	0.005	0.093	0.0	0.0	0.0	1.0	0.0	300.0	0.07
13.1902581668	50.0	0.01	0.009	0.093	0.0	0.0	0.0	1.0	0.0	300.0	0.07
13.1902581668	50.0	0.01	0.015	0.093	0.0	0.0	0.0	1.0	0.0	300.0	0.07
13.1902581668	50.0	0.01	0.01	0.093	0.0	0.0	0.0	1.0	0.0	300.0	0.07
13.1902581668	50.0	0.01	0.02	0.093	0.0	0.0	0.0	1.0	0.0	300.0	0.07
13.1902581668	50.0	0.01	0.03	0.093	0.0	0.0	0.0	1.0	0.0	300.0	0.07
13.1902581668	50.0	0.01	0.04	0.093	0.0	0.0	0.0	1.0	0.0	300.0	0.07
13.1902581668	50.0	0.01	0.05	0.093	0.0	0.0	0.0	1.0	0.0	300.0	0.07
13.1902581668	50.0	0.01	0.0	0.093	0.0	0.0	0.0	1.0	0.0	300.0	0.07
13.1902581668	50.0	0.01	0.1	0.093	0.0	0.0	0.0	1.0	0.0	300.0	0.07
13.1902581668	50.0	0.01	1e-06	0.093	0.0	0.0	0.0	1.0	0.0	300.0	0.07

Figure 3: Case A:Error Function Table of T_2 varied

Error(%)	K	$T1$	$T2$	$T3$	$T4$	$T5$	R_{min}	V_{max}	V_{min}	C_{base}	VOV
8.11366274535	50.0	0.01	0.0	0.15	0.0	0.0	0.0	1.0	0.0	300.0	0.07
12.3992244166	50.0	0.01	0.0	0.009	0.0	0.0	0.0	1.0	0.0	300.0	0.07
12.5229910801	50.0	0.01	0.0	0.005	0.0	0.0	0.0	1.0	0.0	300.0	0.07
12.5527365427	50.0	0.01	0.0	0.1	0.0	0.0	0.0	1.0	0.0	300.0	0.07
12.6552923217	50.0	0.01	0.0	0.05	0.0	0.0	0.0	1.0	0.0	300.0	0.07
12.8378904067	50.0	0.01	0.0	0.01	0.0	0.0	0.0	1.0	0.0	300.0	0.07
13.0242710785	50.0	0.01	0.0	0.02	0.0	0.0	0.0	1.0	0.0	300.0	0.07
13.1902581668	50.0	0.01	0.0	0.093	0.0	0.0	0.0	1.0	0.0	300.0	0.07
13.1902581668	50.0	0.01	0.0	0	0.0	0.0	0.0	1.0	0.0	300.0	0.07
13.2038659231	50.0	0.01	0.0	0.002	0.0	0.0	0.0	1.0	0.0	300.0	0.07
13.5739772851	50.0	0.01	0.0	0.08	0.0	0.0	0.0	1.0	0.0	300.0	0.07

Figure 4: Case A:Error Function Table of T_3 varied

Error(%)	K	$T1$	$T2$	$T3$	$T4$	$T5$	R_{min}	V_{max}	V_{min}	C_{base}	VOV
3.23160504169	50.0	0.01	0.0	0.093	0.5	0.0	0.0	1.0	0.0	300.0	0.07
3.59002222362	50.0	0.01	0.0	0.093	0.2	0.0	0.0	1.0	0.0	300.0	0.07
3.75853782402	50.0	0.01	0.0	0.093	0.002	0.0	0.0	1.0	0.0	300.0	0.07
3.78334133651	50.0	0.01	0.0	0.093	0.1	0.0	0.0	1.0	0.0	300.0	0.07
3.78590122308	50.0	0.01	0.0	0.093	0.005	0.0	0.0	1.0	0.0	300.0	0.07
3.79485375129	50.0	0.01	0.0	0.093	0.01	0.0	0.0	1.0	0.0	300.0	0.07
3.7949187945	50.0	0.01	0.0	0.093	0.08	0.0	0.0	1.0	0.0	300.0	0.07
3.79804825674	50.0	0.01	0.0	0.093	0.015	0.0	0.0	1.0	0.0	300.0	0.07
3.79951528661	50.0	0.01	0.0	0.093	0.02	0.0	0.0	1.0	0.0	300.0	0.07
3.80146401435	50.0	0.01	0.0	0.093	0.04	0.0	0.0	1.0	0.0	300.0	0.07
7.80770284558	50.0	0.01	0.0	0.093	0.0	0.0	0.0	1.0	0.0	300.0	0.07
7.80770284558	50.0	0.01	0.0	0.093	1e-06	0.0	0.0	1.0	0.0	300.0	0.07

Figure 5: Case A:Error Function Table of T_4 varied

Error(%)	K	$T1$	$T2$	$T3$	$T4$	$T5$	R_{min}	V_{max}	V_{min}	C_{base}	VOV
3.80490660751	50.0	0.01	0.0	0.093	0.0	0.05	0.0	1.0	0.0	300.0	0.07
3.80591696204	50.0	0.01	0.0	0.093	0.0	0.04	0.0	1.0	0.0	300.0	0.07
3.80829791484	50.0	0.01	0.0	0.093	0.0	0.02	0.0	1.0	0.0	300.0	0.07
3.8129174583	50.0	0.01	0.0	0.093	0.0	0.01	0.0	1.0	0.0	300.0	0.07
3.81391290177	50.0	0.01	0.0	0.093	0.0	0.009	0.0	1.0	0.0	300.0	0.07
3.82119692259	50.0	0.01	0.0	0.093	0.0	0.005	0.0	1.0	0.0	300.0	0.07
3.84928731388	50.0	0.01	0.0	0.093	0.0	0.002	0.0	1.0	0.0	300.0	0.07
3.8984669327	50.0	0.01	0.0	0.093	0.0	0.001	0.0	1.0	0.0	300.0	0.07
7.80770284558	50.0	0.01	0.0	0.093	0.0	0.0	0.0	1.0	0.0	300.0	0.07

Figure 6: Case A:Error Function Table of T_5 varied

SVC placed at Bus-3 with Bus fault at Bus-14

Error(%)	K	$T1$	$T2$	$T3$	$T4$	$T5$	R_{min}	V_{max}	V_{min}	C_{base}	VOV
7.10453882546	58	0.01	0.0	0.093	0.0	0.0	0.0	1.0	0.0	300.0	0.07
7.1046304694	54	0.01	0.0	0.093	0.0	0.0	0.0	1.0	0.0	300.0	0.07
7.10466277049	56	0.01	0.0	0.093	0.0	0.0	0.0	1.0	0.0	300.0	0.07
7.10474592362	50.0	0.01	0.0	0.093	0.0	0.0	0.0	1.0	0.0	300.0	0.07
7.10475196026	52	0.01	0.0	0.093	0.0	0.0	0.0	1.0	0.0	300.0	0.07
7.10519530894	60	0.01	0.0	0.093	0.0	0.0	0.0	1.0	0.0	300.0	0.07
7.10791070492	100	0.01	0.0	0.093	0.0	0.0	0.0	1.0	0.0	300.0	0.07
7.10800600037	80	0.01	0.0	0.093	0.0	0.0	0.0	1.0	0.0	300.0	0.07
7.10804683306	70	0.01	0.0	0.093	0.0	0.0	0.0	1.0	0.0	300.0	0.07
7.1144440258	1000	0.01	0.0	0.093	0.0	0.0	0.0	1.0	0.0	300.0	0.07
7.11444692255	500	0.01	0.0	0.093	0.0	0.0	0.0	1.0	0.0	300.0	0.07
7.11447638865	800	0.01	0.0	0.093	0.0	0.0	0.0	1.0	0.0	300.0	0.07
7.11452749885	300	0.01	0.0	0.093	0.0	0.0	0.0	1.0	0.0	300.0	0.07
7.11473625211	200	0.01	0.0	0.093	0.0	0.0	0.0	1.0	0.0	300.0	0.07

Figure 7: Case B:Error Function Table of K varied

Error(%)	K	$T1$	$T2$	$T3$	$T4$	$T5$	R_{min}	V_{max}	V_{min}	C_{base}	VOV
2.42300798337	50.0	0	0.0	0.093	0.0	0.0	0.0	1.0	0.0	300.0	0.07
2.43643376927	50.0	0.002	0.0	0.093	0.0	0.0	0.0	1.0	0.0	300.0	0.07
11.4736808106	50.0	0.005	0.0	0.093	0.0	0.0	0.0	1.0	0.0	300.0	0.07
14.2562477111	50.0	0.0095	0.0	0.093	0.0	0.0	0.0	1.0	0.0	300.0	0.07
14.3396309553	50.0	0.03	0.0	0.093	0.0	0.0	0.0	1.0	0.0	300.0	0.07
14.3615918355	50.0	0.01	0.0	0.093	0.0	0.0	0.0	1.0	0.0	300.0	0.07
14.4006539249	50.0	0.05	0.0	0.093	0.0	0.0	0.0	1.0	0.0	300.0	0.07
14.7601712023	50.0	0.015	0.0	0.093	0.0	0.0	0.0	1.0	0.0	300.0	0.07
14.8625125072	50.0	0.02	0.0	0.093	0.0	0.0	0.0	1.0	0.0	300.0	0.07
15.3544283948	50.0	0.04	0.0	0.093	0.0	0.0	0.0	1.0	0.0	300.0	0.07
15.4891842427	50.0	0.009	0.0	0.093	0.0	0.0	0.0	1.0	0.0	300.0	0.07

Figure 8: Case B:Error Function Table of T_1 varied

Error(%)	K	$T1$	$T2$	$T3$	$T4$	$T5$	R_{min}	V_{max}	V_{min}	C_{base}	VOV
14.3615918355	50.0	0.01	0.002	0.093	0.0	0.0	0.0	1.0	0.0	300.0	0.07
14.3615918355	50.0	0.01	0.005	0.093	0.0	0.0	0.0	1.0	0.0	300.0	0.07
14.3615918355	50.0	0.01	0.009	0.093	0.0	0.0	0.0	1.0	0.0	300.0	0.07
14.3615918355	50.0	0.01	0.015	0.093	0.0	0.0	0.0	1.0	0.0	300.0	0.07
14.3615918355	50.0	0.01	0.01	0.093	0.0	0.0	0.0	1.0	0.0	300.0	0.07
14.3615918355	50.0	0.01	0.02	0.093	0.0	0.0	0.0	1.0	0.0	300.0	0.07
14.3615918355	50.0	0.01	0.03	0.093	0.0	0.0	0.0	1.0	0.0	300.0	0.07
14.3615918355	50.0	0.01	0.04	0.093	0.0	0.0	0.0	1.0	0.0	300.0	0.07
14.3615918355	50.0	0.01	0.05	0.093	0.0	0.0	0.0	1.0	0.0	300.0	0.07
14.3615918355	50.0	0.01	0.0	0.093	0.0	0.0	0.0	1.0	0.0	300.0	0.07
14.3615918355	50.0	0.01	0.1	0.093	0.0	0.0	0.0	1.0	0.0	300.0	0.07
14.3615918355	50.0	0.01	1e-06	0.093	0.0	0.0	0.0	1.0	0.0	300.0	0.07

Figure 9: Case B:Error Function Table of T_2 varied

Error(%)	K	$T1$	$T2$	$T3$	$T4$	$T5$	R_{min}	V_{max}	V_{min}	C_{base}	VOV
12.4844139505	50.0	0.01	0.0	0.15	0.0	0.0	0.0	1.0	0.0	300.0	0.07
14.266218884	50.0	0.01	0.0	0.002	0.0	0.0	0.0	1.0	0.0	300.0	0.07
14.3615918355	50.0	0.01	0.0	0.093	0.0	0.0	0.0	1.0	0.0	300.0	0.07
14.3615918355	50.0	0.01	0.0	0	0.0	0.0	0.0	1.0	0.0	300.0	0.07
14.478774997	50.0	0.01	0.0	0.1	0.0	0.0	0.0	1.0	0.0	300.0	0.07
14.5363676448	50.0	0.01	0.0	0.005	0.0	0.0	0.0	1.0	0.0	300.0	0.07
14.9117819365	50.0	0.01	0.0	0.05	0.0	0.0	0.0	1.0	0.0	300.0	0.07
15.0490776551	50.0	0.01	0.0	0.01	0.0	0.0	0.0	1.0	0.0	300.0	0.07
15.191782695	50.0	0.01	0.0	0.08	0.0	0.0	0.0	1.0	0.0	300.0	0.07
15.1932345236	50.0	0.01	0.0	0.009	0.0	0.0	0.0	1.0	0.0	300.0	0.07
15.3076450292	50.0	0.01	0.0	0.02	0.0	0.0	0.0	1.0	0.0	300.0	0.07

Figure 10: Case B:Error Function Table of T_3 varied

Error(%)	K	$T1$	$T2$	$T3$	$T4$	$T5$	R_{min}	V_{max}	V_{min}	C_{base}	VOV
2.61445262859	50.0	0.01	0.0	0.093	0.5	0.0	0.0	1.0	0.0	300.0	0.07
3.00935313227	50.0	0.01	0.0	0.093	0.2	0.0	0.0	1.0	0.0	300.0	0.07
3.19471871056	50.0	0.01	0.0	0.093	0.002	0.0	0.0	1.0	0.0	300.0	0.07
3.21859856529	50.0	0.01	0.0	0.093	0.1	0.0	0.0	1.0	0.0	300.0	0.07
3.22301823825	50.0	0.01	0.0	0.093	0.005	0.0	0.0	1.0	0.0	300.0	0.07
3.2292351691	50.0	0.01	0.0	0.093	0.08	0.0	0.0	1.0	0.0	300.0	0.07
3.23239066844	50.0	0.01	0.0	0.093	0.01	0.0	0.0	1.0	0.0	300.0	0.07
3.23498199672	50.0	0.01	0.0	0.093	0.015	0.0	0.0	1.0	0.0	300.0	0.07
3.23656530902	50.0	0.01	0.0	0.093	0.02	0.0	0.0	1.0	0.0	300.0	0.07
3.2386077134	50.0	0.01	0.0	0.093	0.04	0.0	0.0	1.0	0.0	300.0	0.07
7.10474592362	50.0	0.01	0.0	0.093	0.0	0.0	0.0	1.0	0.0	300.0	0.07
7.10474592362	50.0	0.01	0.0	0.093	1e-06	0.0	0.0	1.0	0.0	300.0	0.07

Figure 11: Case B:Error Function Table of T_4 varied

Error(%)	K	$T1$	$T2$	$T3$	$T4$	$T5$	R_{min}	V_{max}	V_{min}	C_{base}	VOV
3.2420888475	50.0	0.01	0.0	0.093	0.0	0.05	0.0	1.0	0.0	300.0	0.07
3.2432577793	50.0	0.01	0.0	0.093	0.0	0.04	0.0	1.0	0.0	300.0	0.07
3.24586538053	50.0	0.01	0.0	0.093	0.0	0.02	0.0	1.0	0.0	300.0	0.07
3.25065444394	50.0	0.01	0.0	0.093	0.0	0.01	0.0	1.0	0.0	300.0	0.07
3.25158145602	50.0	0.01	0.0	0.093	0.0	0.009	0.0	1.0	0.0	300.0	0.07
3.26079149159	50.0	0.01	0.0	0.093	0.0	0.005	0.0	1.0	0.0	300.0	0.07
3.29002525693	50.0	0.01	0.0	0.093	0.0	0.002	0.0	1.0	0.0	300.0	0.07
3.34122981868	50.0	0.01	0.0	0.093	0.0	0.001	0.0	1.0	0.0	300.0	0.07
7.10474592362	50.0	0.01	0.0	0.093	0.0	0.0	0.0	1.0	0.0	300.0	0.07

Figure 12: Case B:Error Function Table of T_5 varied

All parameters varied simultaneously.

Error(%)	K	$T1$	$T2$	$T3$	$T4$	$T5$	R_{min}	V_{max}	V_{min}	C_{base}	VOV
3.03028052446	100	0	0.0	0.3	0.002	0.02	0.0	1.0	0.0	300.0	0.07
3.03035388086	100	0	0.0	0.3	0.02	0.002	0.0	1.0	0.0	300.0	0.07
3.03038159951	50.0	0	0.0	0.15	0.002	0.02	0.0	1.0	0.0	300.0	0.07
3.03040165596	50.0	0	0.0	0.15	0.02	0.002	0.0	1.0	0.0	300.0	0.07
3.03086194466	50.0	0	0.002	0.15	0.01	0.01	0.0	1.0	0.0	300.0	0.07
3.03095326512	100	0	0.002	0.3	0.01	0.01	0.0	1.0	0.0	300.0	0.07
3.03112834935	100	0	0.002	0.3	0.02	0.002	0.0	1.0	0.0	300.0	0.07
3.03121683474	70	0	0.0	0.15	0.02	0.002	0.0	1.0	0.0	300.0	0.07
3.03125593975	100	0	0.0	0.3	0.02	0.0001	0.0	1.0	0.0	300.0	0.07
3.03125918534	70	0	0.0	0.15	0.002	0.02	0.0	1.0	0.0	300.0	0.07
3.03126613385	100	0	0.0	0.3	0.0001	0.02	0.0	1.0	0.0	300.0	0.07
3.03126613385	100	0	0.05	0.3	0.0001	0.02	0.0	1.0	0.0	300.0	0.07
3.03126613385	100	0	0.005	0.3	0.0001	0.02	0.0	1.0	0.0	300.0	0.07
3.03126613385	100	0	0.002	0.3	0.0001	0.02	0.0	1.0	0.0	300.0	0.07
3.03126613385	100	0	0.02	0.3	0.02	0.02	0.0	1.0	0.0	300.0	0.07
3.03126613385	100	0	0.02	0.3	0.0001	0.02	0.0	1.0	0.0	300.0	0.07
3.03126613385	100	0	0.002	0.3	0.002	0.02	0.0	1.0	0.0	300.0	0.07
3.03151226543	50.0	0	0.0	0.15	0.02	0.0001	0.0	1.0	0.0	300.0	0.07
3.03162955773	50.0	0	0.0	0.15	0.0001	0.02	0.0	1.0	0.0	300.0	0.07
3.03162955773	50.0	0	0.002	0.15	0.002	0.02	0.0	1.0	0.0	300.0	0.07

Figure 13: Error Function Table with SVC at Bus-3 with Bus-6 fault

Error(%)	K	$T1$	$T2$	$T3$	$T4$	$T5$	R_{min}	V_{max}	V_{min}	C_{base}	VOV
2.40906099699	70	0	0.0	0.3	0.002	0.02	0.0	1.0	0.0	300.0	0.07
2.40940301076	50.0	0	0.0	0.3	0.01	0.01	0.0	1.0	0.0	300.0	0.07
2.40955027271	100	0	0.0	0.5	0.002	0.02	0.0	1.0	0.0	300.0	0.07
2.40959687923	50.0	0	0.0	0.3	0.002	0.01	0.0	1.0	0.0	300.0	0.07
2.40959735825	50.0	0	0.0	0.3	0.01	0.002	0.0	1.0	0.0	300.0	0.07
2.40963417018	70	0	0.0	0.3	0.02	0.002	0.0	1.0	0.0	300.0	0.07
2.40964277797	100	0	0.0	0.5	0.02	0.002	0.0	1.0	0.0	300.0	0.07
2.40978632149	70	0	0.002	0.5	0.01	0.01	0.0	1.0	0.0	300.0	0.07
2.40978925943	50.0	0	0.002	0.3	0.01	0.01	0.0	1.0	0.0	300.0	0.07
2.40982594312	100	0	0.005	0.5	0.01	0.01	0.0	1.0	0.0	300.0	0.07
2.40989378028	70	0	0.0	0.5	0.01	0.0001	0.0	1.0	0.0	300.0	0.07
2.40989767717	50.0	0	0.0	0.3	0.02	0.002	0.0	1.0	0.0	300.0	0.07
2.40990744801	100	0	0.0	0.5	0.01	0.01	0.0	1.0	0.0	300.0	0.07
2.40991490485	50.0	0	0.0	0.3	0.002	0.02	0.0	1.0	0.0	300.0	0.07
2.40994957171	70	0	0.002	0.3	0.02	0.002	0.0	1.0	0.0	300.0	0.07
2.40995983196	100	0	0.002	0.5	0.01	0.01	0.0	1.0	0.0	300.0	0.07
2.40996480665	100	0	0.02	0.5	0.0001	0.02	0.0	1.0	0.0	300.0	0.07
2.40996480665	100	0	0.002	0.5	0.0001	0.02	0.0	1.0	0.0	300.0	0.07
2.40996480665	100	0	0.05	0.5	0.0001	0.02	0.0	1.0	0.0	300.0	0.07
2.40996480665	100	0	0.005	0.5	0.0001	0.02	0.0	1.0	0.0	300.0	0.07

Figure 14: Error Function Table with SVC at Bus-3 with Bus-14 fault

Error(%)	K	$T1$	$T2$	$T3$	$T4$	$T5$	R_{min}	V_{max}	V_{min}	C_{base}	VOV
3.21479915177	100	0	0.05	0.01	0.01	0.0	0.0	1.0	0.0	300.0	0.07
3.21793240677	56	0	0.05	0.01	0.01	0.0	0.0	1.0	0.0	300.0	0.07
3.21895663481	100	0	0.02	0.01	0.01	0.0	0.0	1.0	0.0	300.0	0.07
3.22102787137	100	0	0.0	0.002	0.0	0.0	0.0	1.0	0.0	300.0	0.07
3.22102787137	100	0	0.005	0.002	0.0	0.0	0.0	1.0	0.0	300.0	0.07
3.22102787137	100	0	0.05	0.002	0.0	0.0	0.0	1.0	0.0	300.0	0.07
3.22102787137	100	0	0.002	0.002	0.0	0.0	0.0	1.0	0.0	300.0	0.07
3.22102787137	100	0	0.02	0.002	0.0	0.0	0.0	1.0	0.0	300.0	0.07
3.22102787137	100	0	1e-06	0.002	0.0	0.0	0.0	1.0	0.0	300.0	0.07
3.22207353177	50.0	0	0.05	0.01	0.01	0.0	0.0	1.0	0.0	300.0	0.07
3.22459666431	100	0	0.002	0.01	0.0	0.0	0.0	1.0	0.0	300.0	0.07
3.22459666431	100	0	0.005	0.01	0.0	0.0	0.0	1.0	0.0	300.0	0.07
3.22459666431	100	0	1e-06	0.01	0.0	0.0	0.0	1.0	0.0	300.0	0.07
3.22459666431	100	0	0.05	0.01	0.0	0.0	0.0	1.0	0.0	300.0	0.07
3.22459666431	100	0	0.0	0.01	0.0	0.0	0.0	1.0	0.0	300.0	0.07
3.22459666431	100	0	0.02	0.01	0.0	0.0	0.0	1.0	0.0	300.0	0.07
3.22678783716	56	0	0.02	0.002	0.01	0.0	0.0	1.0	0.0	300.0	0.07
3.23049553506	56	0	0.02	0.01	0.01	0.0	0.0	1.0	0.0	300.0	0.07
3.23059336466	56	0	1e-06	0.002	0.0	0.0	0.0	1.0	0.0	300.0	0.07

Figure 15: Error Function Table with SVC at Bus-4 with Bus-3 fault

Error(%)	K	$T1$	$T2$	$T3$	$T4$	$T5$	R_{min}	V_{max}	V_{min}	C_{base}	VOV
3.63907130286	50.0	0	0.05	0.01	0.01	0.0	0.0	1.0	0.0	300.0	0.07
3.63952909269	56	0	0.05	0.01	0.01	0.0	0.0	1.0	0.0	300.0	0.07
3.64733750438	100	0	0.05	0.01	0.01	0.0	0.0	1.0	0.0	300.0	0.07
3.65142323747	56	0	0.02	0.002	0.01	0.0	0.0	1.0	0.0	300.0	0.07
3.65296824532	50.0	0	0.02	0.002	0.01	0.0	0.0	1.0	0.0	300.0	0.07
3.65408597242	50.0	0	0.05	0.002	0.0	0.0	0.0	1.0	0.0	300.0	0.07
3.65408597242	50.0	0	0.005	0.002	0.0	0.0	0.0	1.0	0.0	300.0	0.07
3.65408597242	50.0	0	0.0	0.002	0.0	0.0	0.0	1.0	0.0	300.0	0.07
3.65408597242	50.0	0	0.02	0.002	0.0	0.0	0.0	1.0	0.0	300.0	0.07
3.65408597242	50.0	0	0.002	0.002	0.0	0.0	0.0	1.0	0.0	300.0	0.07
3.65408597242	50.0	0	1e-06	0.002	0.0	0.0	0.0	1.0	0.0	300.0	0.07
3.65468426884	56	0	1e-06	0.002	0.0	0.0	0.0	1.0	0.0	300.0	0.07
3.65468426884	56	0	0.0	0.002	0.0	0.0	0.0	1.0	0.0	300.0	0.07
3.65468426884	56	0	0.002	0.002	0.0	0.0	0.0	1.0	0.0	300.0	0.07
3.65468426884	56	0	0.005	0.002	0.0	0.0	0.0	1.0	0.0	300.0	0.07
3.65468426884	56	0	0.02	0.002	0.0	0.0	0.0	1.0	0.0	300.0	0.07
3.65468426884	56	0	0.05	0.002	0.0	0.0	0.0	1.0	0.0	300.0	0.07
3.65482339015	100	0	0.02	0.01	0.01	0.0	0.0	1.0	0.0	300.0	0.07
3.65579717403	100	0	0.005	0.002	0.0	0.0	0.0	1.0	0.0	300.0	0.07

Figure 16: Error Function Table with SVC at Bus-4 with Bus-12 fault

Appendix B

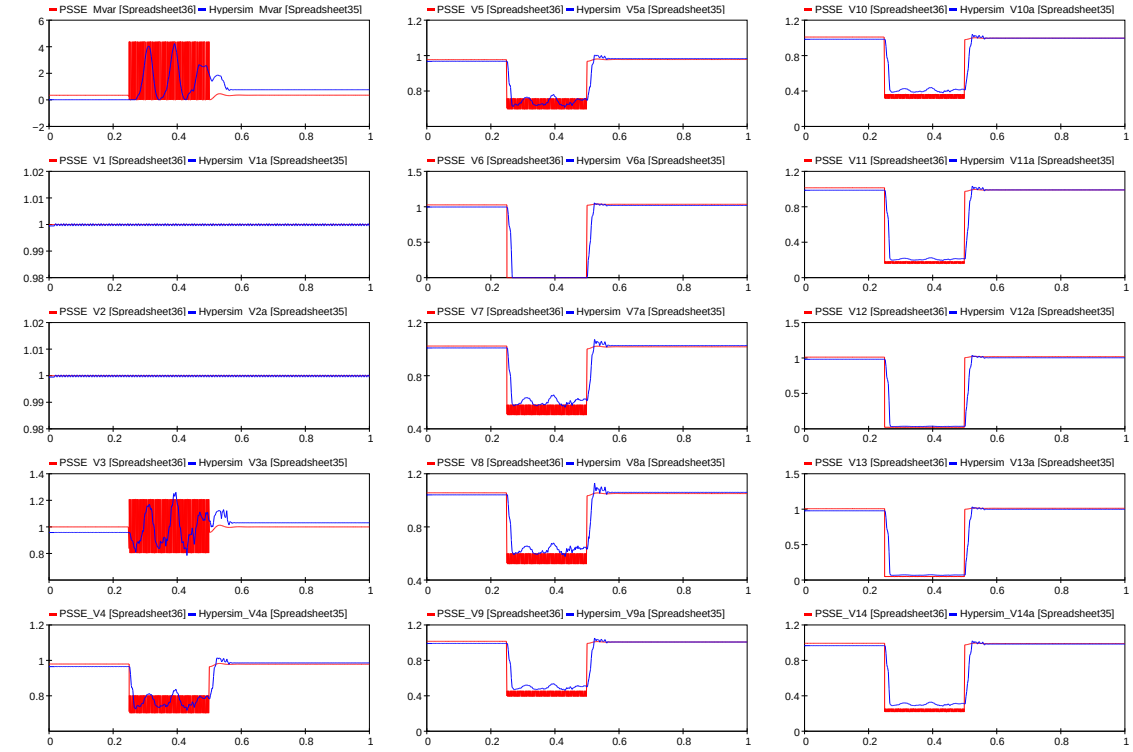

Figure 17: Bus 6 fault with SVC at Bus 3

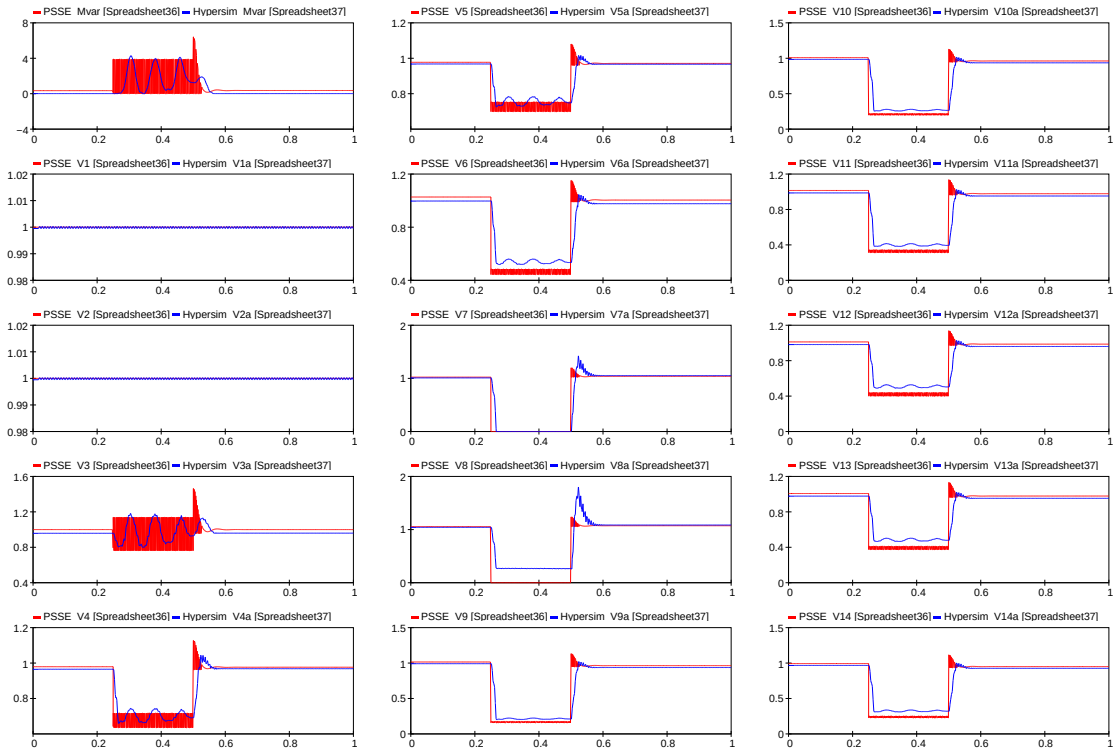

[Spreadsheet36] case7_csv_svc@3 − E:\Individual\Malavika\2017\14bus_with_SVC\Psse_thesis_results\svc@3
[Spreadsheet37] bus7fault_svcbus3 − E:\Individual\Malavika\2017\14bus_with_SVC\hyper_test_cases_3_30_2017\svc@3
Printed for p 1

Figure 18: Bus 7 fault with SVC at Bus 3

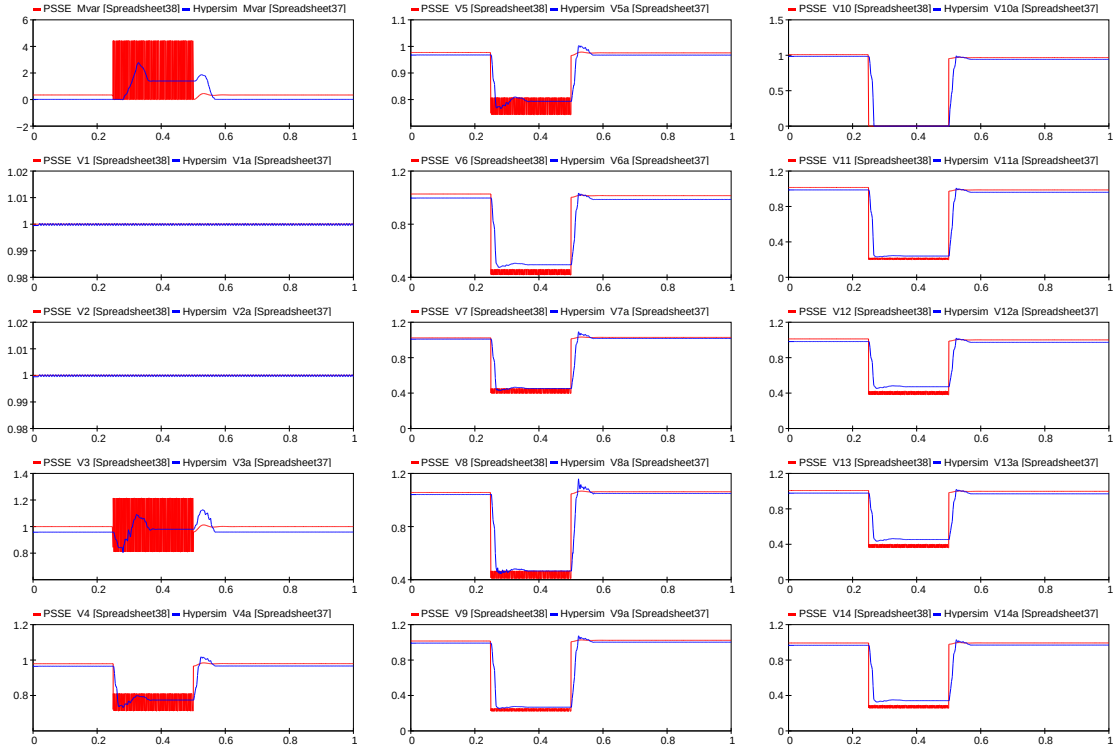

[Spreadsheet37] bus10fault_svcbus3 − E:\Individual\Malavika\2017\14bus_with_SVC\hyper_test_cases_3_30_2017\svc@3
[Spreadsheet38] case10_csv_svc@3 − E:\Individual\Malavika\2017\14bus_with_SVC\Psse_thesis_results\svc@3
Printed for p 1

Figure 19: Bus 10 fault with SVC at Bus 3

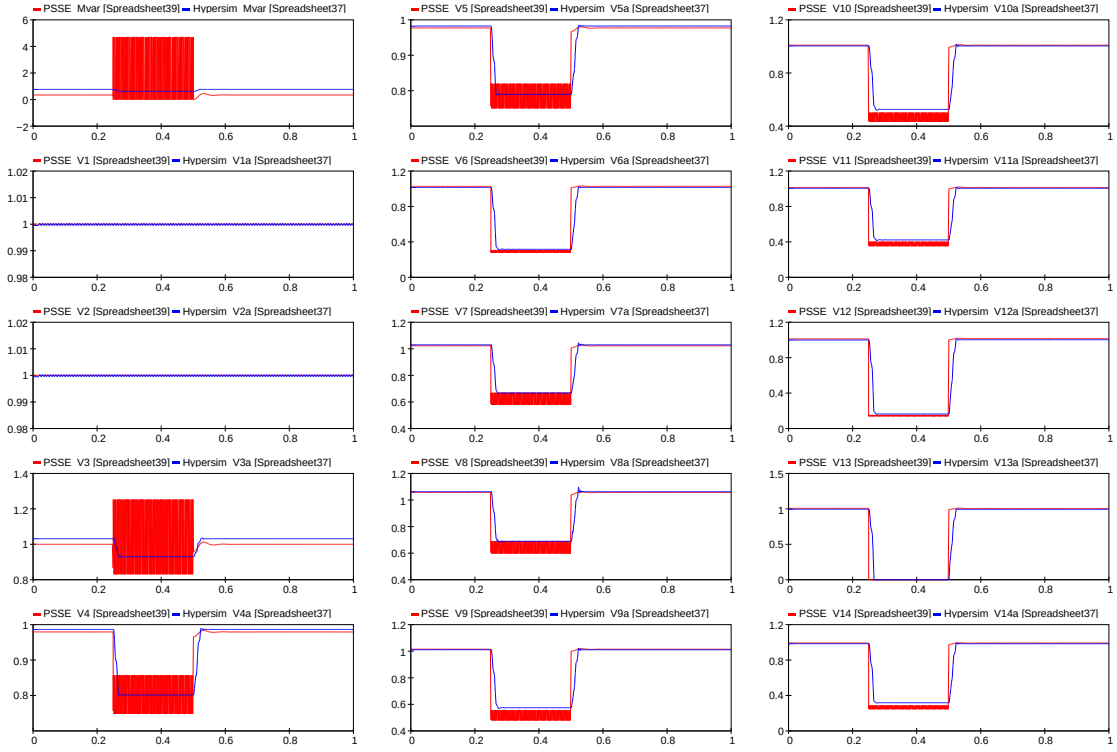

Figure 20: Bus 14 fault with SVC at Bus 3

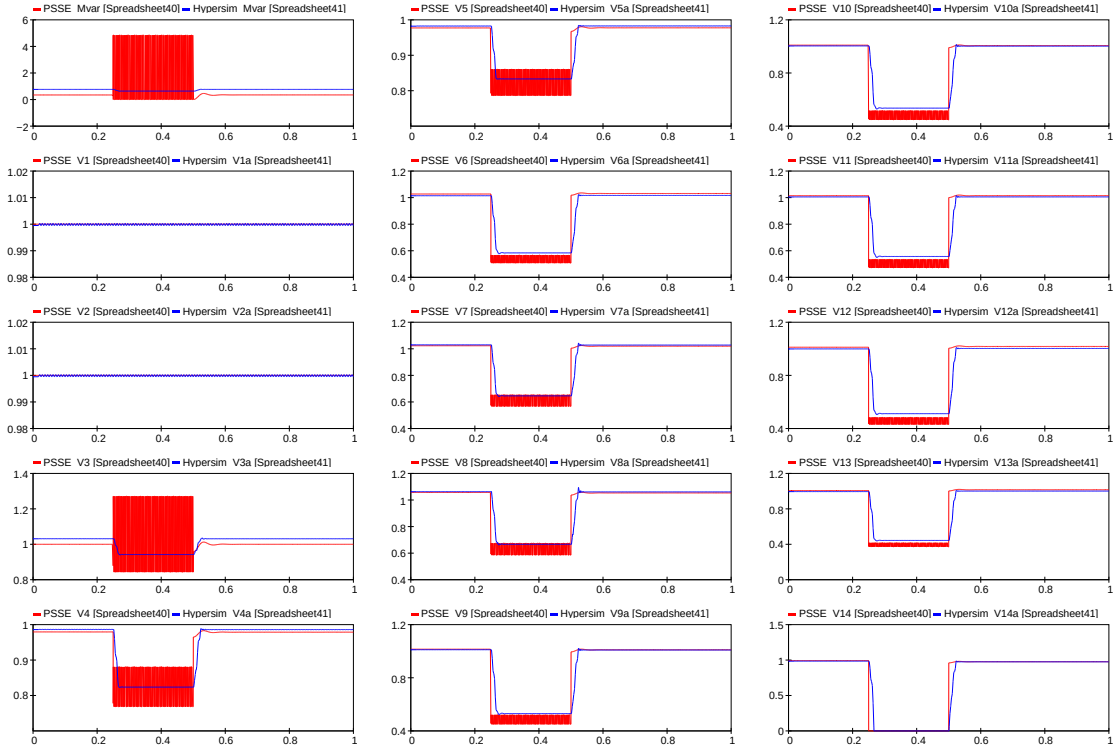

[Spreadsheet40] case14_csv_svc@3 − E:\Individual\Malavika\2017\14bus_with_SVC\Psse_thesis_results\svc@3
[Spreadsheet41] bus14fault_svcbus3 − E:\Individual\Malavika\2017\14bus_with_SVC\hyper_test_cases_3_30_2017\svc@3
Printed for p 1

Figure 21: Bus 6 fault with SVC at Bus 3

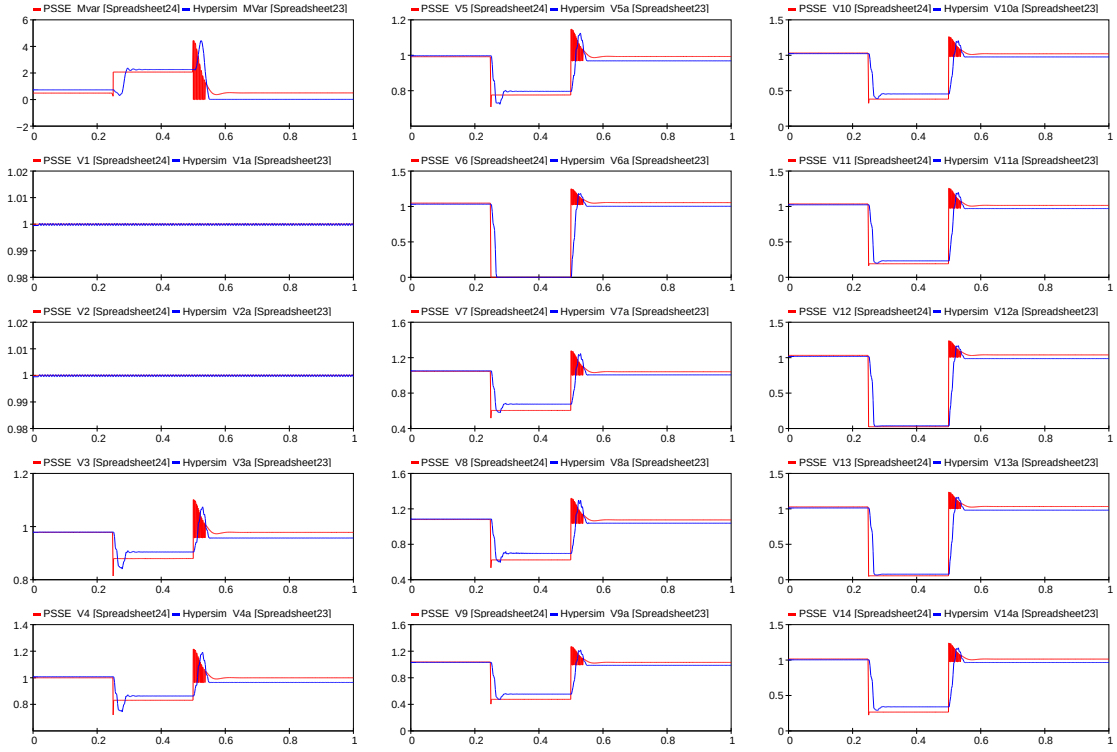

Figure 22: Bus 6 fault with SVC at Bus 4

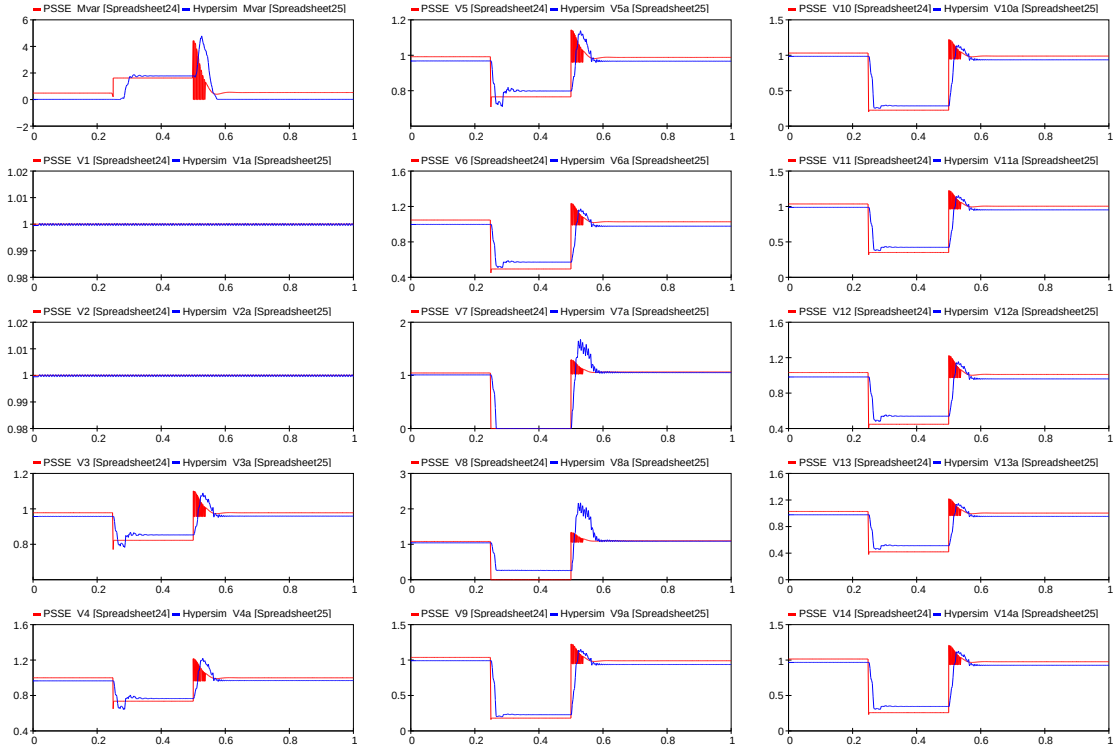

Figure 23: Bus 7 fault with SVC at Bus 4

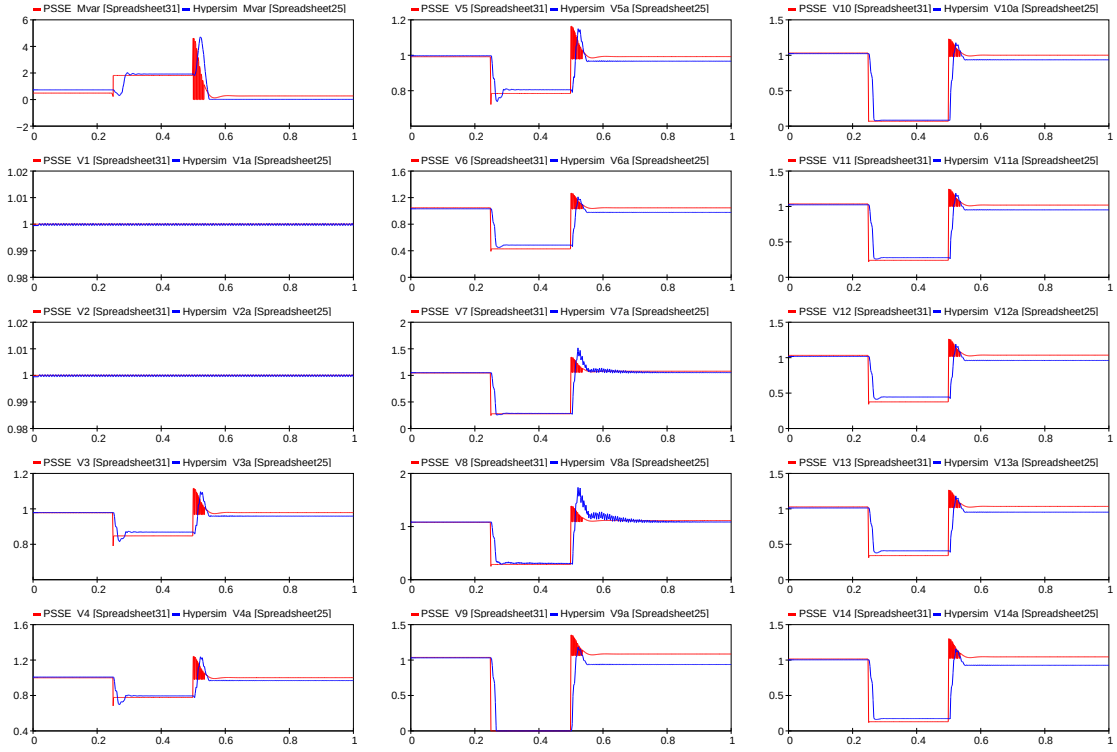

Figure 24: Bus 9 fault with SVC at Bus 4

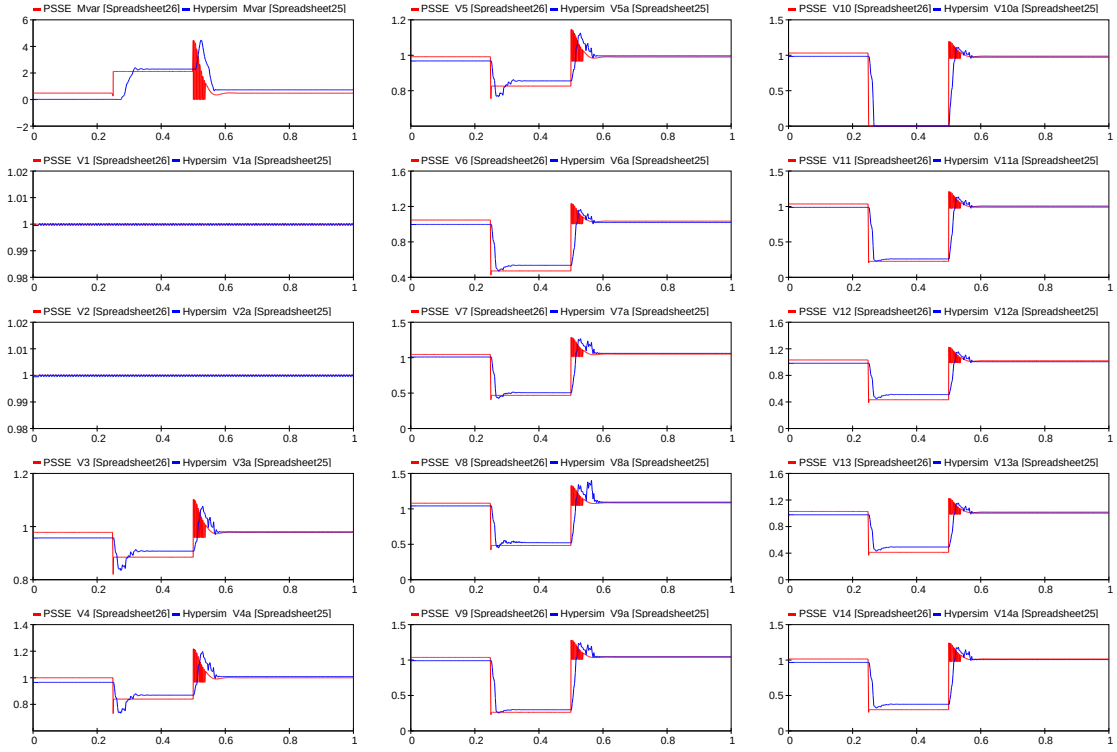

Figure 25: Bus 10 fault with SVC at Bus 4

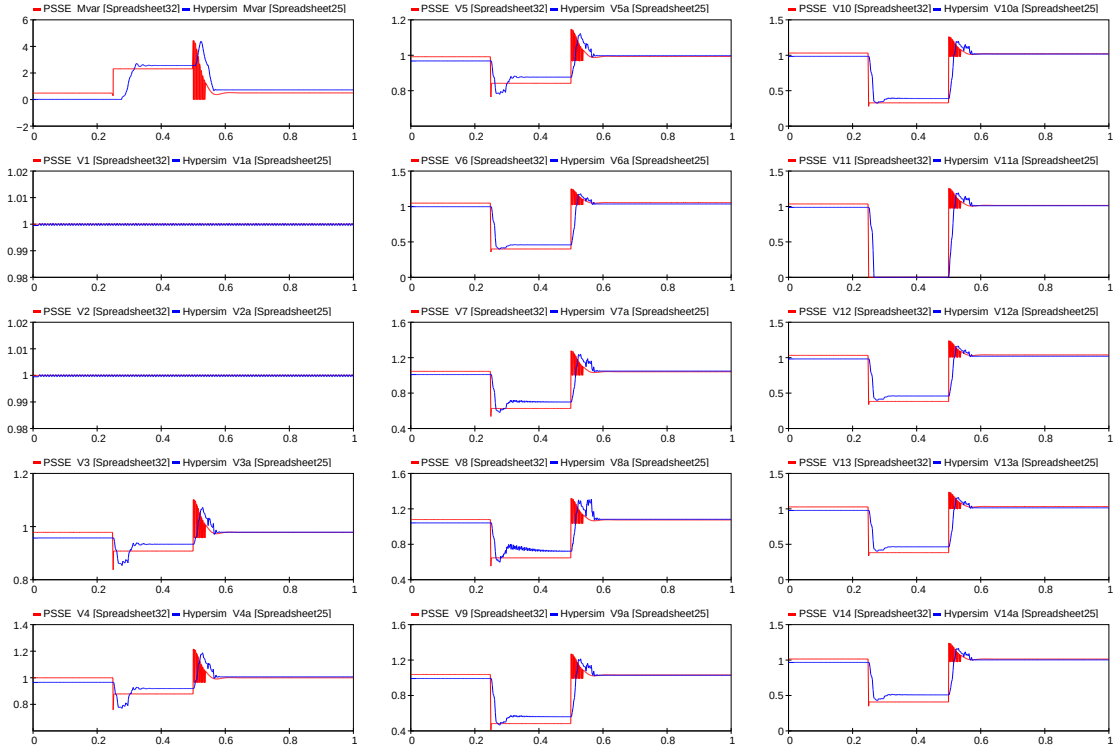

Figure 26: Bus 11 fault with SVC at Bus 4

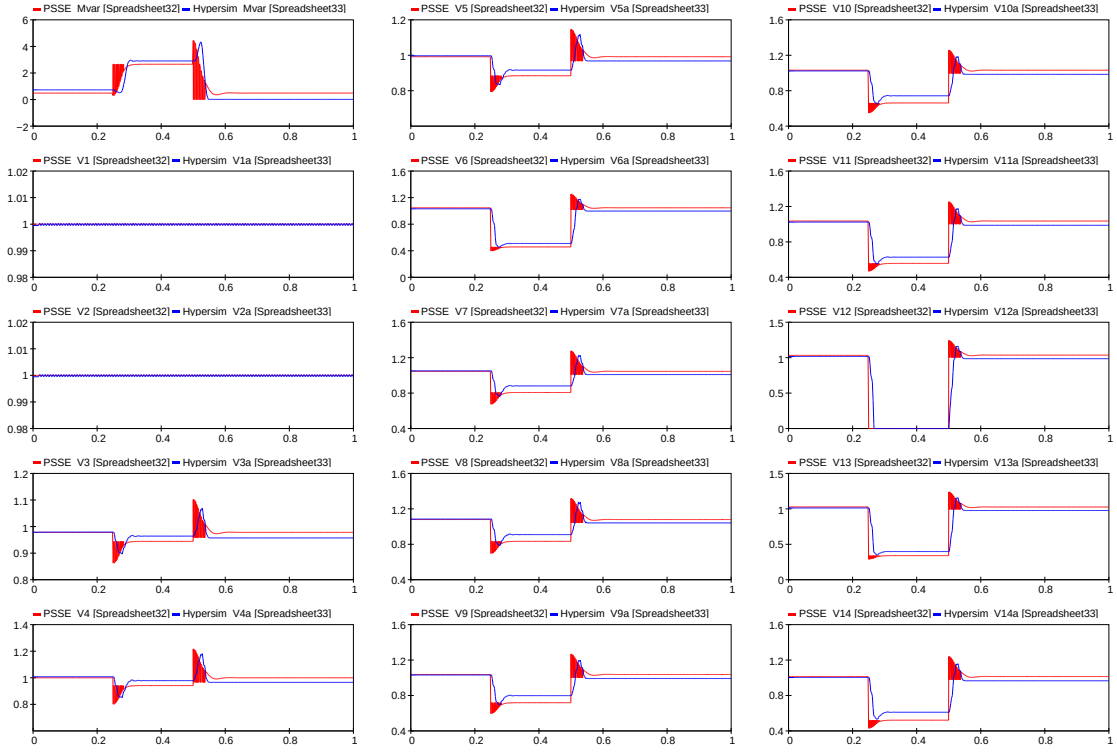

[Spreadsheet32] case12_csv_svc@4 − E:\Individual\Malavika\2017\14bus_with_SVC\Psse_thesis_results\svc@4
[Spreadsheet33] bus12fault_svcbus4 − E:\Individual\Malavika\2017\14bus_with_SVC\hyper_test_cases_3_30_2017\svc@4
Printed for p 1

Figure 27: Bus 12 fault with SVC at Bus 4

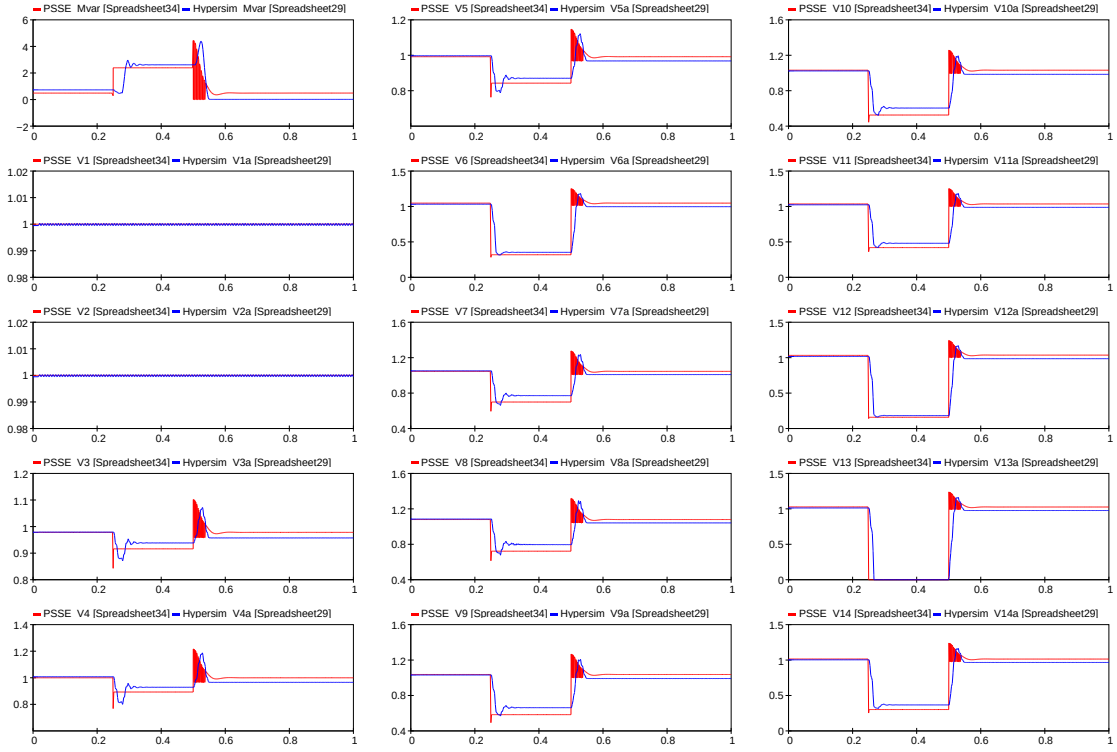

[Spreadsheet29] bus13fault_svcbus4 − E:\Individual\Malavika\2017\14bus_with_SVC\hyper_test_cases_3_30_2017\svc@4
[Spreadsheet34] case13_csv_svc@4 − E:\Individual\Malavika\2017\14bus_with_SVC\Psse_thesis_results\svc@4
Printed for p 1

Figure 28: Bus 13 fault with SVC at Bus 4

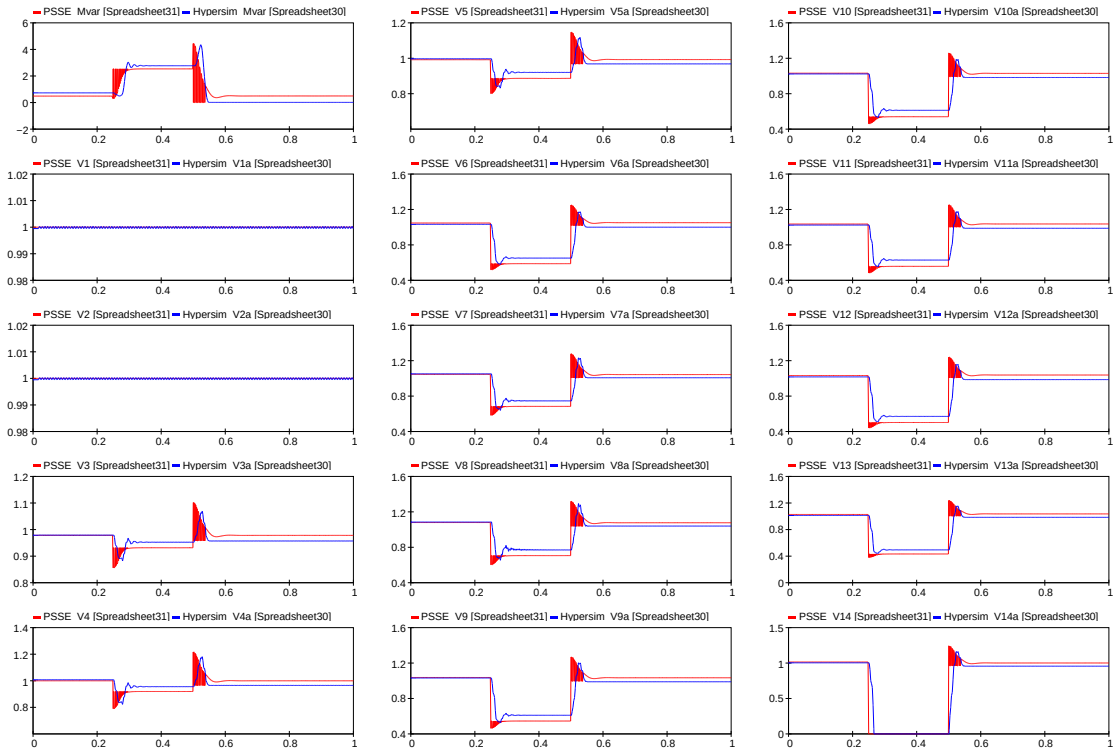

[Spreadsheet30] bus14fault_svcbus4 – E:\Individual\Malavika\2017\14bus_with_SVC\hyper_test_cases_3_30_2017\svc@4
[Spreadsheet31] case14_csv_svc@4 – E:\Individual\Malavika\2017\14bus_with_SVC\Psse_thesis_results\svc@4
Printed for p 1

Figure 29: Bus 14 fault with SVC at Bus 4

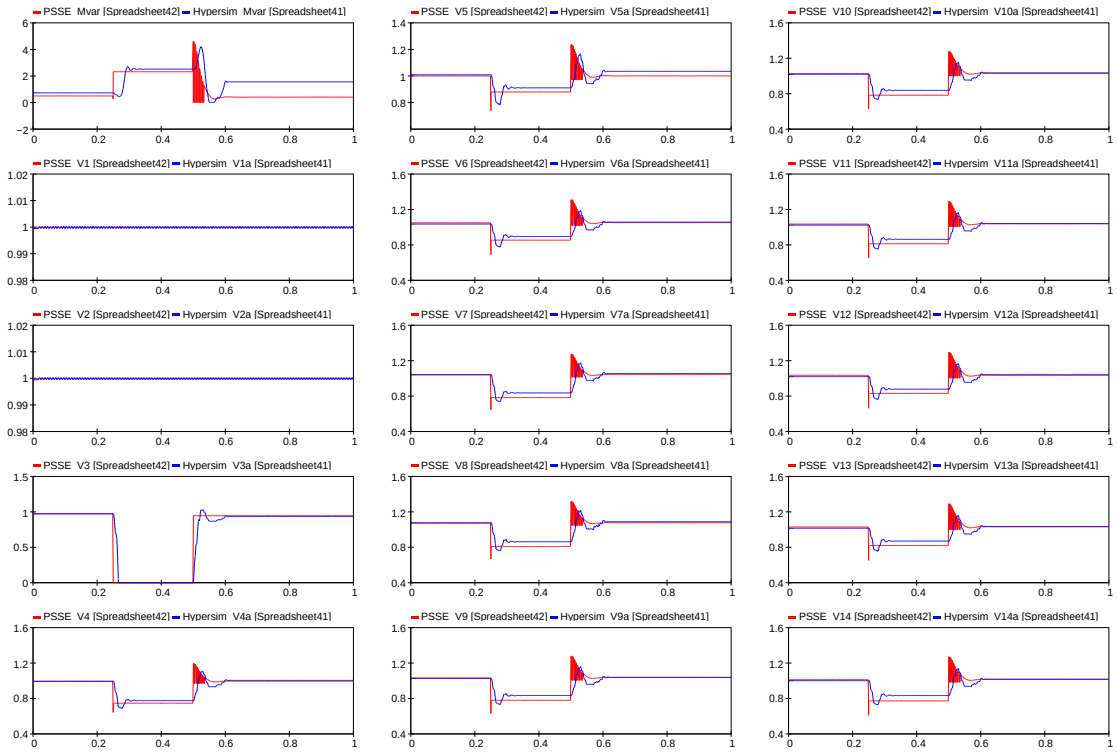

[Spreadsheet41] bus3fault_svcbus5 – E:\Individual\Malavika\2017\14bus_with_SVC\hyper_test_cases_3_30_2017\svc@5
[Spreadsheet42] case3_csv_svc@5 – E:\Individual\Malavika\2017\14bus_with_SVC\Psse_thesis_results\svc@5
Printed for p 1

Figure 30: Bus 3 fault with SVC at Bus 5

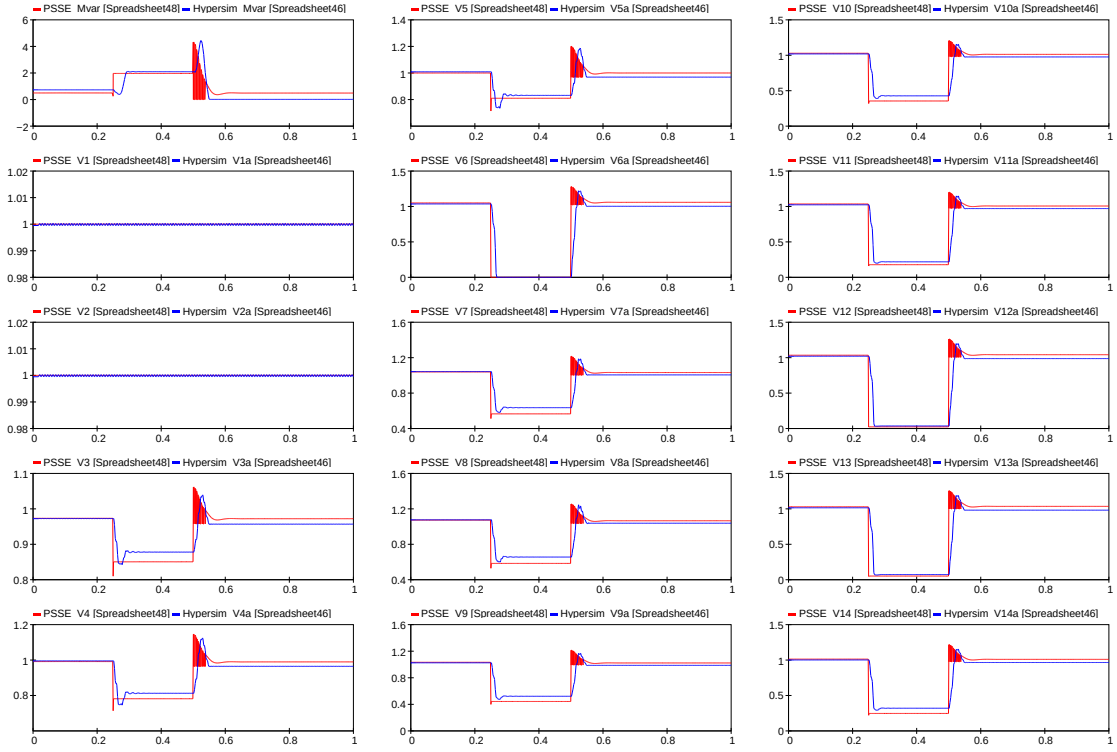

[Spreadsheet46] bus6fault_svcbus5 – E:\Individual\Malavika\2017\14bus_with_SVC\hyper_test_cases_3_30_2017\svc@5
[Spreadsheet48] case6_csv_svc@5 – E:\Individual\Malavika\2017\14bus_with_SVC\Psse_thesis_results\svc@5
Printed for p 1

Figure 31: Bus 6 fault with SVC at Bus 5

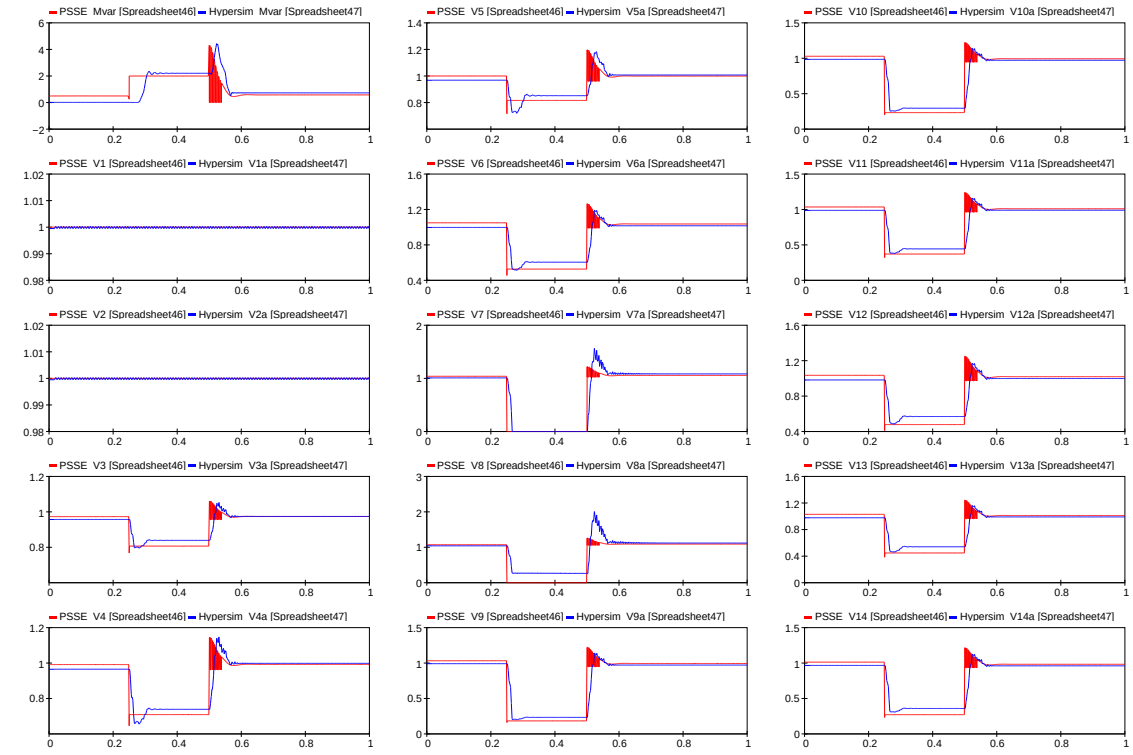

[Spreadsheet46] case7_csv_svc@5 − E:\Individual\Malavika\2017\14bus_with_SVC\Psse_thesis_results\svc@5
[Spreadsheet47] bus7fault_svcbus5 − E:\Individual\Malavika\2017\14bus_with_SVC\hyper_test_cases_3_30_2017\svc@5
Printed for p 1

Figure 32: Bus 7 fault with SVC at Bus 5

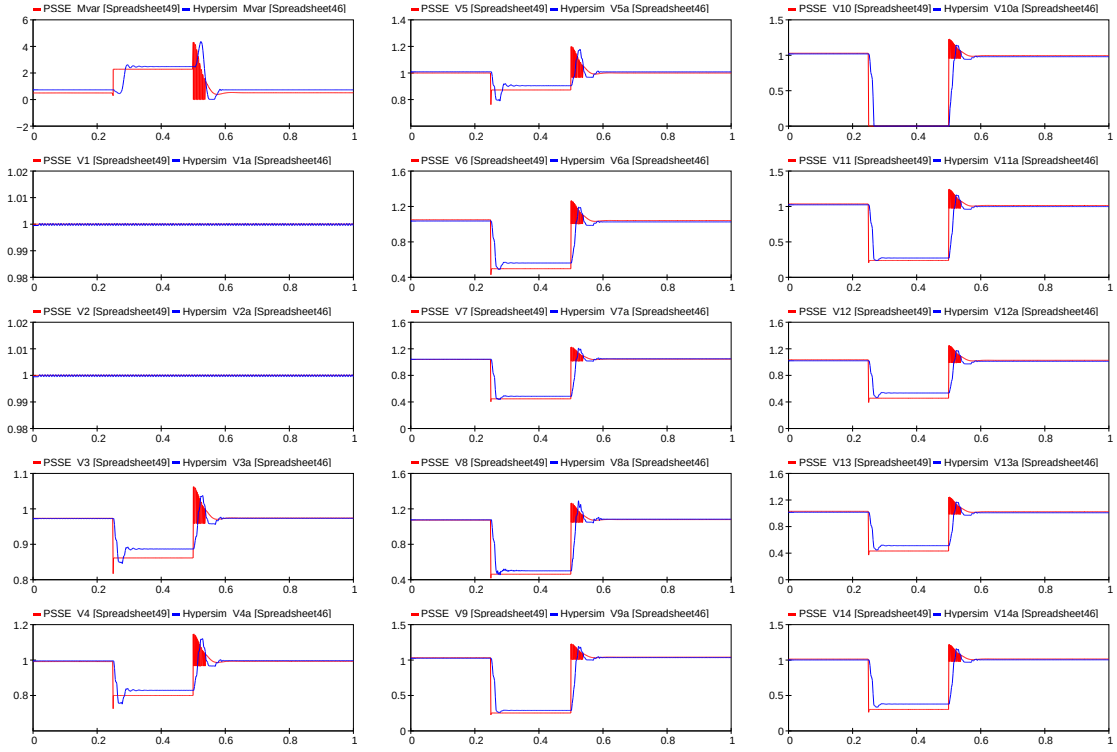

[Spreadsheet46] bus10fault_svcbus5 − E:\Individual\Malavika\2017\14bus_with_SVC\hyper_test_cases_3_30_2017\svc@5
[Spreadsheet49] case10_csv_svc@5 − E:\Individual\Malavika\2017\14bus_with_SVC\Psse_thesis_results\svc@5
Printed for p 1

Figure 33: Bus 10 fault with SVC at Bus 5

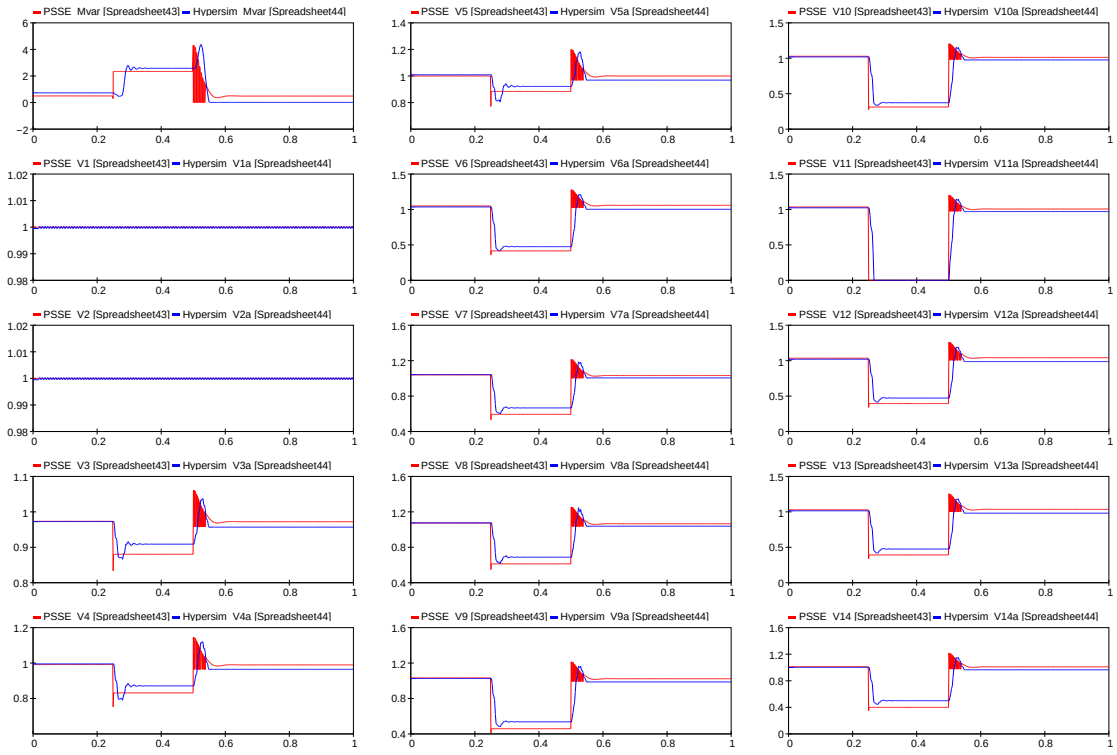

[Spreadsheet43] case11_csv_svc@5 − E:\Individual\Malavika\2017\14bus_with_SVC\Psse_thesis_results\svc@5
[Spreadsheet44] bus11fault_svcbus5 − E:\Individual\Malavika\2017\14bus_with_SVC\hyper_test_cases_3_30_2017\svc@5
Printed for p 1

Figure 34: Bus 11 fault with SVC at Bus 5

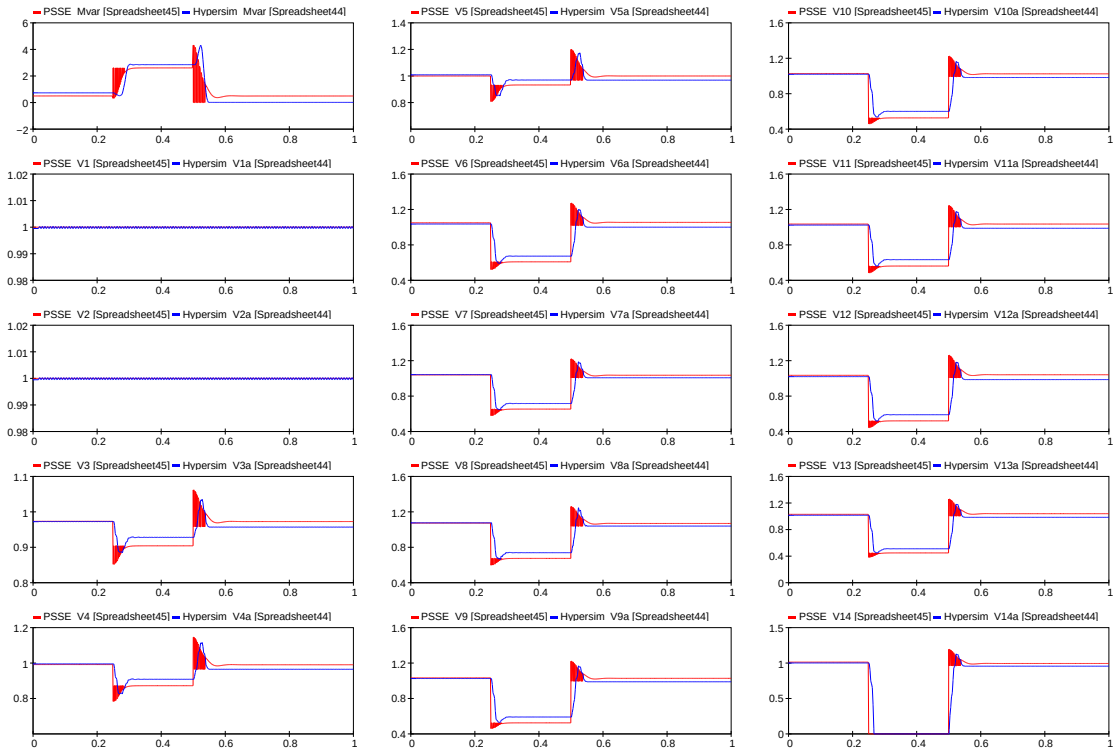

Figure 35: Bus 14 fault with SVC at Bus 5

Vita

Malavika Vasudevan Menon was born in India, in 1992. She received her Bachelor of Technology degree in Electronics and Communication Engineering from Mahatma Gandhi University, Kerala, India, in 2014. She joined the University of New Orleans in Spring, 2015 to pursue a Master's degree in Electrical Engineering.

She joined the Power and Energy Research Laboratory under Dr. Parviz Rastgoufard in 2015 and worked on projects in the area of Power systems transmission modeling, simulation, and design and gained knowledge in using the software platforms such as PSS/E, EMTP, Hypersim for steady state, dynamic, and hardware-in-the-loop modeling and simulation of power systems.